8209428

Kang, Joo-Myung

FINITE ELEMENT ANALYSIS OF THE HEAT AND MASS TRANSFER IN A MAGMA BODY

The University of Oklahoma PH.D. 1981

University Microfilms International 300 N. Zeeb Road, Ann Arbor, MI 48106

THE UNIVERSITY OF OKLAHOMA

GRADUATE COLLEGE

FINITE ELEMENT ANALYSIS OF THE HEAT AND MASS TRANSFER IN A MAGMA BODY

A DISSERTATION

SUBMITTED TO THE GRADUATE FACULTY

in partial fulfillment of the requirement for the

degree of

DOCTOR OF PHILOSOPHY

BY

JOO-MYUNG KANG

NORMAN, OKLAHOMA

1981

FINITE ELEMENT ANALYSIS OF THE HEAT AND MASS TRANSFER

IN A MAGMA BODY

APPROVED BY

J.L. Ahern, Ph.D. (Chairman)

R.D. Evans, Ph.D.

D. Tiab, Ph.D.

J.D. Morris, Ph.D.

H. Crichlow, Ph.D.

L.W. White, Ph.D.

ACKNOWLEDGMENTS

The author wishes to express his sincere gratitude and appreciation to his thesis committee members, Dr. J. L. Ahern, Dr. J. D. Morris, Dr. R. D. Evans, Dr. D. Tiab, Dr. H. B. Crichlow and Dr. L. W. White. The author is particularly indebted to his thesis adviser, Dr. J. L. Ahern, who gave so generously of his time throughout the investigation and in the preparation of this thesis. His guidance, support, encouragement, stimulation and understanding made this thesis possible.

His gratitude is extended to Dr. A. Satake for his advise and stimulation in finite element analysis. Thanks are due to Mrs. M. Fitch Hauser who helped in proofreading and Cathy for her superb typing.

Finally, I am indebted to my parents for teaching me the importance and necessity of education, and to my wife and sons for their patience and encouragement which made this thesis possible.

ABSTRACT

In this study problems of heat and mass transfer in a geothermal reservoir are solved numerically by the finite element analysis for development of geothermal exploration. The problems under investigation are unsteady free convection within a magma body and a two phase Stefam problem associated with moving boundaries. These geological phenomena require a large amount of computer storage as a result of the need to provide increased resolution near a small interesting area of the huge domain. Thus, a consideration to reduce the number of unknown variables is necessary; the penalty method of finite element analysis is employed to solve the time dependent free convection problem. The purpose of the unsteady free convection model is to investigate the effect of convection on the temperature and streamline distribution within a geothermal reservoir (magma body). The one dimensional, two phase Stefan formulation, which has dependent melting temperature on depth, is developed by the finite element method after using the Duvaut's transformation to resolve the discontinuity of the temperature gradient on the solid-liquid interface. This model is used to investigate the effect of the latent heat of fusion on the solidification of magma.

In a time dependent free convection model, convection is generated by density changes due to temperature variations. The results of this study show that the convection gives larger temperature gradients at the upper portion of the magma than the lower portion. Consequently, the heat

transported from the bottom of the magma by convection prevents the roof of the magma body from freezing, or slows the freezing process at the upper portion of the magma, until almost all of the lower portion of the magma is frozen.

The conductive moving boundary model developed in this study indicates that the solidification of magma takes more time when the latent heat of fusion is considered. The convective moving boundary model shows that the temperature gradients in the upper portion of the magma are more steep than those in the lower by transporting the heat at the bottom upward.

NOMENCLATURE

C	Specific heat
D	Domain
d	Characteristic length
D_e, ∂D_e	Domain of element, boundary of element
g	Gravitational acceleration
H_{ij}, G_{ij}, F_i, K_{ij}	Coefficients of matrix
I, G	Global functional, penalty functional
K	Thermal conductivity
ℓ, L	Latent heat per volume, latent heat per mass
N	Interpolation function
n_x, n_y	Components of unit normal vector in x and y direction
P	Pressure
$P(\underset{\sim}{x})$	Position function of the interface
Pr	Prandtl number
Ra	Rayleigh number
$S(t)$, $M(t)$, $I(t)$	Solid domain, melted domain, solid-liquid interface
T	Temperature
T_1, U_1, V_1, $\bar{\theta}_1$, $\bar{U}_1$, $\bar{V}_1$	Values of essential boundary condition
Tm	Transformation temperature
t_1, t_2, t_3	Values of natural boundary condition
T_h, T_c	Temperatures at hot and cold wall
U, V	Velocities in x and y directions
$\hat{U}$, $\hat{V}$, $\hat{T}$, $\hat{\theta}$	Functions of initial conditions
x, y	Cartesian coordinates in two dimensions

α	Thermal diffusivity
β	Coefficient of thermal expansion
γ	Slope of the Clapeyron curve
δ	Variational operator
∂D	Boundary of the domain
ε	Penalty parameter
ρ, ρ_o	Density, reference density
ξ, η	Natural coordinates
θ	Non-dimensionalized temperature
ν	Kinematic viscosity
ω	Vorticity
Ψ	Stream function
[F]	Force vector
[K]	Stiffness matrix
[M]	Mass matrix
$( )_x$, $( )_y$	First derivative of each subscript
∇	Gradient operator
∇^2	Laplacean operator
$\big\|_S$, $\big\|_L$	Values of gradient at the interface

TABLE OF CONTENTS

Chapter | Page

LIST OF FIGURES

Figure		Page

LIST OF TABLES

CHAPTER I

INTRODUCTION

During the last decade geothermal energy has received much attention as a way to meet future energy needs under the assumption of the ultimate depletion of fossil fuel energy. The advantages of geothermal energy over fossil fuel energy are a wide variety of applications, a clean form of energy, and the immense amount of potential energy stored in the earth's interior. These advantages provide an impetus for the development of geothermal exploration. In addition, a substantial amount of hot liquid rock, called magma, rises along the deep cracks in the earth's crust to the depth where it can be tapped by available drilling techniques. Thus, geological or mechanical efforts to utilize a geothermal reservoir as an energy resource have been attempted.

A sequence of stages of intrusion, upward heat transfer, and solidification of hot rock (batholith) have been studied to help assess geothermal reservoirs in terms of the temperature profile and the size of batholiths. Numerous analytical and numerical solutions for the behavior of the magma have been derived by many authors such as Jaeger (1961), Shimazu (1961), McKenzie (1968), Richter (1973), and Korio (1979). The solutions from previous works are not general enough to describe this mechanism because of some oversimplified assumptions, such as no convection effect and no phase change considerations.

In this paper, the formation of a geothermal reservoir associated with a magma chamber, which is an important criterion for the development of geothermal exploration, will be studied as a heat transfer problem with moving boundaries.

The problems of the present study will now be described. As an initial condition a batholith, a molten phase of rock, at a known temperature and at a known mode is intruded into the country rock at a given temperature. After the intrusion, it is subject to the geothermal gradient. The phase change is determined by the melting temperature. This description represents the boundary conditions of the present problem.

The physical properties of the batholith and the country rocks are assumed to have the same values. The molten portion behaves as a laminar incompressible Newtonian fluid under the Boussinesq assumption.

The problem under consideration may be characterized as a free convection problem with moving boundaries. Thus, the problem is divided into two parts to be analyzed systematically.

1-1. Time Dependent Free Convection Model

The purpose of this model is to investigate the heat transfer mechanism of the magma and country rock governed by not only the conductive heat equation outside the magma but also the convective heat transport inside the magma which most previous workers disregarded. From the geological point of view, the convective heat transfer produced by any temperature variations is necessarily a transient phenomenon because the temperature gradient decreases eventually by conductive heat loss through the country rock and convective heat transfer. Then, the molten phase of magma finally becomes solidified after a period of a time.

The convection effect of a magma can give different shape to the batholith depending upon the geological situation. Shaw (1965) pointed out that the forced convection of granitic magma can result in the formation of dikes under certain conditions; on the other hand, a stock-like batholith can be formed by natural convection. Therefore, the effect of the convective heat transfer inside the batholith on the formation of the batholith should be considered with the same degree of importance as the conductive heat transfer. In this model, the general mechanisms governing the motions and temperatures of a magma are formulated mathematically, and the formulated equations are analyzed numerically. The governing equations consist of the continuity equation, momentum equation, energy equation, and equation of state.

The governing equations are formulated variationally by using the penalty method (*) and are discretized by the finite element method with respect to space, and furthermore discretized by the finite difference method with respect to time.

After the finite element method emerged as one of the most effective tools of numerical analysis for structural and solid mechanics, its application to the fluid problem was demonstrated for the first time by Taylor and Hood (1974), and later refined by Zienkiewicz and Gallagher (1975), and Reddy (1979-b).

A finite element method based on the penalty functional formulation is developed for the unsteady free convection problem in Chapter II.

* The penalty method, originated from R. Courant (1945), is developed by Zienkiewicz and Heinrich (1973), Reddy (1979), et al., for application to fluid dynamics.

Reddy and Satake (1980) showed that the penalty formulation has more computational advantages than the direct velocity-pressure formulation (Taylor, 1975) by reducing the number of unknowns. In the penalty formulation the pressure term can be dropped by imposing the incompressibility condition as a constraint into the variational formulations associated with the governing equations.

It is necessary to note that these mathematical formulations are derived under the Boussineseq assumption. This model is used to calculate the temperatures and velocity field inside the batholith.

1-2. Moving Boundary Problem

Immediately after the intrusion of magma into the country rock, the magma is assumed to have sufficient heat to melt the country rock which it contacts. The position of the magma-country rock interface is determined by the conduction equation or the energy equation including the effect of the latent heat which is liberated or absorbed with phase changes. The characteristics of the phenomena considered herein are essentially the same as the Stefan problems treated from the point of view of the heat balance.

The essential assumptions for the treatment of a Stefan problem are:

1. The existence of a transformation temperature at which one phase changes to another with emission or absorption of latent heat
2. The existence of a moving intersurface of separation between two phases.

The analytical solutions known by Jaeger (1961) and Tikhonov (1963) are applicable for one dimensional and one phase Stefan problems since the solutions are obtained by using special characteristics of one dimensional case. In order to solve two phase and two dimensional Stefan problems, numerical approaches are needed. The discontinuity of the temperature gradient, which is the principal cause of difficulty in the numerical approaches to Stafan problems, is resolved by introducing the Duvaut's transformation (1976). Since the development of the Duvaut's transformation, Atthey (1973) and Crowley (1977) solved numerically for one dimensional and two phase Stefan problems, and Ichikawa (1977) and Kikuchi (1977) analyzed the water-ice cases, for which the transformation temperature is constant (zero), by various numerical methods.

Ahern and Turcotte (1979), who corrected Shimazu's results (1961) investigated the effect of convection by simulating this phenomenon with a one dimensional finite difference model. In their model the rate of convection was obtained from Rossby's experimental equation showing that the Nusselt number is a function of the Rayleigh number.

In the present study we will extend the application of the Stefan principles to a problem which has a changing melting temperature with depth and includes the convective effect. The finite element scheme is employed to solve the problem numerically. First of all, to determine the effect of latent heat on the solidification of magma with migration, the one dimensional conductive moving boundary formulation is constructed using the conduction equation. To analyze the upward magma migration mechanism simulated by Ahern (1978) and Shimazu (1961) which used the finite difference model, the development of moving boundary formulation including the convective terms is necessary. To my knowledge, the moving boundary model constructed for the energy equation is the first such approach to the Stefan problem. It is impractical because of the technical difficulty caused by the domain iteration procedure to extend the model at hand to the two dimensional analysis of magma migration by introducing moving boundary conditions into the unsteady free convection model.

CHAPTER II

FREE CONVECTION FORMULATION

2-1. Governing Equations

After the magma is intruded into country rock, a large body of hot magma is surrounded by cold country rock which has been subject to the geothermal gradient. This temperature variation gives rise to variations in the properties of the magma, such as the density and viscosity. All mobilization or transport mechanisms in the magma are produced by these mechanical or thermal instabilities (density and viscosity variations) (Spera, 1980).

The transport mechanisms can be generally classified into two types: forced convection, the mass transfer of fluid as a result of an externally applied force; and free convection which results from the gravitational force on a fluid with inconsistent density due to temperature gradients. In the present study, free convection, which is physically analogous to the present problem is of prime concern.

Since analysis including the full effects of the variations of physical properties associated with free convection flow is so complicated, the Boussinesq approximation will be used. In the Boussinesq approximation, "Variations of all fluid properties other than the density are ignored completely. Variations of the density are ignored except as they give rise to a gravitational force" (Tritton, 1977). Thus, time dependent two dimensional flow of a laminar Newtonian, Boussinesq, incompressible fluid will be considered in the present investigation. The relevant momentum equations (Navier-Stokes equations) are given as follows since incompressibility conditions are satisfied in an approximate sense in the penalty method.

$$U_t + UU_x + VU_y = -\frac{1}{\rho} P_x + \nu[2U_{x,x} + (U_y + V_x)_y] \tag{1}$$

$$V_t + UV_x + VV_y = -\frac{1}{\rho} P_y + \nu[2V_{y,y} + (U_y + V_x)_x] + g\beta(T - T_o) \tag{2}$$

in D

where ρ is density, ν kinematic viscosity, g gravitational acceleration, β thermal expansion coefficient, T_o reference temperature, U horizontal velocity, V vertical velocity, P pressure, D domain. It is necessary to note that U_t, U_x, U_y, V_t, V_x, V_y, T_t, P_x, P_y, $(\ )_y$, $(\ )_x$ denote first derivatives with respect to each subscript and $U_{x,x}$, $U_{y,y}$, $T_{x,x}$, $T_{y,y}$ are second derivatives with respect to x,y, respectively.

The continuity equation can be written as

$$U_x + V_y = 0 \qquad \text{in D} \tag{3}$$

The energy equation is

$$T_t + UT_x + VT_y = \alpha(T_{x,x} + T_{y,y}) \qquad \text{in D} \tag{4}$$

where α is isotropic thermal diffusivity. Equation 4 does not include the viscous-energy-dissipation term due to friction in the fluid because the effect of that term is negligibly small for most engineering applications where the flow velocities are small (Ozisik,1977).The derivation of Navier-Stokes equations from Newton's 2nd law, the continuity equation and the heat conduction equation are described in Appendix 1.

The boundary conditions are:

$$T = T_1 \qquad U = U_1 \qquad V = V_1 \qquad \text{in } \partial D_1 \tag{5}$$

$$t_1 = (2\nu \cdot U_x - \frac{P}{\rho})n_x + \nu(U_y + V_x)n_y$$

$$t_2 = \nu(U_y + V_x)n_x + (2\nu \cdot V_y - \frac{P}{\rho})n_y \qquad \text{in } \partial D_2 \tag{6}$$

$$t_3 = \alpha(T_x n_x + T_y n_y)$$

where n_x, n_y are normal derivatives to the boundaries:

T_1, U_1, V_1 the values of essential (Dirichlet) boundary conditions of temperature and velocities.

t_1, t_2, t_3 the values of natural (Neumann) boundary conditions of each variable.

∂D_1 denotes the portions of the boundary on which the variables are specified.

∂D_2 denotes the portions of the boundary on which the tractions of the variables are specified.

Initial conditions associated with the governing equations are given as

$$
\begin{aligned}
U(x,y,o) &= \hat{U}(x,y) \\
V(x,y,o) &= \hat{V}(x,y) \\
T(x,y,o) &= \hat{T}(x,y)
\end{aligned}
\tag{7}
$$

where $\hat{U}$, $\hat{V}$, $\hat{T}$ are initial functions of velocities and temperature respectively.

It is usually convenient to nondimensionalize the governing equations by the dimensionless parameters and variables for the usual treatment of the thermal flow problems.

$$x = x^*d,\ y = y^*d,\ U = U^*\frac{\alpha}{d},\ V = V^*\frac{\alpha}{d},\ \theta = \frac{T - T_c}{T_h - T_c}$$

$$P = \rho V^2 p^*,\ t = t^*\frac{d^2}{\alpha}$$

where d is a characteristic length, U a characteristic velocity, T_h a temperature at hot wall, T_c a temperature at cold wall and the starred quantities denote the dimensionless variables, θ is dimensionless temperature. The stars on the variables will be omitted for convenience hereafter.

By introducing the following nondimensional parameters:

$$Pr = \frac{\nu}{\alpha} \qquad \text{Prandtl number}$$

$$Ra = \frac{g\beta(T - T_o)d^3}{\nu\alpha} \qquad \text{Rayleigh number,}$$

we can rewrite the governing equations as:

$$U_t + UU_x + VU_y = -P_x + Pr \, . \, (2U_{x,x} + (U_y + V_x)_y) \tag{8}$$

$$V_t + UV_x + VV_y = -P_y + Pr \, . \, (2V_{y,y} + (U_y + V_x)_x) + Ra \, . \, Pr \, . \, \theta$$

$$U_x + V_y = 0 \tag{10}$$

$$\theta_t + U \, . \, \theta_x + V \, . \, \theta_y = \theta_{x,x} + \theta_{y,y} \tag{11}$$

in D

with boundary conditions

$$t_1 = (2Pr \, . \, U_x - P)n_x + Pr \, . \, (U_y + V_x)n_y$$

$$t_2 = Pr \, . \, (U_y + V_x)n_x + (2Pr \, . \, V_y - P)n_y \qquad \text{in } \partial D_2 \tag{12}$$

$$t_3 = \theta_x n_x + \theta_y n_y$$

$$
\left.\begin{aligned}
\theta &= \bar{\theta}_1 \\
U &= \bar{U}_1 \\
V &= \bar{V}_1
\end{aligned}\right\} \quad \text{in } \partial D_1 \tag{13}
$$

The initial conditions become

$$
\begin{aligned}
\theta(x,y,o) &= \hat{\theta}(x,y) \\
U(x,y,o) &= \hat{U}(x,y) \\
V(x,y,o) &= \hat{V}(x,y)
\end{aligned} \tag{14}
$$

2-2. Penalty Functional Formulation

The finite element formulation is derived from the Rayleigh-Ritz-Galerkin philosophy of constructing approximation functions whose linear combinations represent the unknown solutions. The introduction of the Galerkin integrals which do not require the construction of a functional is necessary in the problem where the convective (nonlinear) terms are important. Furthermore, problems which need large computer storage require another consideration to reduce the number of unknowns. Thus, the penalty formulation, which was refined by Zienkiewicz (1975) and Reddy (1979-a), is employed to solve the system of equations defined by (1), (2), (3), and (4). The penalty method consists of incorporating the penalty function into the variational formulation associated with these equations.

The penalty function corresponds to the incompressibility condition which is appended with the penalty term. Thus, the approximate solution converges into the true solution as the constraint is satisfied more closely.

Hence

$$\int_D \Big[[U_t + U \,.\, U_x + V \,.\, U_y + P_x - Pr \,.\, [2U_{x,x} + (U_y + V_x)_y]\delta U$$

$$+ [V_t + U.V_x + V.V_y + P_y - Pr \,.\, [2V_{y,y} + (U_y + V_x)_x - Ra \,.\, Pr \,.\, \theta]\delta V$$

$$+ [U_x + V_y]\delta p$$

$$+ [\theta_t + U\theta_x + V\theta_y - \theta_{x,x} - \theta_{y,y}]\delta\theta \Big] dD = 0 \tag{15}$$

By use of integration by parts

$$\int_D \Big[[U_t\delta U + (U \,.\, U_x + V \,.\, U_y)\delta U + Pr \,.\, [2U_x\delta U_x + (U_y + V_x)\delta U_y]$$

$$+ [V_t\delta V + (U \,.\, V_x + V \,.\, V_y)\delta V + Pr \,.\, [2V_y\delta V_y + U_y + V_x)\delta V_x]$$

$$- Pr \,.\, Ra \,.\, \theta\delta V$$

$$+ [\theta_t\delta\theta + (U\theta_x + V\theta_y)\delta\theta - \theta_x\delta\theta_x - \theta_y\delta\theta_y]$$

$$- [P(\delta U_x + \delta V_y) + (U_x + V_y)\delta p] \Big] dD$$

$$+\int_{\partial D}[Pr\ .\ [2U_x\delta U\ .\ n_x + (U_y + V_x)\delta U\ .\ n_y + 2V_y\delta V\ .\ n_y$$

$$+ (U_y + V_x)\delta V\ .\ n_x]$$

$$+ [p\delta U\ .\ n_x + p\delta V\ .\ n_y + \theta_x N_x + \theta_y N_y]\ dS \tag{16}$$

For the moment, let's examine the following term

$$-\int_D P(\delta U_x + \delta V_y)\ dD + \int_{\partial D_1}(P\delta U\ .\ n_x + P\delta V\ .\ n_y)\ dS \tag{17}$$

Since the arbitrary functions U, V satisfy the incompressibility condition, the first term vanishes. The second term disappears when the velocity is specified on the boundary. Thus, pressure does not appear in the penalty method. The above variational statements can be rewritten in penalty formulation forms

$$\delta I + \delta G = 0 \tag{18}$$

where $\delta I = \int_D [U_t\delta U + (U\ .\ U_x + V\ .\ U_y)\delta U + Pr\ .\ [2U_x\delta U_x + (U_y + V_x)\delta U_y]$

$$+ [V_t\delta V + (U\ .\ V_x + V\ .\ V_y)\delta V + Pr\ .\ [2V_y\delta V_y + (U_y + V_x)\delta V_x]$$

$$- Pr\ .\ Ra\ .\ \theta\delta V\ .\ [\theta_t\ .\ \delta\theta + (U\ .\ \theta_x + V\ .\ \theta_y)\delta\theta - \theta_x\delta\theta_y$$

$$- \theta_y\delta\theta]dD$$

$$+ \int_{\partial D} Pr \cdot [2U_x \delta U \cdot n_x + (U_y + V_x)\delta U \cdot n_y + 2V_y \delta V \cdot n_y$$

$$+ (U_y + V_x)\delta V \cdot n_x] + [\theta_x N_x + \theta_y n_y]dS \qquad (19)$$

$$G = \frac{\varepsilon}{2}\int_D (U_x + V_y)^2 dD \qquad (20)$$

where G is the penalty function and ε is penalty parameter. Zienkiewicz (1977) and Reddy (1979-a) proved theoretically that the penalty function converges to zero as ε goes toward infinity. In other words, the approximate solution converges into the actual solution as ε is increased to infinity. But, in practical computation the selection of the value for ε is crucial to yield accurate results. In the penalty method, the pressure is obtained by

$$p = -\varepsilon(U_x + V_y) \qquad (21)$$

because the pressure corresponds to the Lagrange multiplier which is associated with the incompressibility constraint in this system.

2-3. Finite Element Formulation

The finite element method was introduced as a tool of numerical approximation for the problems associated with structural mechanics. The applications of the finite element method to the problems of fluid flow have only been developed in recent years.

The finite element method assumes that the governing equations over a given global domain hold in each subdomain, called a finite element.

Thus, the relevant equations for a typical element are derived from the global governing equations using the variational method. Then, the unknown primitive variables U, V, θ are approximated by a series of interpolation functions (or shape functions) in each element. As a result, the associated equations for a typical element are discretized in matrix form. The global approximations over the given domain are constructed by assembling these elements at the continuous interelement boundaries.

We can introduce the following interpolation functions of the variables U, V, and θ over the subdomain

$$
\begin{aligned}
U &= \Sigma U_i N_i(x,y) \\
V &= \Sigma V_i N_i(x,y) \qquad (22) \\
\theta &= \Sigma \theta_i N_i(x,y)
\end{aligned}
$$

where N_i denotes the interpolation function corresponding to node i and U_i, V_i, θ_i, the values of variables at the ith node of the element. By substituting equation 22 into equation 18, we obtain

$$
\sum_i \delta U_i \int_{De} [U_{j,t} \cdot N_j \cdot N_i + (U\Sigma U_j N_{j,x} + V\Sigma U_j N_{j,y})N_i +
$$

$$
\varepsilon \cdot (\Sigma U_j N_{j,x} + \Sigma V_j N_{j,y})N_{i,x} + Pr \cdot [2N_{i,x}\Sigma U_j N_{j,x} +
$$

$$
(\Sigma U_j N_{j,y} + \Sigma V_j N_{j,x})N_{i,y}]dxdy
$$

$$\sum_i \delta V_i \int_{De} V_{j,t} \cdot N_j N_i + (U\Sigma V_j N_{j,x} + V\Sigma V_j N_{j,y}) N_i +$$

$$Pr \cdot [2N_{i,y}\Sigma V_j N_{j,y} + (\Sigma V_j N_{j,y} + \Sigma V_j N_{j,x}) N_{i,x}]$$

$$- Pr \cdot Ra \cdot \theta \cdot N_i + \varepsilon N_{i,y}(\Sigma V_j N_{j,x} + \Sigma V_j N_{j,y})]dxdy$$

$$+ \Sigma\delta\theta_i \int_{De} [\theta_{j,y} \cdot N_j \cdot N_i + (U\Sigma\theta_j N_{j,x} + V\Sigma\theta_j N_{j,y}) N_i + N_{i,x}\Sigma\theta_j N_{j,x}$$

$$+ N_{i,y}\Sigma\theta_j N_{j,y}]dxdy \; .$$

$$- \Sigma\delta U_i \int_{\partial De} t_1 N_i dS - \Sigma\delta V_i \int_{\partial De} t_2 N_i dS - \Sigma\delta\theta_i \int t_3 N_i dS \qquad (23)$$

where

$$t_1 = (2Pr \cdot U_x - p)n_x + Pr(U_y + V_x)n_y$$

$$t_2 = Pr(U_y + V_x)n_x + (2Pr \cdot V_y - p)\, n_y \qquad (24)$$

$$t_3 = (\theta_x n_x + \theta_y n_y)$$

D_e, ∂D_e denote a domain of element, and a boundary of element respectively. Collecting the coefficients of the variables δU_i, δV_i and $\delta\theta_i$ respectively, we can have the following matrix forms

$$\begin{bmatrix} M^e & 0 \\ 0 & M^e \end{bmatrix} \cdot \begin{bmatrix} U_t \\ V_t \end{bmatrix} + \left[\begin{array}{c|c} H + Pr.[2G^1 + G^2] + \varepsilon.G^1 & Pr.G^{21} + \varepsilon.G^{12} \\ \hline Pr.G^{21} + \varepsilon.G^{12} & H + Pr.[2G^2 + G^1] + \varepsilon.G^2 \end{array}\right] \cdot \begin{bmatrix} U \\ V \end{bmatrix} = \begin{bmatrix} F^1 \\ F^2 \end{bmatrix} \tag{25}$$

$$[M^e][\theta_t] + [H + G^1 + G^2][\theta] = [F^3] \tag{26}$$

where $$H_{ij} = \int (U \cdot N_{j,x} + V \cdot N_{j,y}) \cdot N_i dxdy \tag{27}$$

$$G^1_{ij} = \int N_{i,x} N_{j,x} dxdy \tag{28}$$

$$G^2_{ij} = \int N_{i,y} N_{j,y} dxdy \tag{29}$$

$$G^{12}_{ij} = \int N_{i,x} N_{j,y} dxdy \tag{30}$$

$$G^{21}_{ij} = \int N_{i,y} N_{j,x} dxdy \tag{31}$$

$$F^1_i = \int t_1 N_i dS \tag{32}$$

$$F^2_i = \int t_2 N_i dS + \int Pr \cdot Ra. \theta . N_i \, dxdy \tag{33}$$

$$F^3_i = \int t_3 N_i dS$$

$$M^e_{ij} = \int N_i \cdot N_j \cdot dxdy \tag{35}$$

One of the important steps in the finite element analysis is the selection of the interpolation functions associated with the shape of an element.

Zienkiewicz (1979) showed that quadrilateral elements give more accurate solutions than the triangular elements in the penalty formulation. Also, linear interpolation functions and the more refined meshes have computational advantages over the high order interpolation functions because of the difficulty of the integration. Thus, a bilinear quadrilateral interpolation function is used in the present formulation:

$$
\begin{aligned}
N_1 &= \frac{1}{4ab}(b-x)(a-y) \\
N_2 &= \frac{1}{4ab}(b+x)(a-y) \\
N_3 &= \frac{1}{4ab}(b+x)(a+y) \\
N_4 &= \frac{1}{4ab}(b-x)(a+y)
\end{aligned}
\tag{36}
$$

where N_1, N_2, N_3, and N_4 are interpolation functions at nodal point 1, 2, 3, and 4 in the element.

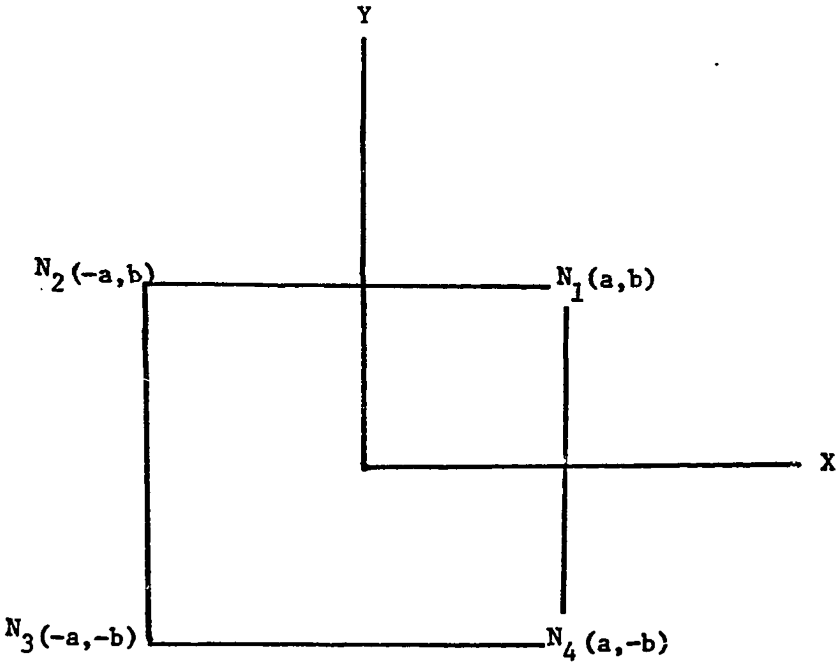

Figure 2-1, The Rectangular Element

The nonlinear term in the matrix [H] requires an iterative technique which computes the value at the (m+1)th iteration, assuming the values at the mth iteration to be known, until the computed values show sufficient convergence.

The finite element equations discretized with respect to space should be discretized further with respect to time for time dependent problems.

There are generally two discretization methods for time dependent problems. The interpolation function is regarded as being dependent upon space as well as upon time such that:

$$\frac{\partial U(\underset{\sim}{x},t)}{\partial t} = \frac{\partial N_i(\underset{\sim}{x},t)}{\partial t} \cdot U_i \tag{37}$$

The second method involves the temporal operator being introduced as the time derivative of a variable at a node from the relation

$$\frac{\partial U(\underset{\sim}{x},t)}{\partial t} = N_i(\underset{\sim}{x}) \frac{\partial U_i(t)}{\partial t} \tag{38}$$

In the present study the second approach is employed for the time approximation. An advantage of the second method over the first method is the decrease in computational dimensions requiring the finite element in time (Chung, 1978).

Hence, we can rewrite equations 25 and 26 in standard matrix form

$$[M][\underset{\sim}{U}_t] + [K(\underset{\sim}{U})][\underset{\sim}{U}] = [F] \tag{39}$$

where [M] is conventionally called the mass matrix, $\underset{\sim}{U}$ unknown solution vector, [K] stiffness matrix, [F] force vector. The finite difference schemes for time dependent problems is given by

$$\theta \cdot (\underset{\sim}{U}_{n+1})_t + (1-\theta) \cdot (\underset{\sim}{U}_n)_t = (\underset{\sim}{U}_{n+1} - \underset{\sim}{U}_n)/\Delta t \tag{40}$$

where $(\ )_t$ denotes the derivative with respect to time, $\underset{\sim}{U}_{n+1}$, $\underset{\sim}{U}_n$ are unknown variables at the n+1, and nth time step.

The following values of θ are generally used for time dependent problems.

$$\theta = \begin{array}{rl} 0, & \text{forward-difference} \\ 1/2, & \text{Crank-Nicholson} \\ 2/3, & \text{Galerkin} \\ 1, & \text{backward-difference} \end{array}$$

The Crank-Nicholson and Galerkin schemes will be tested for convergence and accuracy in the present study. From equation 40, we obtain:

$$[M](U_n)_t + [K]U_n = F_n \text{ at nth time step} \tag{41}$$

$$[M](U_{n+1})_t + [K]U_{n+1} = F_{n+1} \text{ at (n+1)th time step} \tag{42}$$

Multiplying equation (40) with [M], then substituting equations 41 and 42 into 40, we have

$$\begin{aligned}[][[M] + \Delta t[K(U_{n+1})]\theta]\left\{U_{n+1}\right\} &= [[M] - \Delta t[K(U_n)](1 - \theta)]\left\{U_n\right\} \\ &+ \Delta t[\theta F_{n+1} + (1 - \theta)F_n]\end{aligned} \tag{43}$$

The dependence of the [K] matrix which contains convective terms (non-linear terms) on the solution at n+1th time step requires an iterative procedure.

2-4. Stream Function

The stream function, Ψ, is a useful variable for the analysis of the two dimensional flow. The stream function can be determined from the vorticity equation once the velocity field is known. From the relationship between the stream function and the velocity variables, we have

$$\begin{aligned} U &= \Psi_y \\ V &= -\Psi_x \end{aligned} \tag{44}$$

The vorticity equation is defined by

$$\omega = -(U_y - V_x) \tag{45}$$

Therefore,

$$\begin{aligned} \nabla^2\Psi &= -\omega \\ &= (U_y - V_x) \end{aligned} \tag{46}$$

The Galerkin integral is applied to equation (46) to develop the finite element formulation.

$$\int_D (-\Psi_{x,x} - \Psi_{y,y} + U_y - V_x)\delta\Psi dxdy = 0 \tag{47}$$

Integrating by parts,

$$\int_D [\Psi_x \delta\Psi_x + \Psi_y \delta\Psi_y + (U_y - V_x)] \delta\Psi \, dxdy$$

$$- \int_{\partial D} (\Psi_x \delta\Psi \cdot N_x + \Psi_y \delta\Psi \cdot N_y) dS = 0 \tag{48}$$

The boundary terms vanish since the value of the stream function at the boundary is zero. If we assume the following interpolation functions for Ψ, U, and V, in each element respectively

$$\Psi = \Sigma \Psi_j N_j \qquad U = \Sigma U_j N_j \qquad V = \Sigma V_j N_j \tag{49}$$

substituting equation 49 into equation 38, we obtain

$$\delta\Psi_i \int \{\Psi_j (N_{j,x} N_{i,x} + N_{j,y} J_{i,y}) +$$

$$(V_j N_{j,x} - U_j N_{j,y}) N_i\} dxdy = 0 \tag{50}$$

Collecting the coefficients of $\delta\Psi_i$, we can express the above equation in matrix form

$$[K] \{\Psi\} = \{F\} \tag{51}$$

where
$$K_{ij} = \int (N_{j,x} N_{i,x} + N_{j,y} N_{i,y}) dxdy \tag{52}$$

$$F_i = - \int (V_i N_{i,x} - U_i N_{i,y}) N_i \, dxdy \tag{53}$$

The time dependent, two-dimensional, free convection model, which has been formulated for the first time using the penalty method of finite element analysis, is employed to investigate the heat transfer mechanism of the magma and country rock, primarily the convective heat transport inside the magma. The advantage of this method is that the number of variables is reduced and computation time is correspondingly reduced. The results of this modelling will be given and discussed in Chapter IV.

CHAPTER III

MOVING BOUNDARY FORMULATION

Immediately after the intrusion of magma into the country rock, the magma may have sufficient heat to melt the country rock which it contacts. Also, if the melting takes place along the Clapeyron curve, along which the melting temperature increases with depth, the magma may move upward by melting the country rock above the intrusion and freezing the batholith near its lower boundary [Shimazu (1961), Ahern et al., (1979, 1981)]. The ascent rate of the solid-liquid interface was calculated by Ahern and Turcotte (1979) by using the one dimensional finite difference convective upwelling model, suggesting that the position of the interface is determined by conduction as well as convection including the effect of latent heat.

This section will develop the conductive moving boundary model to investigate the effect of latent heat on the solidification of magma without convection. The magma becomes solidified along the moving solid-liquid interface where the phase change occurs by liberating or absorbing the latent heat. The phenomenon of interest is analogous to the Stefan problem from the point of view of the heat balance. The importance of the moving boundary problem is based on the following points: 1) a domain of the solution of the governing equation is unknown and must be determined as part of the solution procedure and 2) a discontinuity of the temperature gradient on the solid-liquid interface, which is the principal cause of difficulty in numerical approaches to the Stefan problem. The first difficulty is resolved by the domain iteration procedure which is repeated until the solutions from the assumed domain converge to the solutions from the computed domain. The second difficulty is overcome by transforming the discontinuous temperature to the continuous variable defined by Duvaut. Since the development of the Duvaut's transformation, numerical approaches to Stefan problems have been investigated by Atthey (1973) and Crowley (1977) for one dimensional and two phase cases, and Ichikawa (1979) and Kikuchi (1979) for water-ice cases with a fixed freezing temperature. The analytical solutions obtained by Jaeger (1961) and Tikhonov (1963) are applicable for one dimensional and one phase Stefan problems, not all are extensible to two dimensional and two phase cases. In the present study the application of the Stefan principles will be extended to a problem which has a changing melting temperature with depth. The finite element scheme is employed to solve the problem numerically. The essential assumptions for the treatment of a Stefan problem are:

1. The existence of a transformation temperature at which changes from one phase to another result in emission or absorption of latent heat.
2. The existence of a moving intersurface of separation between the two phases.

The above assumptions are satisfied in the following manner in this study. The transformation temperature is given by:

$$T_m = T_{mo} + \frac{P}{\gamma}$$

$$= T_{mo} + \frac{\rho \cdot g \cdot y}{\gamma} \qquad (54)$$

where P is pressure, T_{mo} the transformation temperature at the surface, γ the slope of the Clapeyron curve, ρ density and y depth.

Secondly, the position of the transformation surface is determined by the difference of heat flux across the surface. In other words, the location of the interface can be written in finite difference form at the time $t = n\Delta t$;

$$\rho \cdot L \frac{Y^n - Y^{n-1}}{\Delta t} = K_1 \cdot \nabla T^{n-1}\Big|_S - K_2 \nabla T^{n-1}\Big|_L \qquad (55)$$

where T is temperature, K_i thermal conductivity of the ith phase, L latent heat per mass, and $\Big|_S$, $\Big|_L$ denote the value of temperature gradient at the solid side of the surface, and the liquid side of the surface respectively. The discontinuity of the temperature gradients in the matching condition is the principal difficulty in any numerical or analytical method. Thus, an innovative concept is needed to overcome this discontinuity. The method introduced by Duvaut (1976) transforms the discontinuous temperature field to a continuous variable which determines the phase of the material. Thus, the continuous variable can be differentiated over the whole domain. The continuous variable is denoted as the melting index for convenience.

3-1. Governing Equation

We can generally formulate our problem by heat equations with the boundary conditions, initial conditions, and matching conditions as follows:

$$C_i T_t = \nabla \cdot K_i \nabla T \qquad \text{in } D \tag{56}$$

$$S(t) = \{\underset{\sim}{x} \varepsilon D : T(\underset{\sim}{x},t) < Tm\} \tag{57}$$

$$M(t) = \{\underset{\sim}{x} \varepsilon D: \ T(\underset{\sim}{x},t) > Tm\} \tag{58}$$

$$I(t) = \{\underset{\sim}{x} \varepsilon D: \ T(\underset{\sim}{x},t) = Tm\} \tag{59}$$

where C_i, K_i are mass heat capacity and heat conductivity of the ith phase respectively (i=1, solid; i=2, melted phase), D whole domain, S(t) solid domain, M(t) melted domain, I(t) interface in which phase change occurs, Tm transformation temperature, $\underset{\sim}{x}$ Cartesian coordinate.

Boundary conditions are

$$T = T_1 \qquad \text{on } \partial D_1 \tag{60}$$

where T_1 is the boundary condition and ∂D_1 is an area specified by the essential boundary condition.

Initial conditions are

$$T = T_{so}(x,y,o) \qquad \text{in } S(t) \tag{61}$$

$$T = T_{1o}(x,y,o) \qquad \text{in } M(t) \tag{62}$$

Matching conditions are

$$\rho \cdot L \frac{\underset{\sim}{x}^{n} - \underset{\sim}{x}^{n-1}}{\Delta t} = K_i \nabla T^{n-1}\Big|_S - K_i \cdot \nabla T^{n-1}\Big|_L \quad \text{on } I(t) \tag{63}$$

In the problem where the melting temperature is dependent on the depth, the following transformation of variables is developed to satisfy principles of Duvaut's transformation. From equation 54 we can have the following relationship

$$\dot{T}(x,y,t) = T(x,y,t) - Tm(y) \tag{64}$$

where $\dot{T}$ is a new temperature variable.

Transforming the governing systems using equation 64, we obtain:

governing equation,

$$C_i \mathring{T}_t = K_i \nabla^2 \mathring{T} \qquad \text{in } D \tag{65}$$

initial condition,

$$\dot{T} = T_{so}(x,y,o) - Tm(y) \qquad \text{in } D(t) \tag{66}$$

$$\dot{T} = T_{Lo}(x,y,o) - Tm(y) \qquad \text{in } L(t) \tag{67}$$

boundary condition,

$$\mathring{T} = T_1 - Tm(y) \qquad \text{in } \partial D \tag{68}$$

and matching condition,

$$\rho \cdot L \frac{\underset{\sim}{x}^{n} - \underset{\sim}{x}^{n-1}}{\Delta t} = K_i \nabla \dot{T}^{n-1} \Big|_S - K_i \nabla \dot{T}^{n-1} \Big|_L = [K \cdot \nabla \dot{T}] \tag{69}$$

since Tm(y) is linearly dependent on y, where [ ] denotes the difference of the temperature gradients between the solid side and the melted side. The matching condition can be related to the position of the interface by the following development. If the equation $\underset{\sim}{X} = I(t)$ is given,

$$\frac{d\underset{\sim}{x}}{dt} = \frac{dI(t)}{dt} \tag{70}$$

Thus, we can rewrite the equation X = I(t) inversely

$$t = I^{-1}(\underset{\sim}{X}) = P(\underset{\sim}{X}) \tag{71}$$

By substituting the relationships 70, 71 into the matching condition, we have

$$\rho . L \frac{dI(t)}{dt} = [K_i . \nabla \dot{T}] \tag{72}$$

$$\rho . L = [K_i . \nabla \dot{T}] \frac{dt}{dI(t)}$$

$$= [K_i . \nabla \dot{T}] \frac{\partial (\underset{\sim}{x})}{d\underset{\sim}{x}}$$

$$= [K_i . \nabla \dot{T}] . \nabla P(\underset{\sim}{x}) \tag{73}$$

Hereafter we will omit the dots on the temperature for convenience.

3-2. Duvaut's Transformation

We transform the governing equations associated with discontinuous temperature gradients to continuous variables defined by Duvaut (1975) as follows:

$$\theta(\underset{\sim}{x},t) = \int_{o}^{t} K_1 . T(\underset{\sim}{x},\tau)d\tau \tag{74}$$

For instance, if the phase changes from solid to solid, the first derivative of θ;

$$\nabla\theta(\underset{\sim}{x},t) = \int_{o}^{t} \nabla . K_1 T(\underset{\sim}{x},\tau)d\tau \tag{75}$$

the second derivative of θ;

$$\nabla.\nabla\theta(\underset{\sim}{x},t) = \int_{o}^{t} \nabla.\nabla K_1 T(\underset{\sim}{x},\tau)d\tau$$

$$= -C_1 T(\underset{\sim}{x},o) + C_1 T(\underset{\sim}{x},\tau). \tag{76}$$

If the phase change goes from solid to liquid, we have

$$\theta(\underset{\sim}{x},t) = \int_{o}^{P(x)} K_1 . T(\underset{\sim}{x},\tau)d\tau + \int_{P(x)}^{t} K_2 . T(\underset{\sim}{x},\tau)d\tau \tag{77}$$

The first derivative of the first term in equation 77 is obtained by using Leibnitz rule;

$$\nabla\theta(\underset{\sim}{x},t) = \int_{o}^{P(x)} K_1 \nabla T(\underset{\sim}{x},\tau)d\tau + K_1 T(\underset{\sim}{x},P(\underset{\sim}{x}))\Big|_{S} . \nabla P(\underset{\sim}{X})$$

$$+ \int_{P(x)}^{t} K_2 \nabla T(\underset{\sim}{x},\tau)d\tau - K_2 T(\underset{\sim}{x},P(\underset{\sim}{x}))\Big|_{L} . \nabla P(\underset{\sim}{X})$$

$$= \int_{o}^{t} K_i \nabla T(\underset{\sim}{x},\tau)d\tau \tag{78}$$

since the temperature T is zero on I(t) (interface). The second derivative of $\theta(\underset{\sim}{X},t)$ is

$$\nabla.\nabla\theta(\underset{\sim}{x},t) = \int_{o}^{P(x)} \nabla.K_1 \nabla T(\underset{\sim}{x},\tau)d\tau + K_1 \nabla T(\underset{\sim}{x},P(x))\Big|_{S} . \nabla P(\underset{\sim}{x})$$

$$+ \int_{P(x)}^{t} \nabla.K_2 \nabla T(\underset{\sim}{x}\ \tau)d\tau - K_2 \nabla T(\underset{\sim}{x},P(x))\Big|_{L} . \nabla P(\underset{\sim}{x})$$

$$= \int_{o}^{t} \nabla K_i . \nabla T(\underset{\sim}{x},\tau)d\tau + [K\nabla T(\underset{\sim}{x},P(x)] . \nabla P(\underset{\sim}{x})$$

$$= -C_1 T(\underset{\sim}{x},o) + C_2 T(\underset{\sim}{x},t) + \ell \tag{79}$$

where $\ell = \rho . \underline{L}$.

The subscript denotes the phase: i=1 is the solid and i=2 is the melted phase.

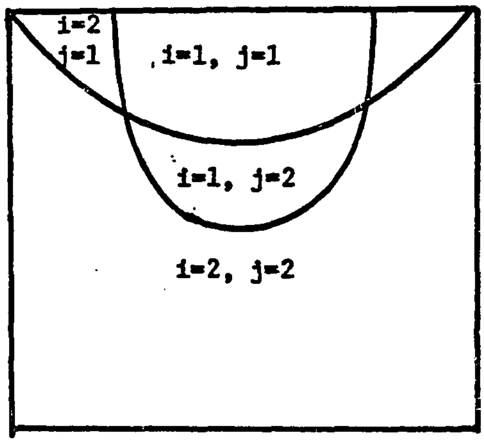

Figure 3-1 The schematic representation of a phase change on the domain (i=j=1: solid i=j=2 liquid)

The domains are determined from the melting temperature as follows

$$S(t) = \underset{\sim}{x}: \theta_t(\underset{\sim}{x}, t) < 0 \qquad (80)$$

$$L(t) = \underset{\sim}{x}: \theta_t(\underset{\sim}{x}, t) > 0 \qquad (81)$$

The governing equations can be rewritten in each case;
From the solid phase to solid phase.

$$\nabla . \nabla \theta(\underset{\sim}{x}, t) = -C_1 T(\underset{\sim}{x}, 0) + C_1 T(\underset{\sim}{x}, t) \qquad (82)$$

from the solid to the melted

$$\nabla.\nabla\theta(\underset{\sim}{x},t) = -C_1T(\underset{\sim}{x},0) + C_2T(\underset{\sim}{x},t) + \ell \quad , \tag{83}$$

from the melted to the melted

$$\nabla.\nabla\theta(\underset{\sim}{x},t) = -C_2T(\underset{\sim}{x},0) + C_2T(\underset{\sim}{x},t) \tag{84}$$

from the melted to the solid

$$\nabla.\nabla\theta(\underset{\sim}{x},t) = -C_2T(\underset{\sim}{x},0) + C_1T(\underset{\sim}{x},t) - \ell. \tag{85}$$

We can rewrite the governing equations explicitly as follows:

$$\frac{C_i}{K_i}\,\theta_t(\underset{\sim}{x},t) - \nabla.\nabla\theta(\underset{\sim}{x},t) = \ell_{ij} + C_jT(\underset{\sim}{x},0) \tag{86}$$

where

$i = j = 1$ at the solid phase

$i = j = 2$ at the melted phase

$$\ell_{ij} = \begin{vmatrix} 0 & \ell \\ -\ell & 0 \end{vmatrix}$$

The initial condition becomes

$$T(x,y,t) = \int_o^t (T_{so}(x,y,o) - Tm(y))d\tau \quad \text{in } S(t) \tag{87}$$

$$T(x,y,o) = \int_o^t (T_{Lo}(x,y,o) - Tm(y))d\tau \quad \text{in } L(t) \tag{88}$$

the boundary condition,

$$\theta(x,y,t) = \int_o^t (T_1 - Tm(y))d\tau \qquad \partial D_1 \tag{89}$$

the matching condition,

$$\theta(x,y,t) = 0 \qquad \text{on } I(t) \tag{90}$$

3-3. Finite Element Formulation

The variational formulation associated with the governing equations will use the Galerkin integral method.

$$\int_D [(\frac{C}{K}\theta_t - \theta_{x,x} - \theta_{y,y} - \ell - C.T(x,y,o)]\delta\theta dxdy = 0 \tag{91}$$

where C, K and ℓ are expressed in matrix form. After integrating the second and third terms of equation 91 by parts, we obtain;

$$\int_D [\frac{C}{K}\theta_t\delta\theta + \theta_x\delta\theta_x + \theta_y\delta\theta_y - \ell\delta\theta - C.T(x,y,o)\delta\theta]dxdy$$
$$- \int_{\partial D} (\theta_x n_x + \theta_y n_y)\delta\theta dS = 0 \tag{92}$$

Assuming that the integral equation holds in each element, the function θ can be interpolated by

$$\theta = \Sigma\theta_j N_j(x,y), \qquad \delta\theta = \Sigma\delta\theta_i N_i(x,y) \tag{93}$$

where N_i, N_j are the interpolation functions corresponding to node i,j respectively and $\theta_j, \delta\theta_i$ the values of the variable at the ith and jth node of the element.

Hence

$$\delta\theta \int_D [\frac{C}{K} (\Sigma\theta_{j,t} N_j) N_i + \theta_j N_{j,x} N_{i,x} + \theta_j N_{j,y} N_{i,y} +$$

$$(\ell + C.T(x,y,o)) N_i] dxdy = 0 \tag{94}$$

Since the function $\delta\theta_i$ is arbitrary, we have

$$\frac{C}{K} [M]\{\theta_t\} + [G^{xx} + G^{yy}] \{\theta\} = F^1 + F^2 \tag{95}$$

$$M_{ij} = \int N_i \cdot N_j \, dxdy \tag{96}$$

$$G_{ij}^{xx} = \int N_{i,x} \cdot N_{j,x} \, dxdy \tag{97}$$

$$G_{ij}^{yy} = \int N_{i,y} \cdot N_{j,y} \, dxdy \tag{98}$$

$$F_i^1 = \int \ell \cdot N_i \, dxdy \tag{99}$$

$$F_i^2 = \int C \cdot T(x,y,o)N_i \cdot dxdy \tag{100}$$

The next step in the development is to discretize the finite element formulation with respect to time by the finite difference scheme (refer to Chapter II).

Thus we have

$$[[M(\frac{C_i}{K_i})_{n+1} + \Delta t.s.[K]]\{\theta\}_{n+1} = [[M(\frac{C_i}{K_i})_n - \Delta t.(1-s).[K]]\{\theta\}_n$$

$$+ \Delta t[s.\{F_1(\ell_{ij})_{n+1} + F_2(C_j)_{n+1}\} + (1-s)\ \{F_1(\ell_{ij})_n$$

$$+ F_2(C_j)_n\}] \tag{101}$$

where $\frac{C_i}{K_i}$, ℓ_{ij} in the bracket indicates the domain corresponding to each time iteration.

The time dependent, one-dimensional conductive moving boundary model developed herein is employed to determine the effect of latent heat on the solidification of magma with migration. The convective moving boundary model, which includes the convection effect, will be developed to investigate the possibility of upward migration of a magma body in Chapter 5.

CHAPTER IV

A COMPARISON OF CONDUCTION MODEL VERSUS FREE CONVECTION MODEL IN THE HEAT DIFFUSION OF GEOTHERMAL RESERVOIR

4-1. Numerical Model

The part played by convection in the heat diffusion of the geothermal reservoir has been a matter of speculation. Jaeger (1964) stated that little evidence of convection exists in basic sheets less than 30 m. thick but that convection does take place in the stock-like bodies of magma more than 30 m. in diameter. The phenomenon of interest can be simulated by the motion of a laminar incompressible, Boussinesq, Newtonian fluid (hot magma) confined in cold country rock. The physics of the problem plays a crucial role in constructing a reasonable model. The finite element method is no exception. In this study the convection is generated by a change of density due to the difference in temperature between hot magma and cold country rock. The problem under consideration is as follows; The geothermal reservoir is assumed to be a rectangular slab of magma 100 m. wide and 50 m. high located 100 m. below the surface (Figure 4-1). The magma was initially intruded over the melting temperature into the country rock which had been subjected to a geothermal gradient. In this model the effect of the geothermal gradient can be disregarded because the temperature difference by geothermal gradients at that depth is negligibly small. The interface between the magma and the country rock is assumed to be impermeable for flow but not insulated for temperature. The surface and vertical wall of the country rock is specified by zero temperature and the lower one by zero temperature gradients. To simplify modelling the physical parameters of the model are given in Table 4-1 and are representative of acidic igneous rocks [Clark (1966), Stein et. al, (1981)].

TABLE 4-1

Physical Parameters of the Model

Parameter	Value	Description
K	0.01 cal/cm sec C	Thermal Conductivity
C	0.25 cal/gm C	Specific Heat
L	80 cal/gm	Latent Heat of Fusion
ρ	3.0 gm/cm^3	Density
g	1000 cm/sec^2	Acceleration of Gravity
ν	10^8 cm^2/sec	Viscosity of Magma
β	3.0×10^{-5} deg C^{-1}	Coefficient of Thermal Expansion
γ	3.6 deg C/Km	Clapeyron Gradient

4-2. Numerical Procedure

The finite element equations are expressed by a set of algebraic equations reduced from a continuous problem described by partial differential equations to a discrete problem. The element equations in (25) - (35) are assembled to obtain the associated global algebraic equations through the appropriate summation of equations for nodes common to adjacent elements.

In problems of interest where both the flow and heat equations are strongly coupled, solution algorithms for the equations must have an iteration procedure because of nonlinearity of coupling terms. The heat and flow equations are solved in a cyclic manner beginning with the heat equation. The velocities for the first iteration are assumed to be zero and the matrix coefficients are computed. Then, the heat equation is solved for the temperature. The velocities are obtained using the computed temperature as the force terms for the flow equations and one cycle of iteration is completed. This process is repeated until the solutions at any two successive iterations satisfies with a specified convergence criterion;

$$\sqrt{\frac{(U_{new} - U_{old})^2 - (V_{new} - V_{old})^2}{U^2_{new} + V^2_{new}}} < 0.1\%$$

where U is a horizontal velocity, and V is a vertical velocity. An appropriate time step to insure convergence and to avoid spurious oscillations in the solution is an important consideration. The θ family approximations will be tested as a time stepping procedure for solutions of the time dependent conduction model. Figure 4-2 shows that the Gälerkin scheme ($\theta = 2/3$ in Equation 43) gives a smoother time approximation of temperatures than Crank-Nicolson's ($\theta = 1/2$) even at the point where temperature changes most rapidly. The use of numerical integration is desirable to evaluate various matrix coefficients in equations (25) → (35) with curved boundaries. In addition, the "reduced integration" required by the penalty method can also be obtained by using numerical integration. Details of the methodology are given in Appendix I. For further theoretical discussion of the reduced integration in the penalty method refer to Zienkiewicz (1977), and Reddy (1979-a). In problems of interest where temperature is a more dependent variable than pressure, the penalty parameter $\varepsilon = 10^{15}$ is shown to give accurate results for this particular model. The actual solution of the algebraic equations is accomplished by a Gaussian Elimination. All of the computation is carried out on an IBM 370/158 computer in double precision.

4-2-1. Arrangement of Mesh. The arrangement of mesh by physical understanding is a key step in the approximation of possible flow and temperature patterns for the problem. The domain at hand is discretized using a 25 x 16 mesh of quadrilateral elements. The mesh spacing is graded finely in order to provide increased resolution near the interface between the hot magma and cold country rock. The elements and nodes are numbered from left to right and from the lower to the upper. (Figure 4-3).

4-2-2. Plotting. The program contains a plotting subroutine that allows finite element meshes, nodal and elemental numbering, contour maps for isotherms and streamlines to be drawn. The description of those methods will be omitted since the generation of plotting follows standard procedures.

4-3. Numerical Results and Discussion

The validity of finite element formulation for unsteady thermal flow is checked by comparing finite difference solutions (Ahern, 1981) with finite element results. Details of the comparison are given in Appendix III.

In this section numerical results for natural convection problems are presented to demonstrate the effect of convection on the heat diffusion of magma. The finite element conduction solutions are compared with the finite element free convection results to discover how convection influences the temperature profile. The velocity field of a magma depends on the rheological characteristics of the fluid, thermal forces, and viscous forces. To simplify the analysis, density differences arising from the composition differences are disregarded. There is a critical value for the onset of convection in hot fluid confined by cold country rock. The critical value is conventionally represented by the Rayleigh number which is considered to be the ratio of buoyancy forces developing convection to viscous forces preventing flow. The magnitude of the Rayleigh number depends on several variables: the viscosity (ν), the thermal expansion coefficient (β), the diffusivity of the fluid (α), and the size of the body and the temperature difference.

Below the critical value for the onset of convection, the temperature distribution is simply governed by conduction with no movement of flow. Above that value, the temperature distribution begins to be influenced by fluid motion. Basically, the larger the value, the more vigorous the convection of the fluid.

Since the applicability of the model at hand is strictly limited to a laminar flow, the turbulent flow of the magma is beyond the scope of this investigation. Spera (1980) indicated that convection does not occur until the Rayleigh number reaches about 1500. Lipps (1971) showed an appropriate criterion for the onset of turbulence is a modified Rayleigh number $[(D/L)^3 * Ra]$ which is greater than about 10^4. D/L is called an an aspect ratio where D is the height and L is the length of the liquid (Figure 4-1). The onset of turbulent flow is known to depend upon the aspect ratio as well as the Rayleigh number. Also, the critical value of the modified Rayleigh number has a wide range which depends upon the boundary conditions and the definition of turbulence. In the present model the Rayleigh number ranges from 10^3 to 10^5 and a Prandtl number 10^8. Turbulent flow seems to be prevented because of large viscosity even if it exceeds the critical modified Rayleigh number. The results are presented in graphic form. These show the development of the patterns of isotherms and streamlines.

Figures 4-4-B to 4-9-B show the development of isotherms by conduction as time advances. Figures 4-4-A to 4-9-A show the temperature field with convection motion at each time increment. Of special interest areFigures 4-8 and 4-9 which show that the convection model diffuses the heat more rapidly than conduction does.

The convection motion begins due to buoyancy forces produced when the temperature variations are introduced through temperature differences between hot magma and cold country rocks (Figure 4-10): Hot liquid tends to rise near the center, cold to fall along the cold boundary. In other words, thin thermal boundary layers emerge on the interface between the magma and the country rock. Thin thermal boundary layers, which become cold because of loss of heat transfered into cold country rocks, fall along the wall.

Therefore, the temperature gradients at the upper boundary of magma are larger than those at lower boundaries (Figure 4-5-A). A series of thermal layers will emerge as the boundary layers convect in a circular motion. The isotherms distort progressively as the convective effects become more apparent (Figures 4-6-A, 4-7-A). As the speed of convective currents increase, the cell breaks into two parts (Figure 4-11). A secondary cell broken from the original represents a set of streamlines with anticlockwise circulation which occurs in the upper central region of the magma (Figures 4-11, 4-12, 4-13). The speed of convective motion decreases gradually with decreasing temperature Then, secondary cells disappear (Figure 4-14) and the original patterns of streamlines come back (Figure 4-15), when the velocity of the convection flow decreases with time. The patters of streamlines remain unchanged until the difference of temperature between the magma and the country rock is terminated. In fact, the magma will be solidified by the freezing temperature long before the temperature differences are eliminated. However, similar results would be obtained if the magma had been considerably hotter than the melting temperature upon emplacement. In unsteady free convection problem the magma is assumed to be kept in a liquid phase even when the temperature in the magma goes below the melting temperature.

The effect of convection is shown by comparing the conduction temperature profile with the convection temperature profile along the representative lines A-A' and B-B' in Figure 3 (Figure 4-16). Figure 4-15 shows that the temperature distribution by the convection model is distorted by the fluid motion, while the isotherms of the conduction are symmetrical to the representative line A-A'.

In summary, the rate of heat diffusion into country rock by the convection model exceeds the value of conduction. The effect of convection on the motion of magma within the batholith gives larger temperature gradients at the upper boundary magma than those at lower ones. There is a possibility that the heat transported upward by thermal convection melts the roof of magma while freezing its lower parts when the effect of latent heat is taken into consideration.

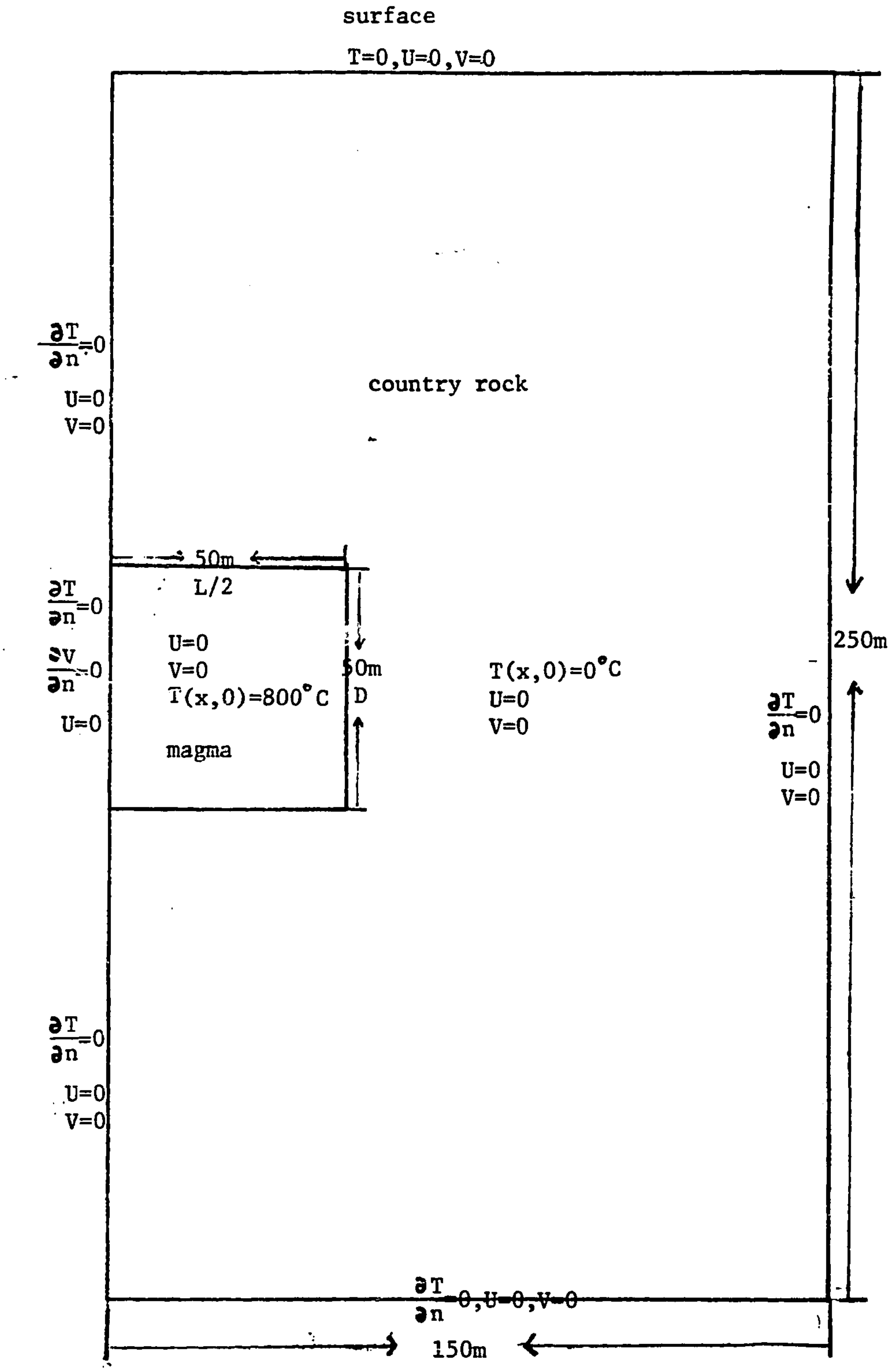

Figure 4-1. A schematic representation of the problem under investigation, showing only right half.

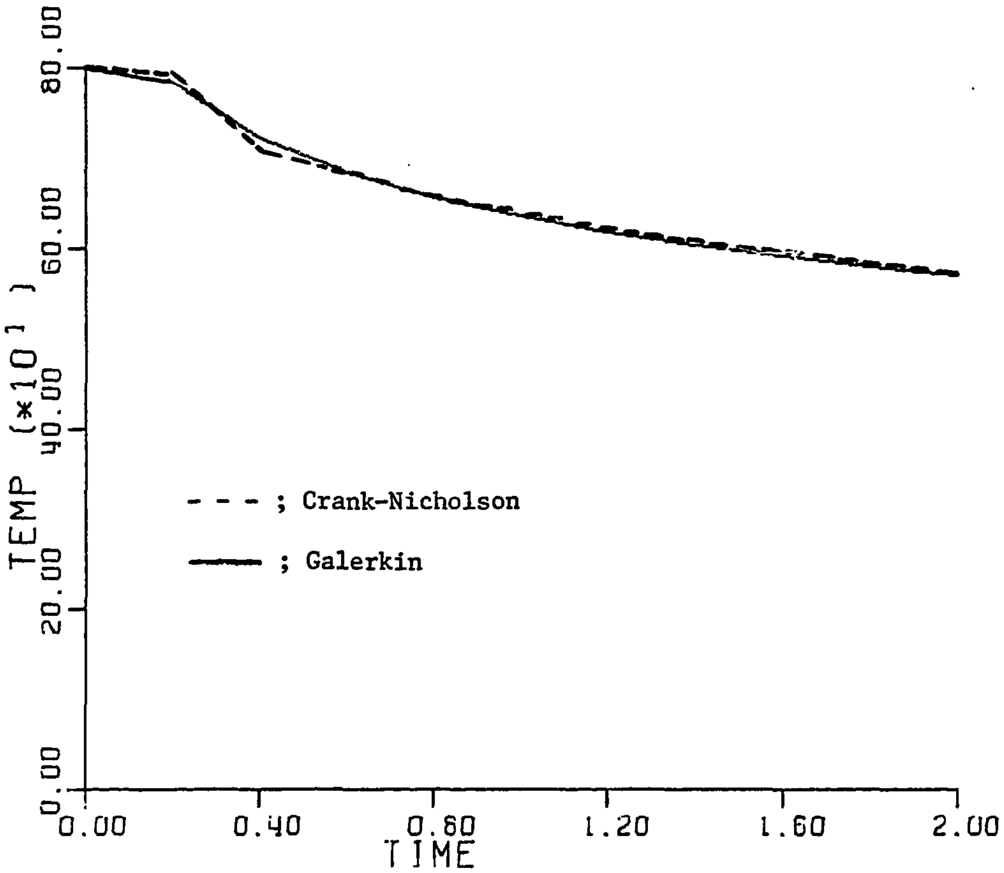

Figure 4-2-a.Temperature change with time at node 200.
Note the instability with the Crank-Nicholson schemes.

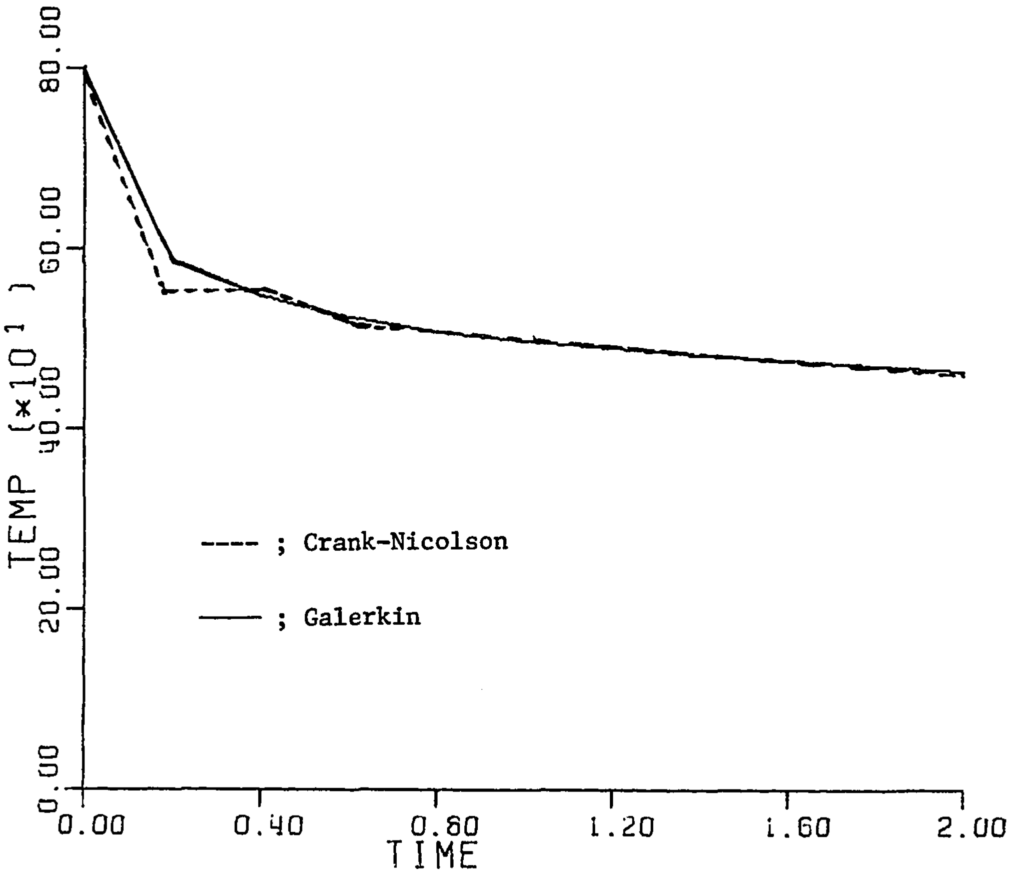

Figure 4-2-b.Temperature change with time at node 277

Figure 4-2. The graphic comparison between Galerkin scheme (θ=2/3) and Crank-Nicolson scheme (θ=1/2) of θ family time approximation at nodes 200,277 where temperature changes sharply (Galerkin: hard line,Crank-Nicolson:dashed line).

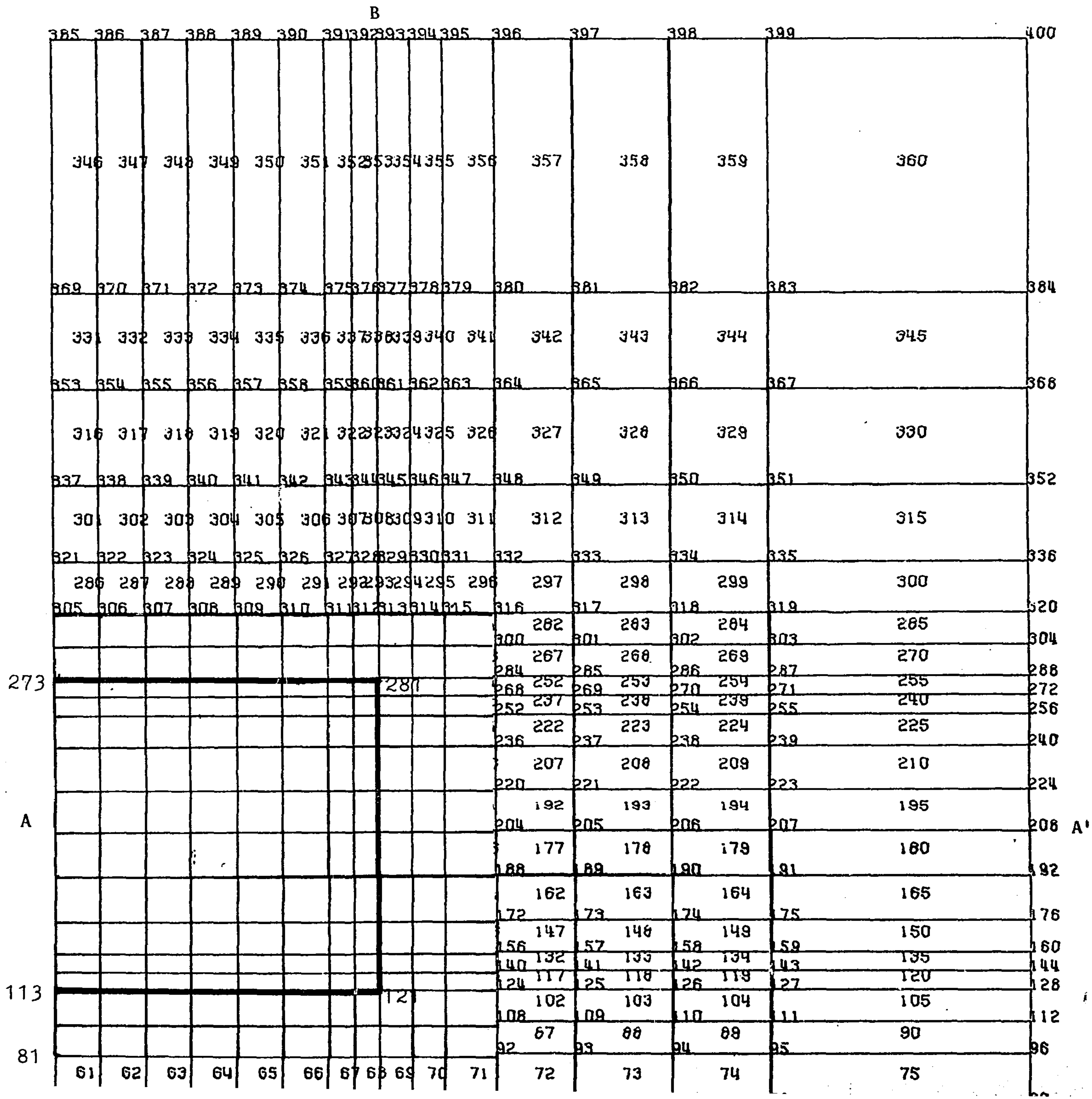

B
A
A'
273
113
81
281
121

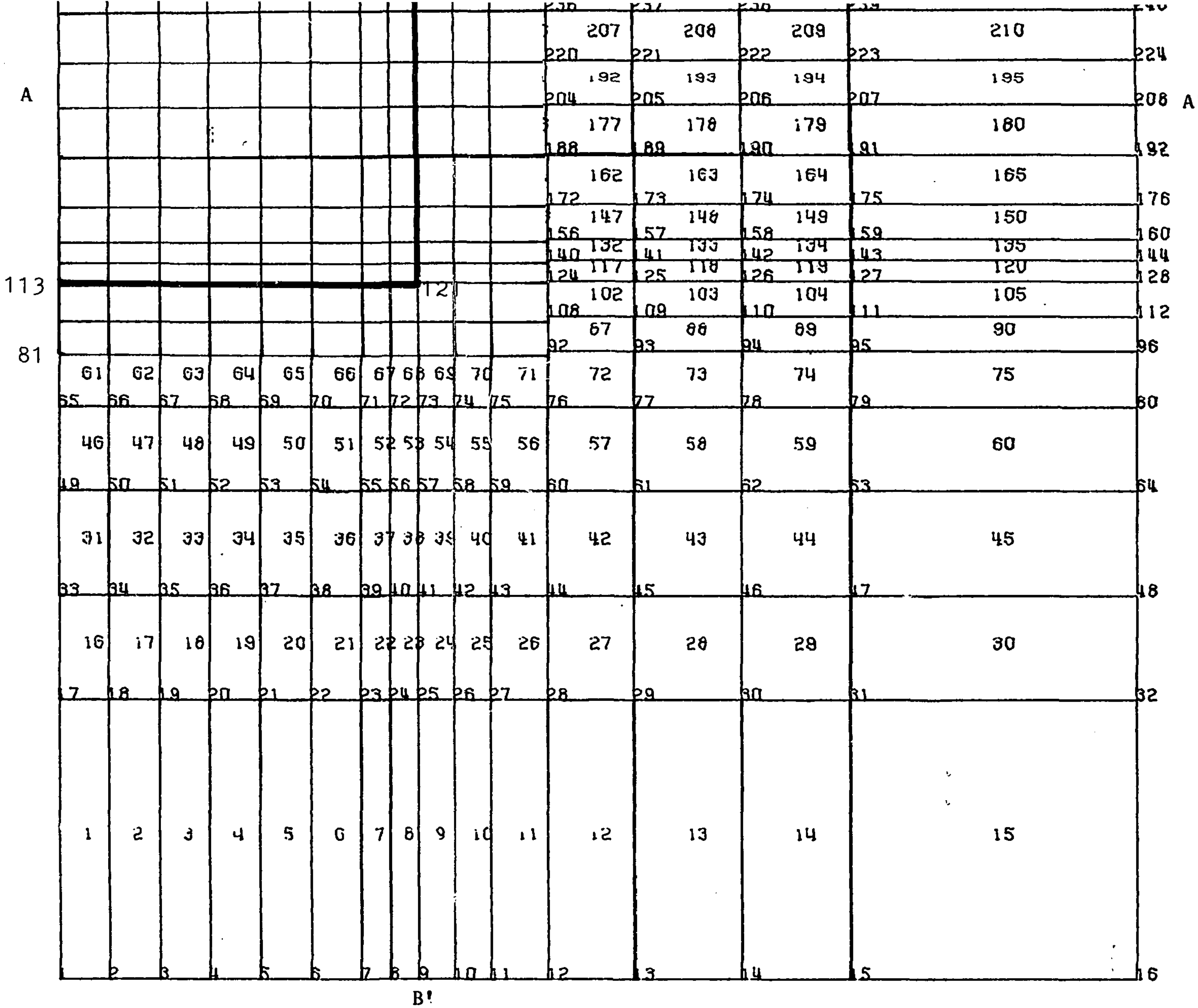

Figure 4-3. Elements (numbered within boxes) and nodes (numbered on corners) for the magma body model. The variable grid spacing is a powerful advantage of the finite element method that allows increased resolution where needed with a relatively small numbered of nodes.

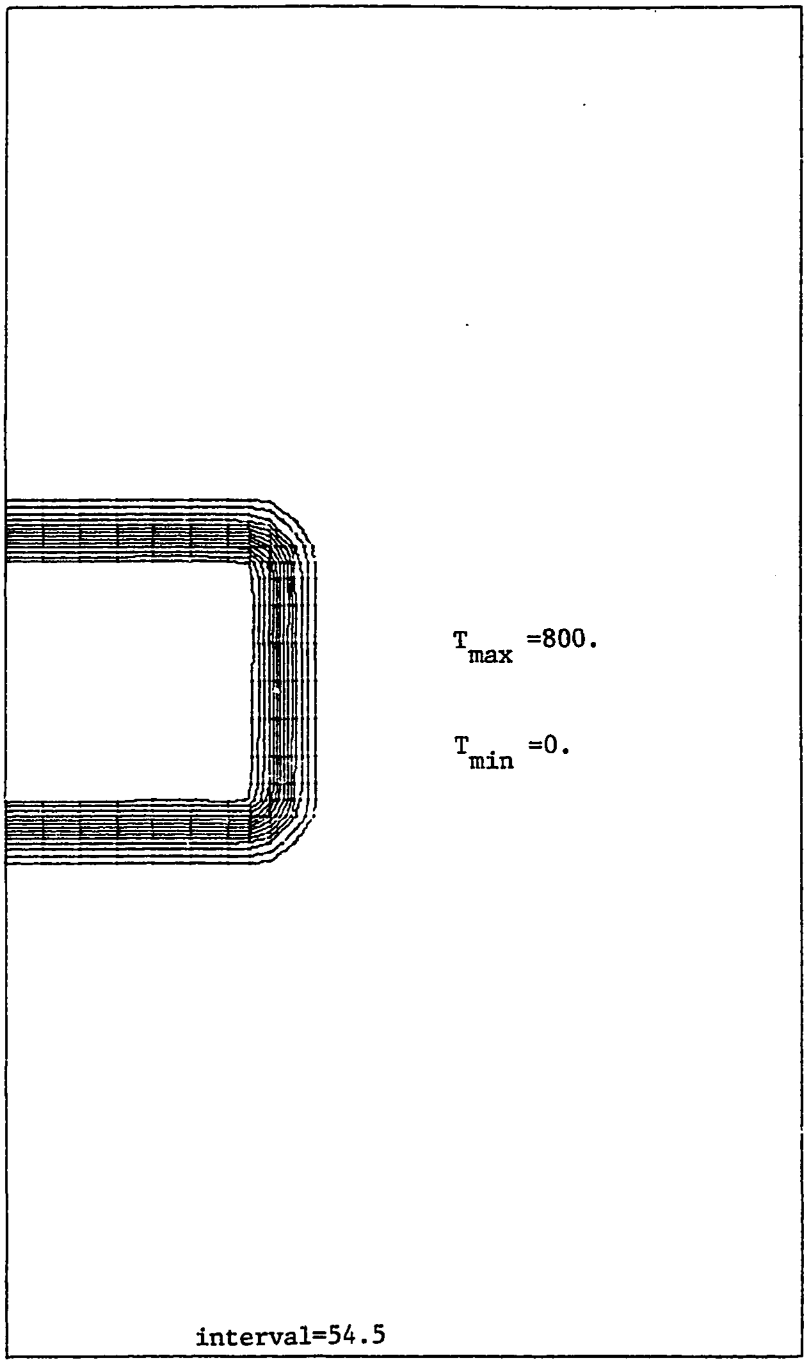

Figure 4-4. Temperature distribution after 0.2 year.

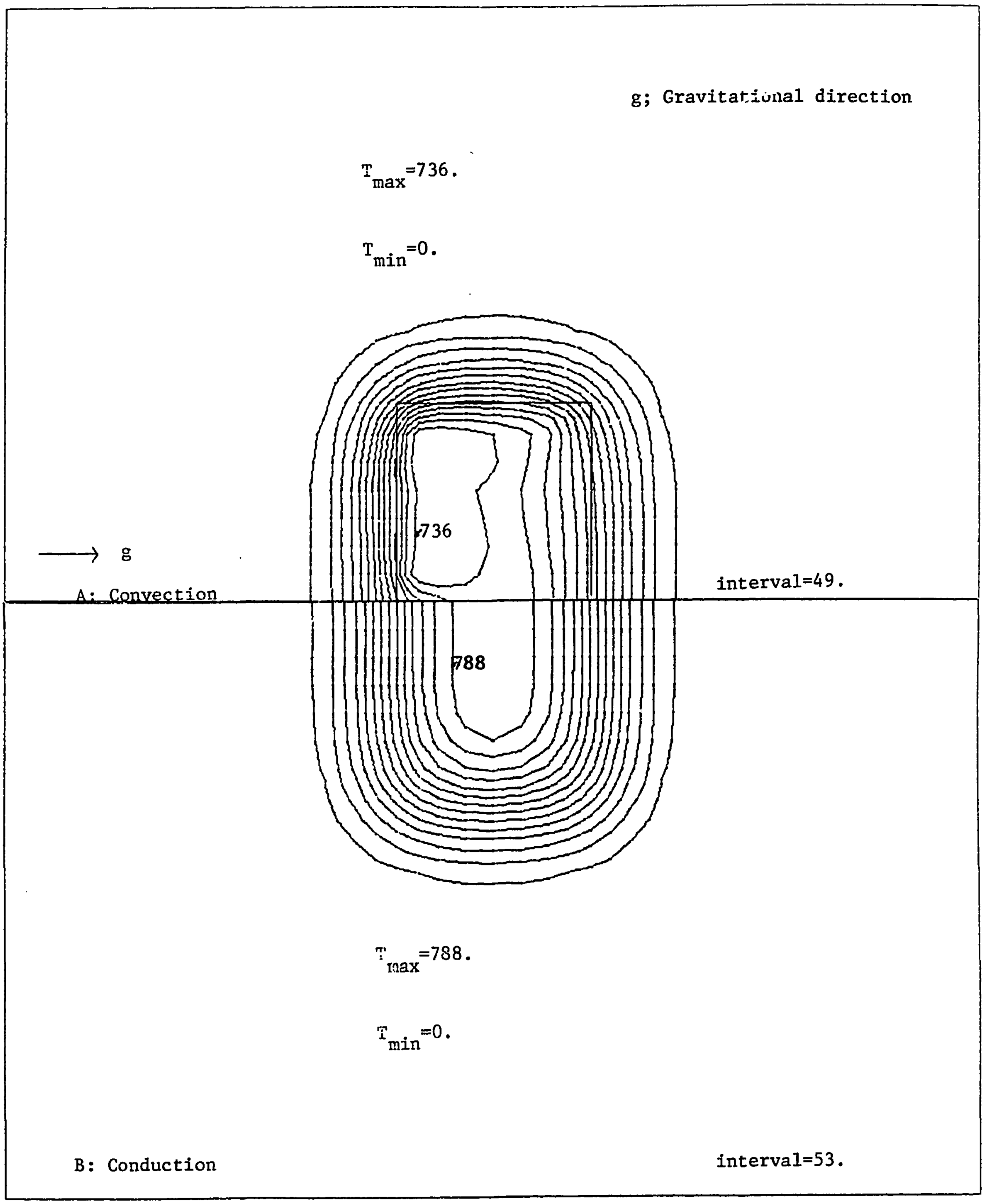

Figure 4-5. Temperature distribution after 2.2 years from (A) Convection model, (B) Conduction model. Note that the temperature gradients are concentrated at the upper portion of the magma body.

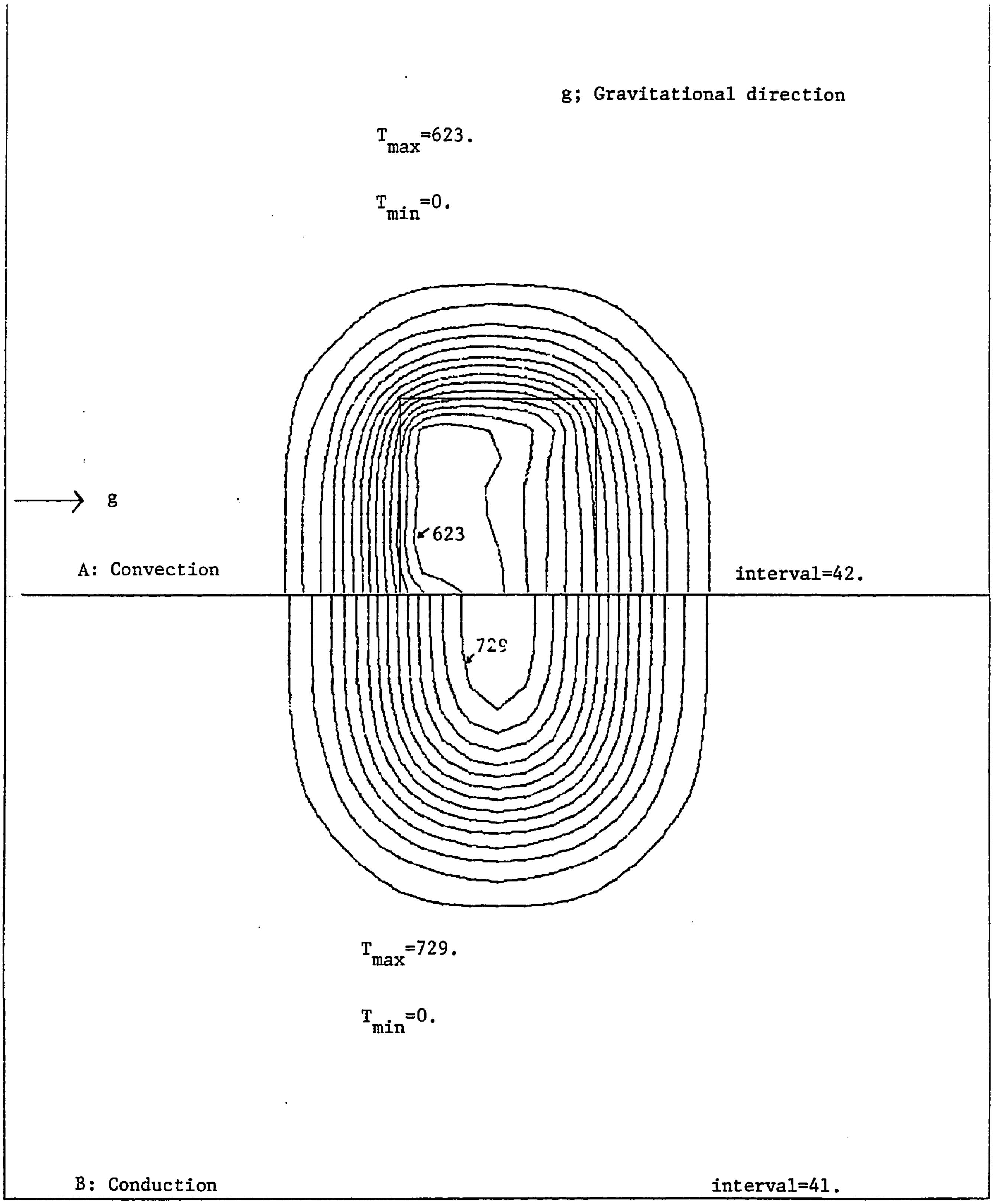

Figure 4-6. Temperature distribution after 4.2 years from (A) Convection model, (B) Conduction model.

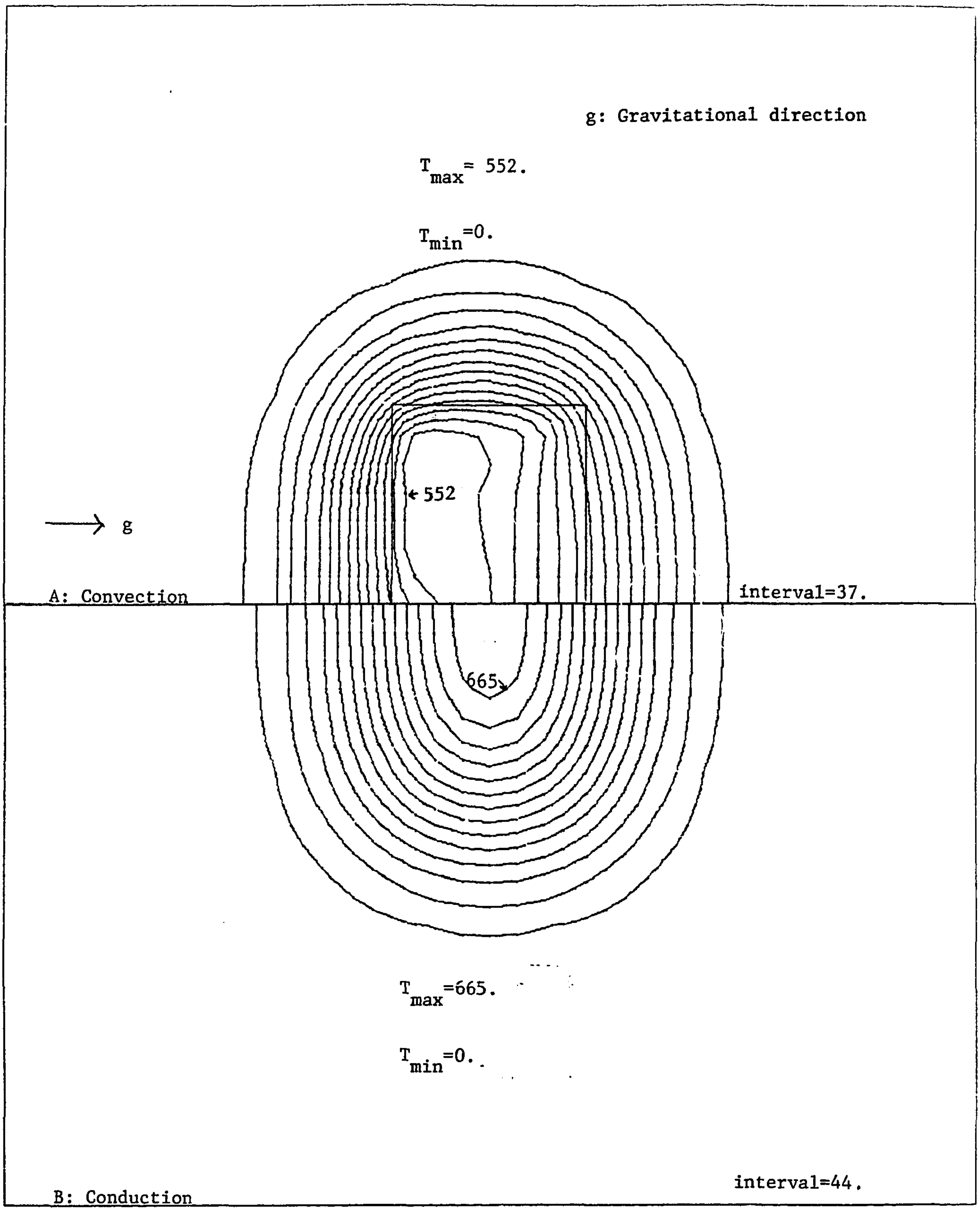

Figure 4-7. Temperature distribution after 6.2 years from (A) Convection model, (B) Conduction model.

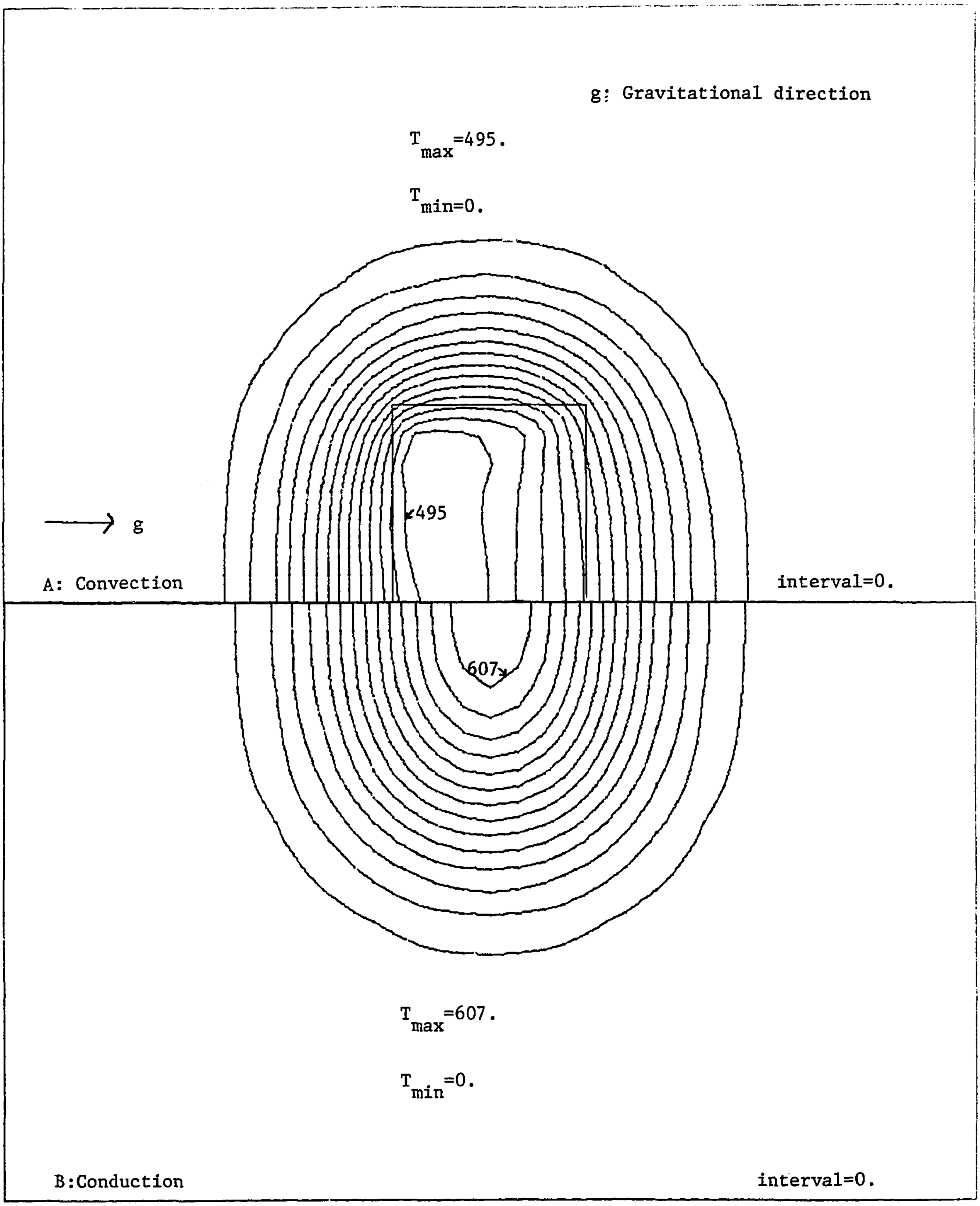

Figure 4-8. Temperature distribution after 8.2 years from (A) Convection model (B) Conduction model.

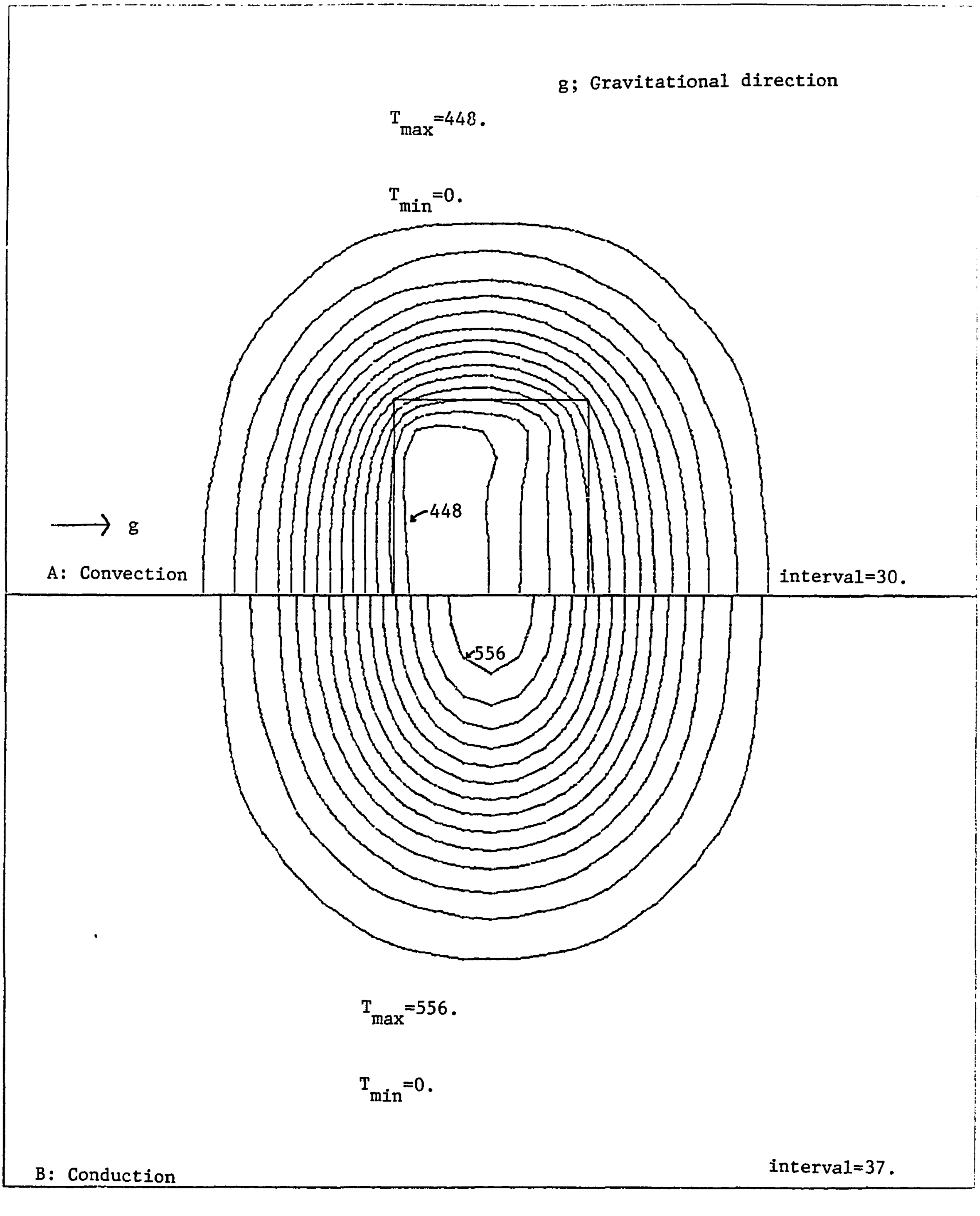

Figure 4-9. Temperature distribution after 10.2 years from (A) Convection model,(B) Conduction model.Note that convective heat transfer exceeds conductive heat transfer into contry rock from magma.

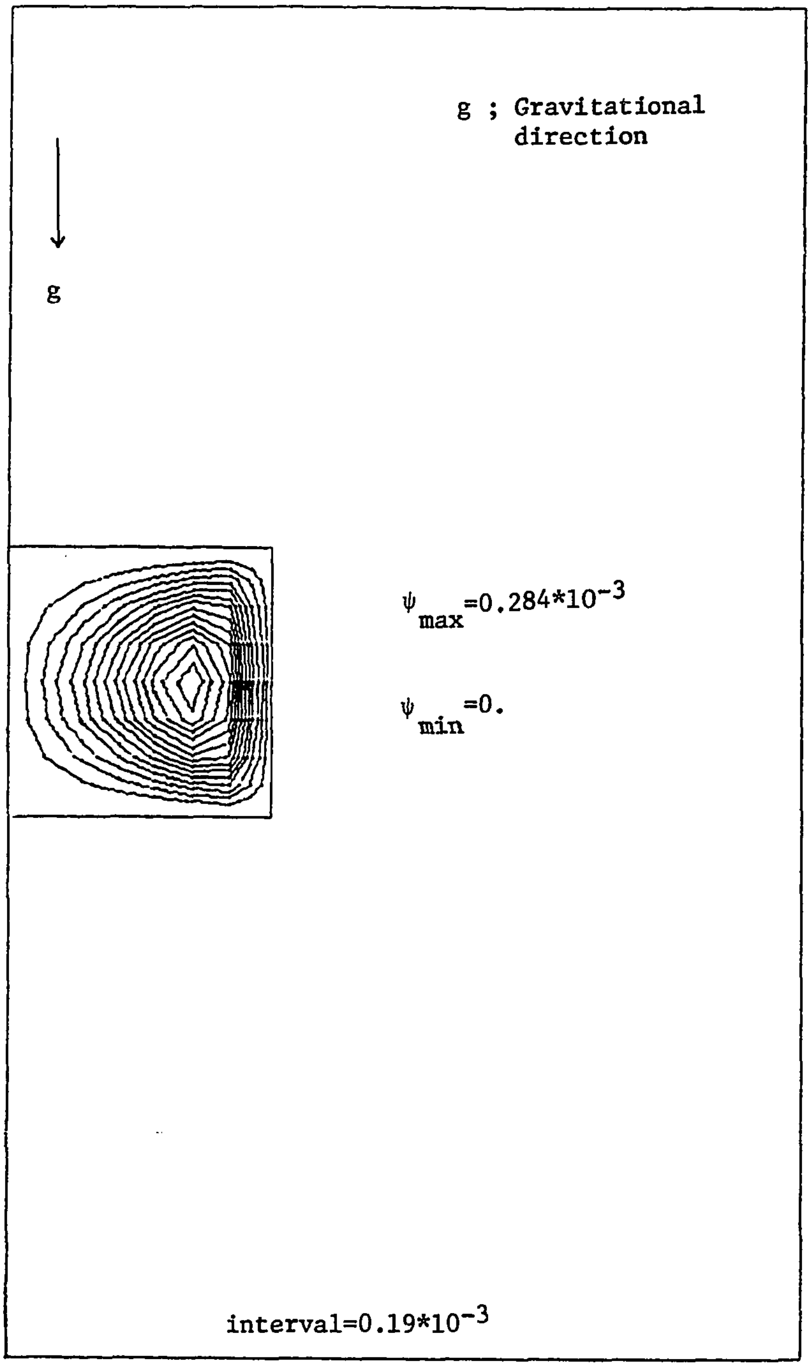

Figure 4-10. Stream lines for convection model after 0.2 year Note that flow is downward at the right edge of the magma body.

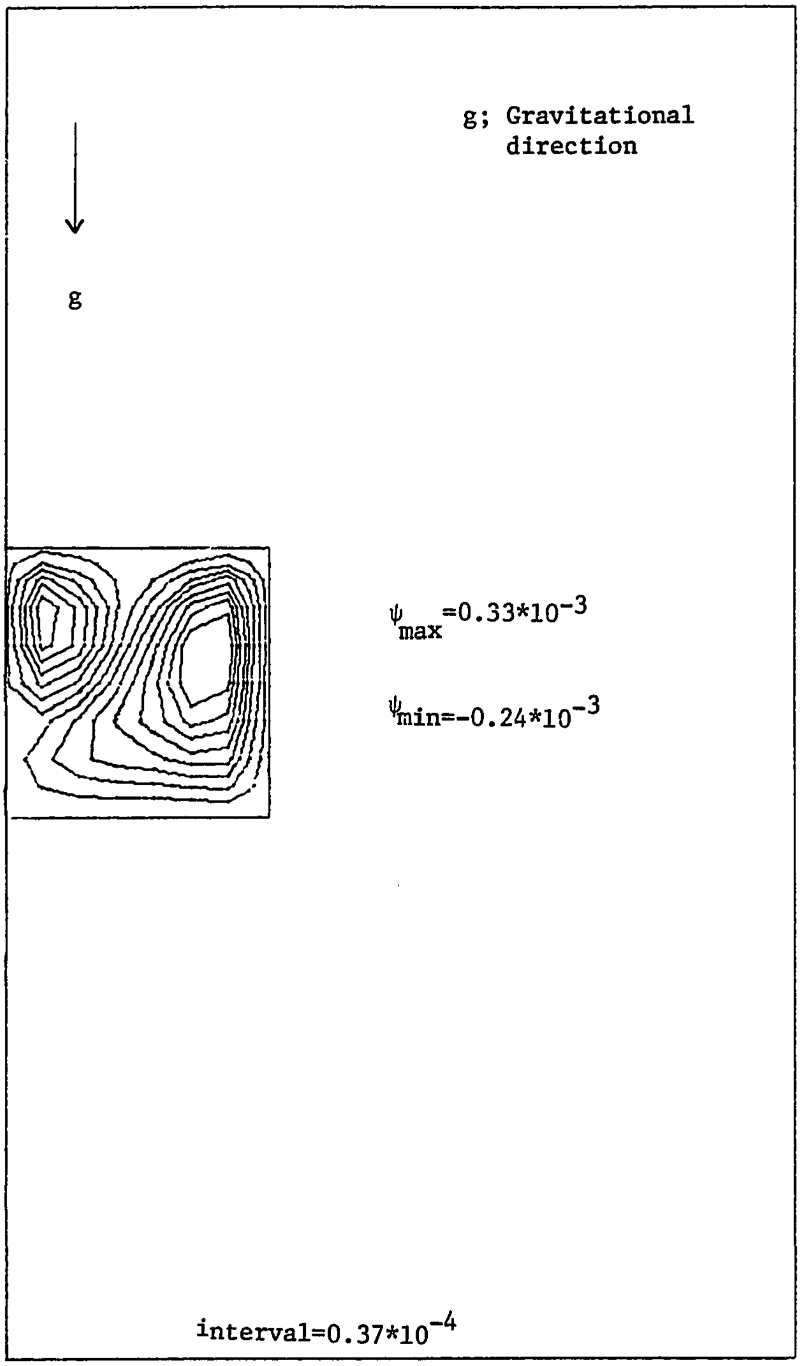

Figure 4-11. Streamlines for convection model after 2.2years Note that the secondary convection cell in the upper left portion of the magma body.

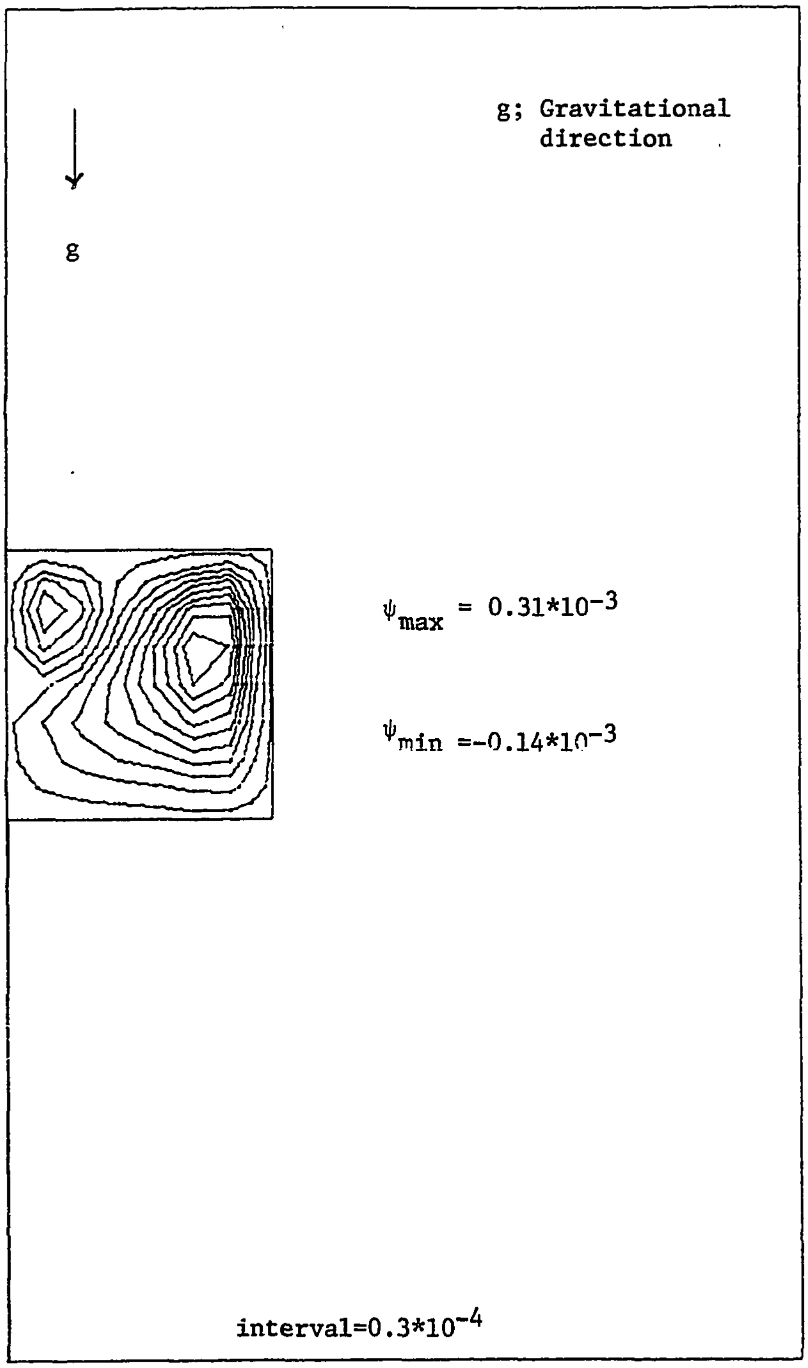

Figure 4-12. Stream lines after 4.2 years.

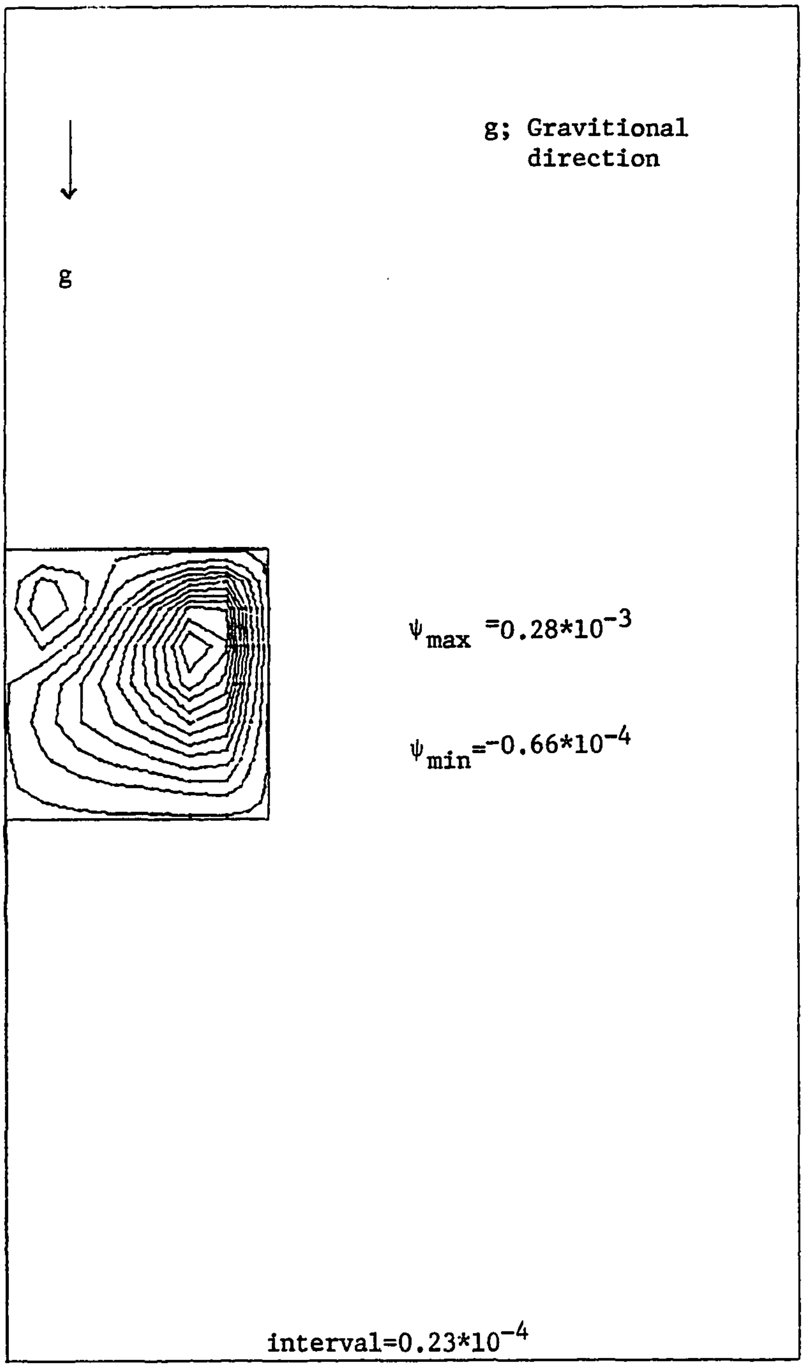

Figure 4-13. Stream lines after 6.2 years.

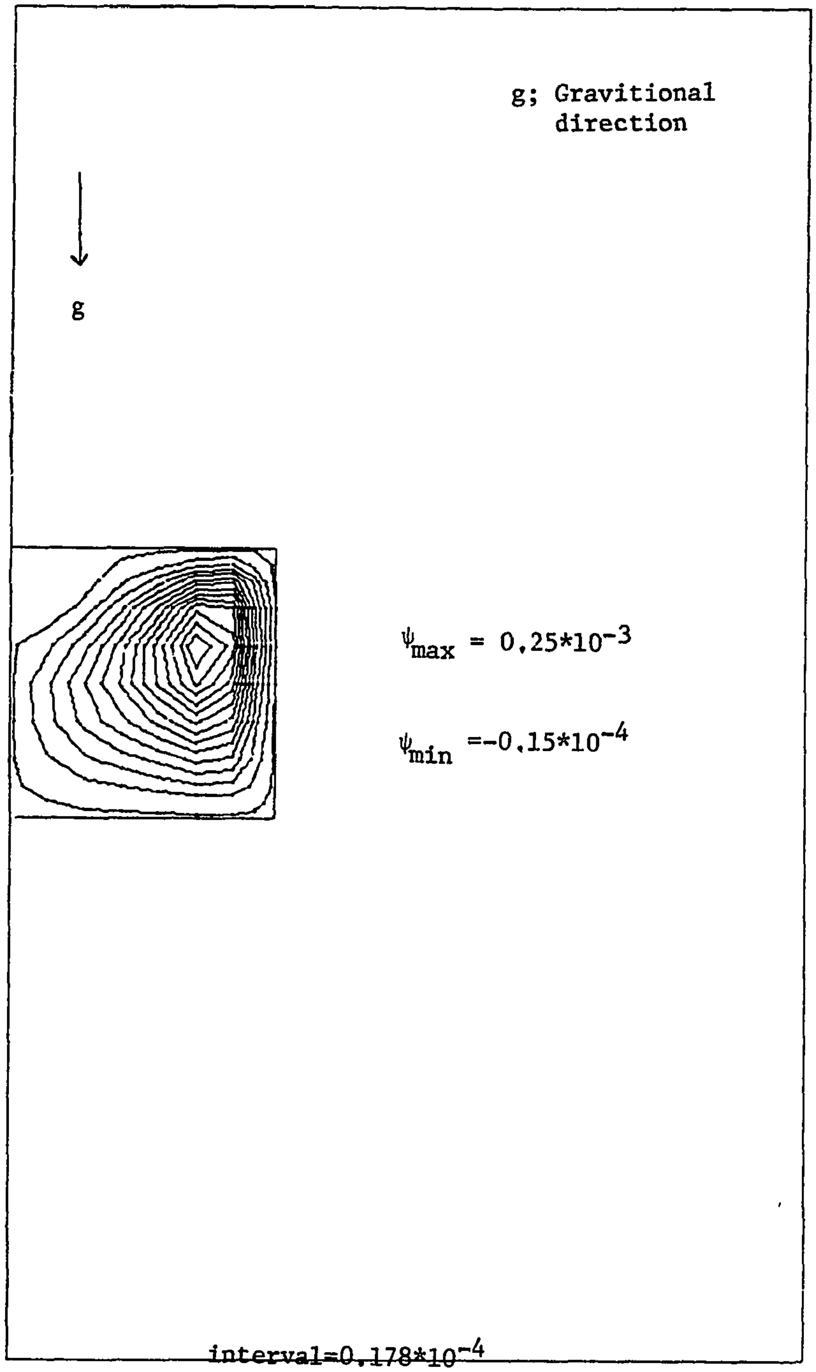

Figure 4-14. Stream lines after 8.2 years. Note the secondary cell is disappeared.

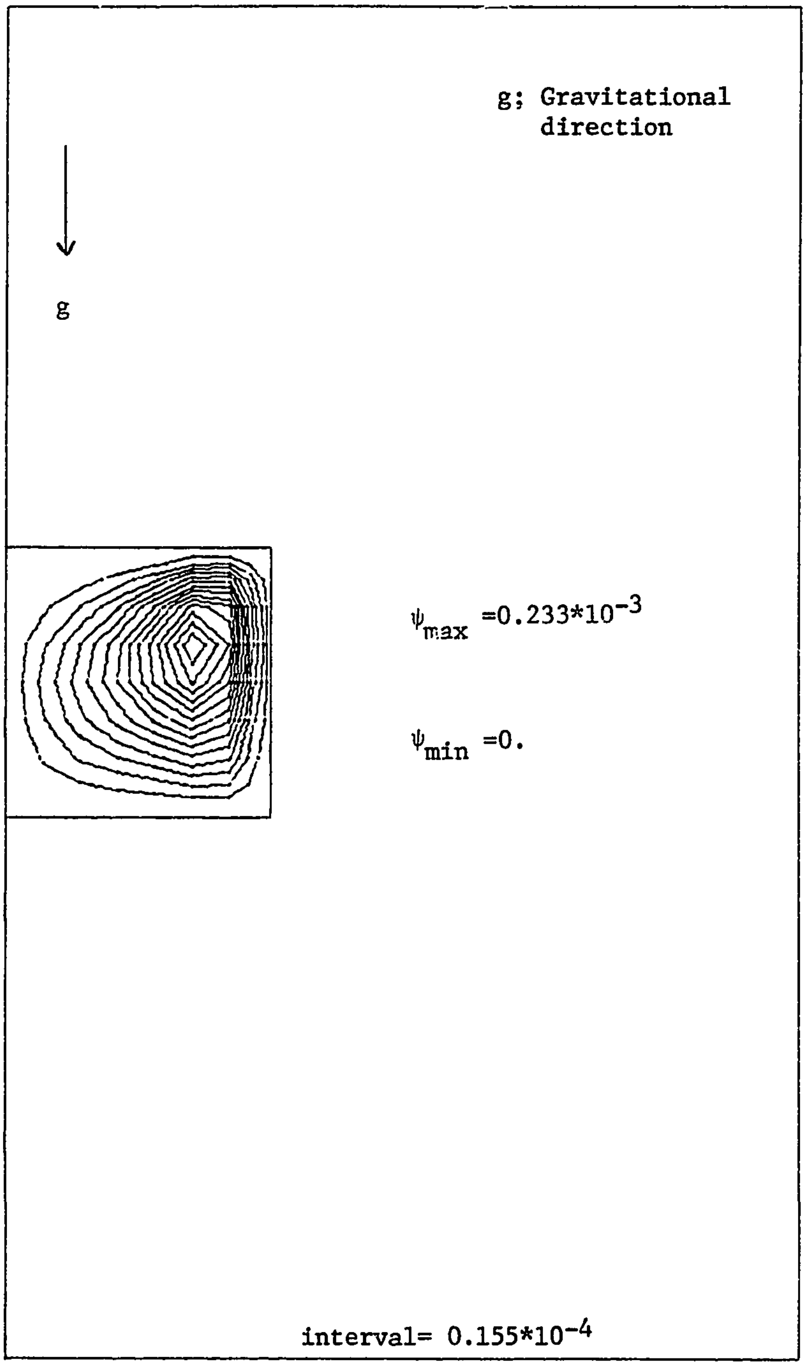

Figure 4-15. Stream lines after 10.2 years. The convection motion reaches the steady state.

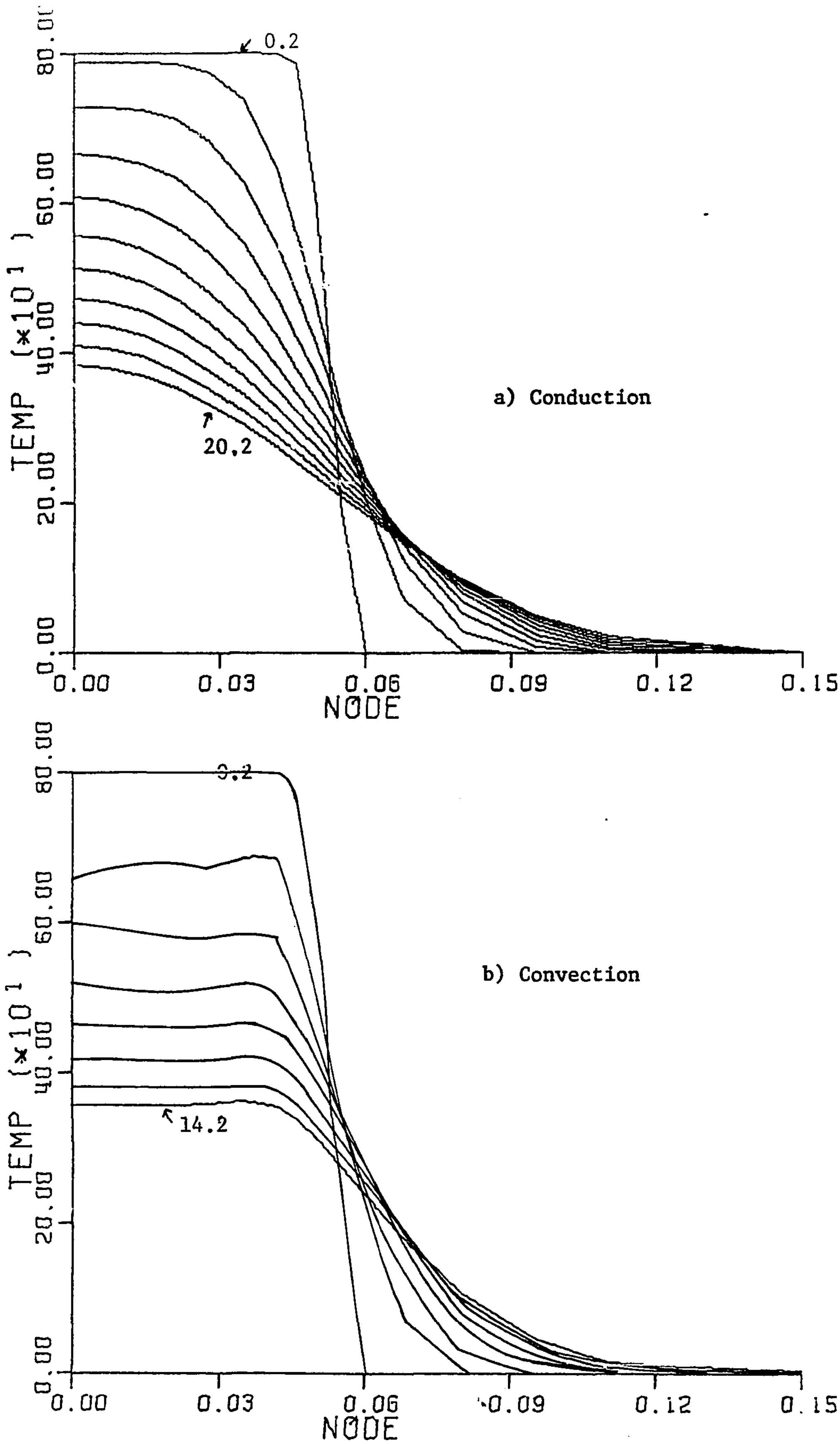

Figure 4-16-A. Temperature distribution along the representative line A-A' at the different time steps a) Conduction b) Convection (time step = 0.2 year).

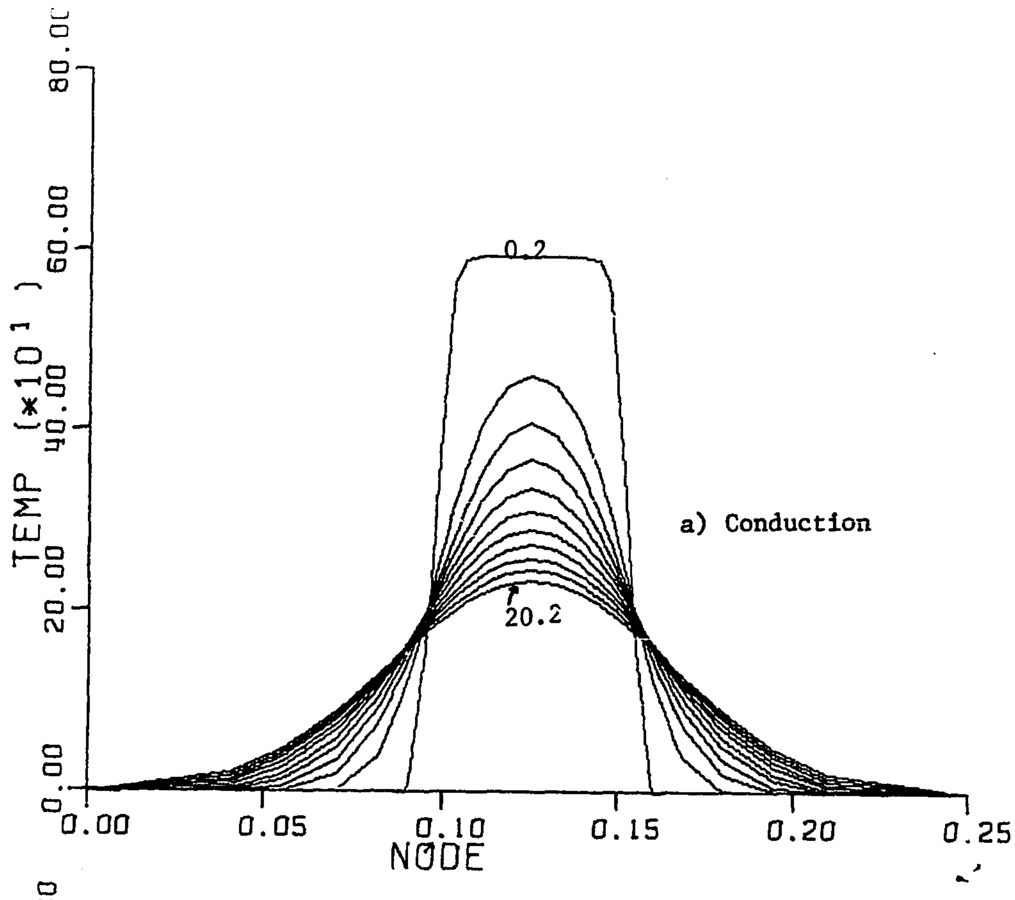

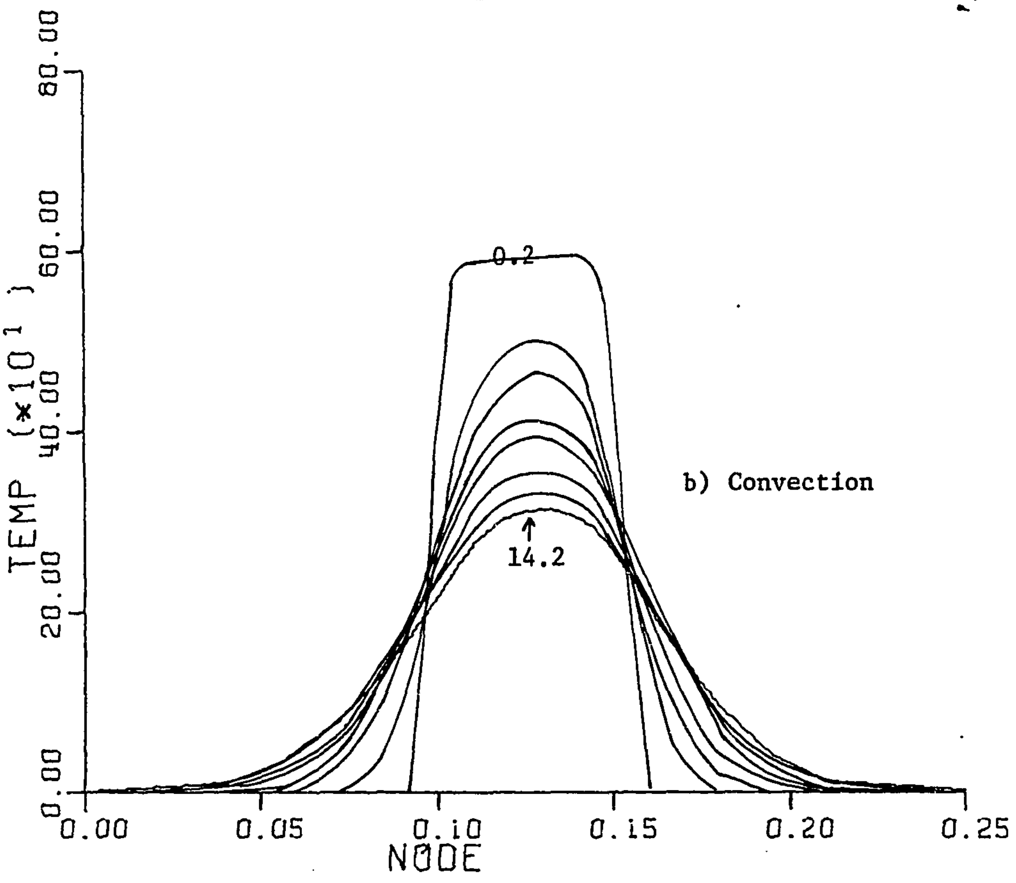

Figure 4-16-B. Temperature distribution along the representative line B-B' at the different steps.(time step = 0.2 year)

CHAPTER V

EFFECT OF THE LATENT HEAT ON THE MIGRATION OF MAGMA

5-1. Convective Moving Boundary Formulation

To analyze the migration of the magma after the emplacement of the the magma into the country rock, two complicated mechanisms are associated with each other. One is free convection which is employed to determine the distribution of the velocity and temperature within the magma and the distribution of the temperature surrounding the magma chamber. The free convection was investigated numerically in the previous chapters. The other mechanism is a moving boundary mechanism used when the position of the solid-liquid interface is determined by the difference of heat flux across it. The conductive moving boundary formulation, which is developed in Chapter 3, is used to determine the effect of the latent heat on the solidification of the magma without convection.

From the free convection model we have learned that the convection motion of the liquid within the batholith results in larger temperature gradients at the top of the magma than at the bottom. This convective motion inhibits the solidification of the upper part of the magma until the freezing front which originated at the bottom reaches the top.

In order to investigate the possibility of upward migration of a magma body, we must develop the convective moving boundary model. This model has an energy equation which includes a convective term to govern the liquid domain. To my knowledge, the moving boundary model, which takes the convective effect into consideration, is the first approach of this type to the Stefan problem. In the present model the moving boundary distinguishes the domain where convective heat transfer occurs from the domain where conductive transfer takes place. In other words, the governing equation (56) remains unchanged when the domain is solid, but the governing equation on the liquid domain must include a convective term, which is the energy equation.

$$C_i(T_t + UT_x) = \nabla \cdot K_i \cdot \nabla T \qquad \text{in } M(t) \qquad (56')$$

If the convective term in equation (56') keeps constant, the energy equation (56) associated with discontinuous temperature gradients can be transformed to the equations with continuous variables defined by Duvaut.

Since the governing equation of the solid domain (conduction equation) is transformed in Chapter 3, the transformation of the energy equation governing the liquid domain is treated as follows:
First of all, the equation 56' is transformed by a new temperature variable defined in equation 64 to satisfy principles of Duvaut's transformation.

$$C_i\ (\dot{T}_t + U(\dot{T}_x + A)) = \nabla \cdot K_i \cdot \nabla\dot{T}$$

where $A = \frac{\rho \cdot g}{\gamma}$ since the first derivative of the melting temperature Tm with respect to depth is constant. The primes on the temperature are omitted for convience.

If the phase changes from liquid to liquid, the first derivative of θ defined in equation 74 is

$$\nabla\theta(x,t) = \int_o^t \nabla \cdot K_1 T(x,\tau)d\tau$$

the second derivative of θ is

$$\begin{aligned}
\nabla \cdot \nabla\theta(x,t) &= \int_o^t \nabla \cdot \nabla K_1 T(x,\tau)d\tau \\
&= C_2 \int_o^t (Tt + U(T_x + A))d\tau \\
&= -C_2 T(x,o) + C_2 T(x,t) + C_2 \int_o^t U(T_x + A)d\tau \qquad (102)
\end{aligned}$$

where the convective term U denotes the vertical velocity in the one dimensional system.

If the phase change goes from solid to liquid, we have

$$\theta(x,t) = \int_o^{p(x)} K_I \cdot T(x,\tau)d\tau + \int_{p(x)}^t K_2 \cdot T(x,\tau)d\tau$$

the first derivative of θ is,

$$\begin{aligned}
\nabla\theta(x,t) &= \int_o^{p(x)} K_I \cdot \nabla T(x,\tau)d\tau + K_1 T(x,p(x))\Big|_S \cdot \nabla p(x) \\
&\quad + \int_{p(x)}^t K_2 \nabla T(x,\tau)d\tau - K_2 T(x,p(x))\Big|_L \cdot \nabla p(x) \\
&= \int_o^t K_1 \nabla T(x,\tau)d\tau
\end{aligned}$$

since the temperature T is zero on the solid-liquid interface.

The second derivative of θ is,

$$\nabla \cdot \nabla\theta(x,t) = \int_0^{p(x)} \nabla K_1 \cdot \nabla T(x,\tau)d\tau + K_1 \cdot \nabla T(x,p(x))\Big|_S \cdot \nabla p(x)$$

$$+ \int_{p(x)}^{t} \nabla K_2 \cdot \nabla T(x,\tau)d\tau - K_2 \cdot \nabla T(x,p(x))\Big|_L \cdot \nabla p(x)$$

$$= \int_0^{p(x)} C_1 \cdot T_t d\tau + \int_{p(x)}^{t} C_2(T_t + U(T_x + A)d\tau + \ell$$

$$= C_1[T(x,p(x)) - T(x,o)] + C_2[T(x,t) - T(x,p(x))]$$

$$+ C_2 \int_{p(x)}^{t} U (T_x + A) d\tau + \ell$$

$$= -C_1T(x,o) + C_2T(x,t) + C_2\int_{p(x)}^{t} U(T_x + A)d\tau + \ell \quad (103)$$

If the phase changes from liquid to solid, we obtain

$$\nabla \cdot \nabla\theta(x,t) = \int_0^{p(x)} \nabla K_2 \cdot \nabla T(x,\tau)d\tau + \int_{p(x)}^{t} \nabla K_1 \cdot \nabla T(x,\tau)d\tau$$

$$= -C_2T(x,o) + C_1T(x,t) + C_2 \int_0^{p(x)} U(T_x + A)d\tau - \ell \quad (104)$$

If the phase changes from solid to solid, we obtain

$$\nabla \cdot \nabla\theta(x,t) = -C_1T(x,o) + C_1T(x,t) \quad (105)$$

Therefore we can rewrite the governing equations in each case to the following generalized governing equation

$$\frac{Ci}{Ki}\,\theta_t(x,t) - \nabla \circ \nabla\theta(x,t) = \ell_{ij} + C_j T(x,o) - F_{ij}$$

$i \;=\; j \;=\; 1$ at the solid phase

$i \;=\; j \;=\; 2$ at the liquid phase

$$\ell_{ij} = \begin{vmatrix} 0 & \ell \\ -\ell & 0 \end{vmatrix}$$

$$F_{11} = 0$$

$$F_{12} = C_2 \int_{p(x)}^{t} U(\, T_x + \; A \;) d\tau$$

$$F_{21} = C_2 \int_{o}^{p(x)} U(\, T_x + \; A \;) d\tau$$

$$F_{22} = C_2 \int_{o}^{t} U(\, T_x + \; A \;) d\tau$$

with the same matching condition as equation (80)

with the same initial condition as equations (87) (88)

with the same boundary condition as equation (89).

Also, the governing equation is discretized in matrix form using the finite element procedure developed in Chapter 3.

5-2. Numerical Procedure

The difference between regular boundary problems and moving boundary problems is basically that the domain of the solution of the governing equation is unknown and must be determined as a part of the solution. In such a problem, additional information is required to relate the solution of the equation to its domain of definition. The present problem links each domain and the solution of the governing equation to every other domain and the corresponding solutions through the balance of the heat flux rate at the magma-country rock interface which involves the latent heat of solidification, and the rate at which liquid is converted into solid. To solve such a problem numerically an iteration procedure is needed for the domain.

The iteration procedures are

1) The solutions are obtained from the governing equation corresponding to the assumed domain
2) The convergence is checked by comparing the solutions from the assumed domain with the solutions from the computed domain
3) This procedure is repeated until the solutions from the computed domain satisfy a specified convergence criterion.

The other procedures are the same as those developed in Chapter 4.

5-3. Numerical Examples

Example 1. First of all, the numerical results from the model developed herein is compared with the known exact solution of a one-dimensional problem (Jaeger, 1964) for the accuracy and validity of the model. The problem for comparison is illustrated in Figure 5-1. The magma with 1 Km thickness is assumed to be located 5 Km below the surface. The initial temperature of the magma was 850 C which is slightly more than the melting temperature at the surface (800 C). The phase of magma is determined by the melting temperature which is dependent on depth. The temperature of the surface is maintained at 0 C. In this problem the geothermal gradient is not considered for comparison with the known analytical solution which did not include the geothermal gradient effect and convection effect. The physical properties of the magma are the same as those of the country rock (Refer to Table 4-1). The latent heat of solidification is of the order of 80 Cal/g.

Jaeger presents the solution to the problem in terms of the time the magma with half width, d, takes to solidify.

$$t_s = \frac{d^2}{4\alpha\lambda^2}$$

where λ is determined from equation

$$\frac{L\sqrt{\pi}}{C(T_s - T_o)} = \frac{e^{-\lambda^2}}{\lambda(1 + \mathrm{erf}\lambda)}$$

L: Latent heat per mass

C: Specific heat

α: Thermal diffusivity

The numerical results from my model agree with Jaeger's solidification time (Refer to Table 5-1). Figure 5-2 to Figure 5-6 shows the temperature distribution as the solidification of magma proceeds through time. In this problem the liquid phase of the magma is initially assumed to consist of 10 meshes. After 345 years two of the meshes of magma, which contact immediately with the country rock, are solidified (Figure 5-2).

Figure 5-3 shows four of ten liquid phases of the magma solidified after 920 years. The temperature distribution after 1840 years, shown in Figure 5-4, incidates four of the ten meshes to remain in the liquid phase. Figure 5-6 shows the temperature distribution of the complete solidification of the magma after 4140 years.

TABLE 5-1

The Comparison of the Numerical Results and Exact Solutions for Solidification of Magma Body

Half Width of the Solidifying Magma (Unit: m)	Exact Solution (years)	Numerical Solution (years)
100	150	160
200	610	600
300	1370	1400
400	2440	2520
500	3400	4100

Example II. The problem under consideration is shown in Figure 5-7. This problem is basically the same as the problem investigated in Example II except that the geothermal gradient is included as a boundary condition of the country rock to describe the solidification of a magma in a more general sense.

The purpose of this problem is to determine the effect of latent heat on the solidification of the magma. The solidification time from the moving boundary model is compared with the time from the conduction model. Also, the temperature distribution from each model is illustrated in graphic form for visual comparison.

The basic difference between the two models is that the temperature corresponding to the latent heat of solidification, which is of the order of

$$320^{o}\ C = \frac{80}{0.25}\ X\ \frac{cal/g}{cal/g^{o}\ C}$$

is added to the portion of the magma remaining in a liquid phase.

The results from the conduction model show that the complete solidification of the magma is achieved after 880 years. If the latent heat is considered in the solidification, the magma becomes solidified to only two-fifths of the liquid phase after 800 years, completing the solidification of the magma after approximately 4500 years. Figure 5-8 shows temperature distribution changing with time for the conduction model. The temperature distribution for the conductive moving boundary model is shown in Figure 5-9. As a result of the comparison of the two models, the latent heat offusion gives a longer solidification time of the magma.

Example III. The purpose of this problem, which includes the convection effect, is to demonstrate the possibility of inhibiting the freezing of the top of the magma chamber until all of the magma is solidified completely. The boundary conditions and initial conditions are shown in Figure 5-7. In a one dimensional analysis of the problem a convective term necessarily denotes the vertical velocity. This vertical velocity transfers heat at the bottom to cause the freezing front to proceed upward. The value of the velocity is assumed to be 1^m/year, large enough to show the effect of convection in the magma body. Figure 5-10 shows the mode of solidification of the magma for the convective moving boundary model. The portions of the magma, which contact immediately with cold country rocks, are frozen after 250 years. Then the bottom of the magma begins freezing by removing heat at the floor upward due to convection in the magma body. It is interesting to note the temperature gradients in the upper portion of the magma to be more steep than those in the lower.

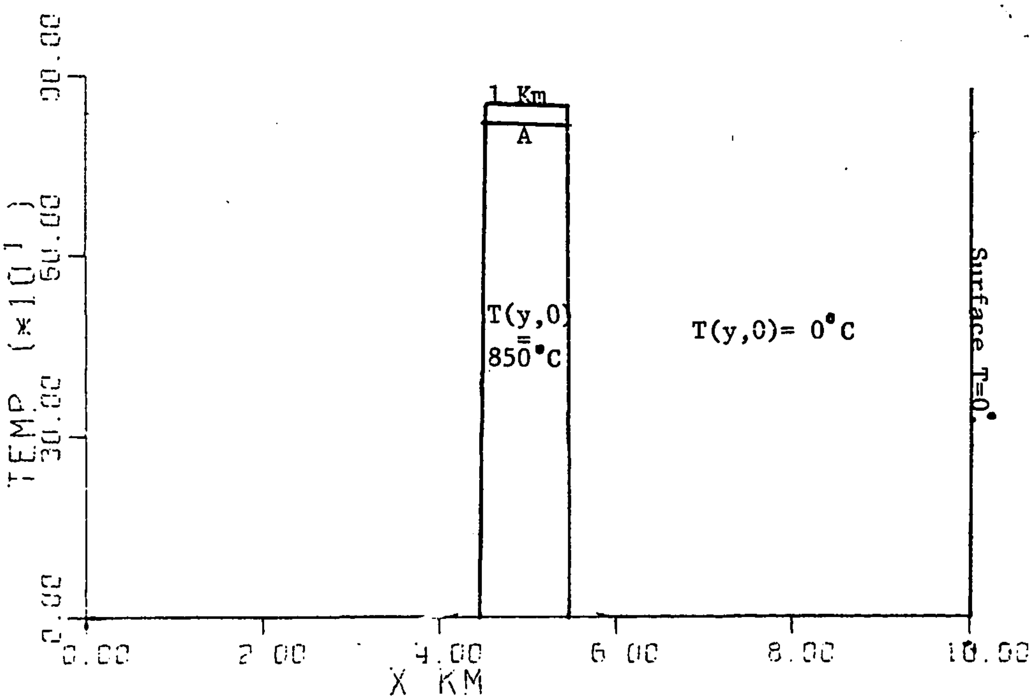

Figure 5-1. A schematic representation of the problem for comparison of conductive moving boundary solution and exact solution (A: slope of the the melting temperature).

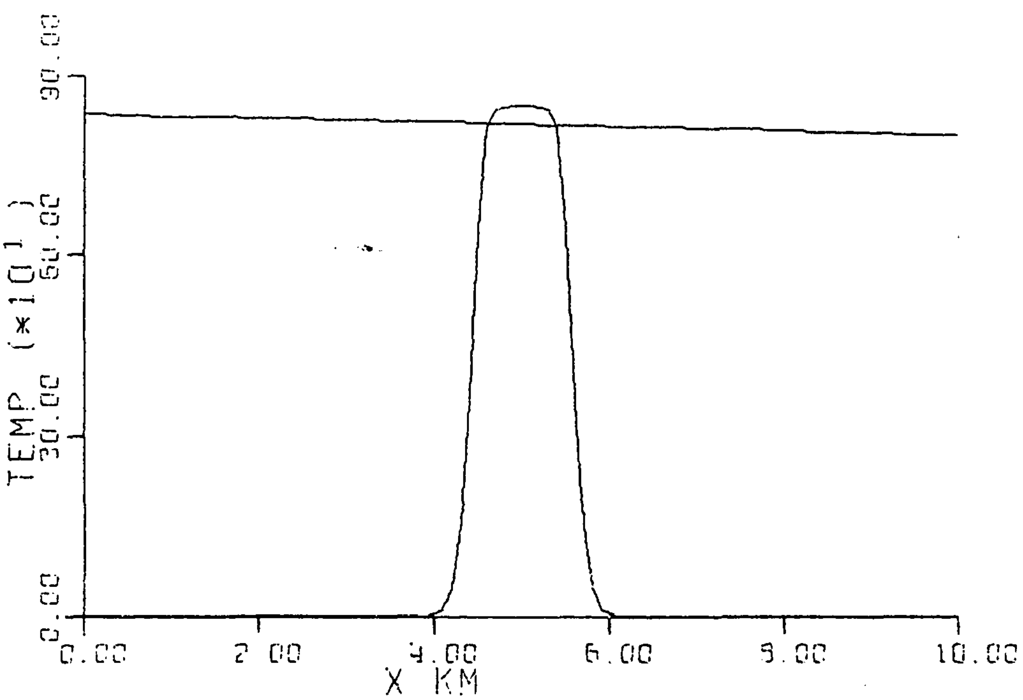

Figure 5-2. Temperature distribution after 345 years for conductive moving boundary model. Note that two portions of the magma, which contacts imediately with the country rock, is freezed. Initially liquid phase of the magma is assumed to consist of 10 meshes.

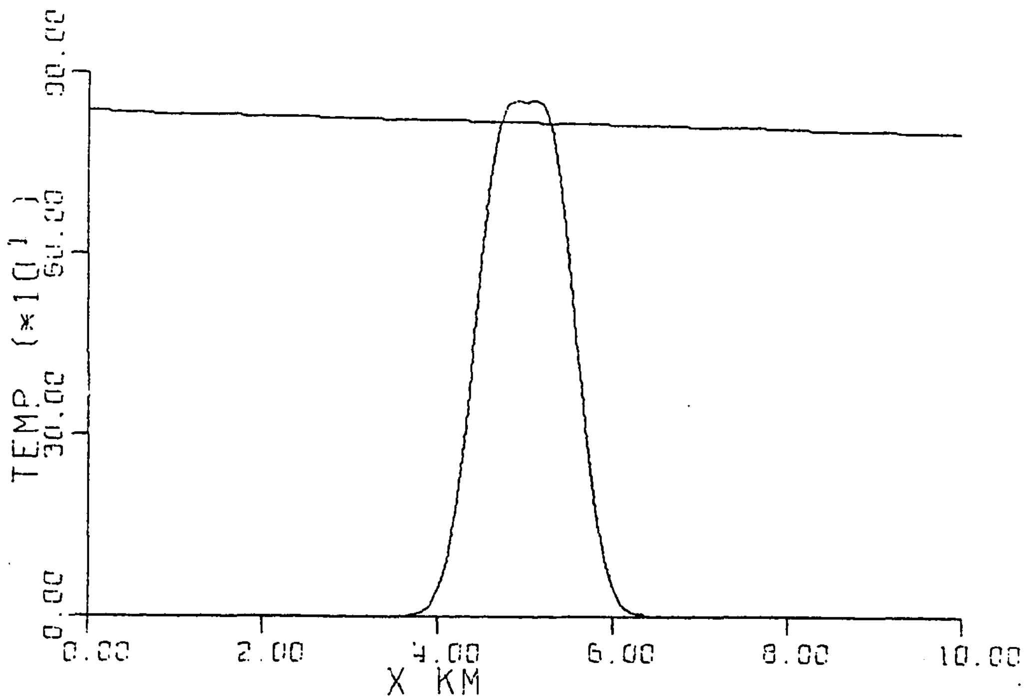

Figure 5-3. Temperature distribution showing four of ten liquid phases of the magma solidified after 920 years from the conductive moving boundary model.

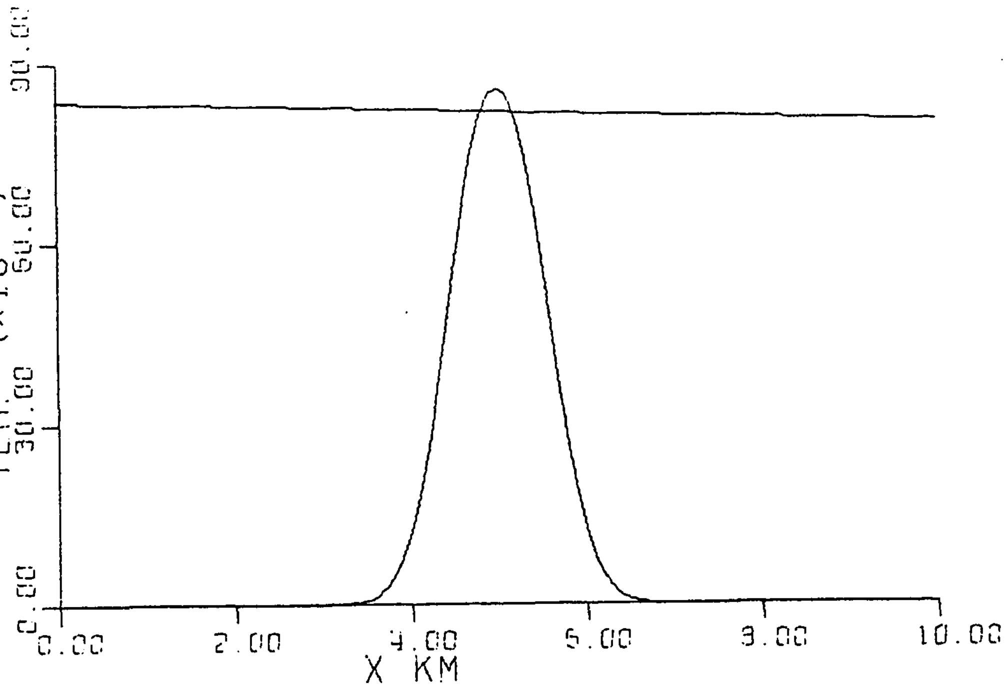

Figure 5-4. Temperature distribution showing four out of ten meshes of the magma remained in liquid phase after 1840 years.

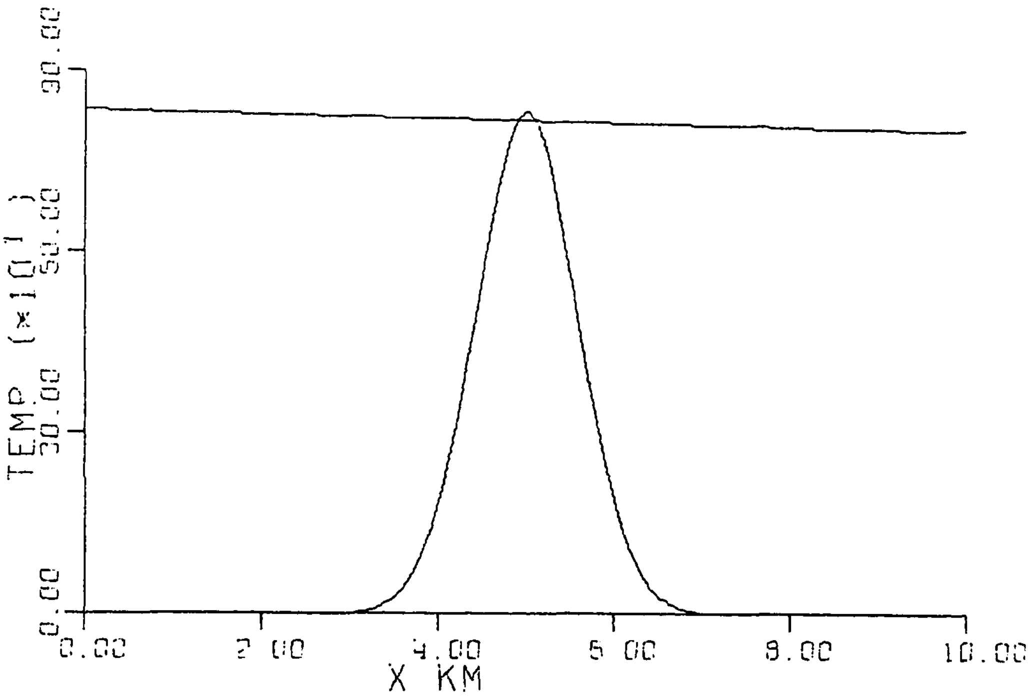

Figure 5-5. Temperature distribution after 2980 years for the conductive moving boundary model. Note that two out of ten meshes of the magma remained in liquid phase.

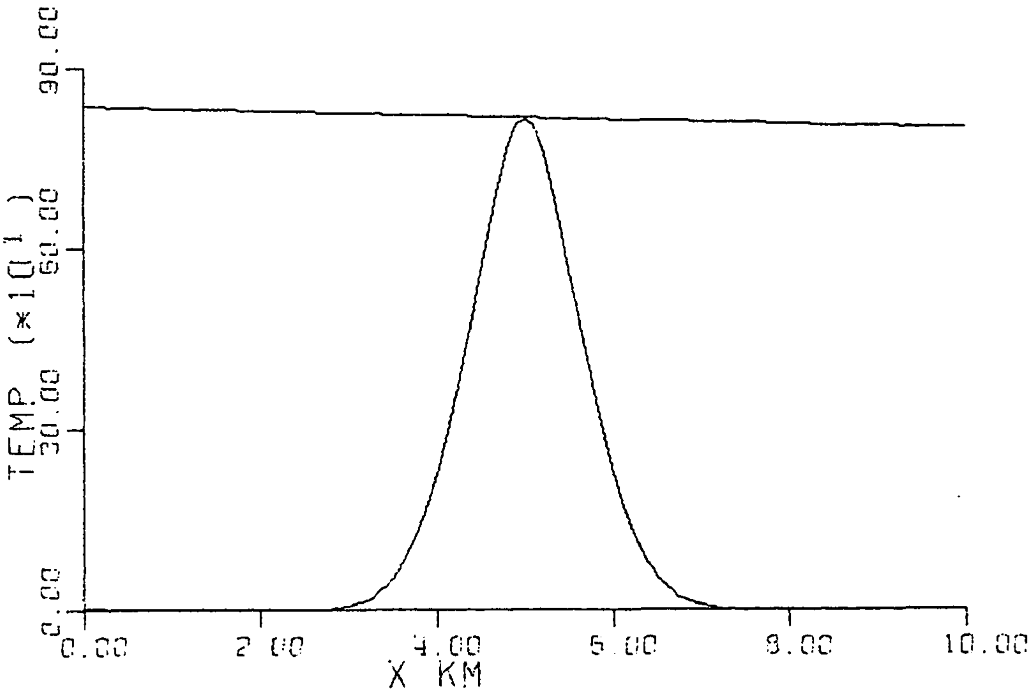

Figure 5-6. Temperature distribution showing the complete solidification of the magma after 4140 years from the conductive moving boundary model.

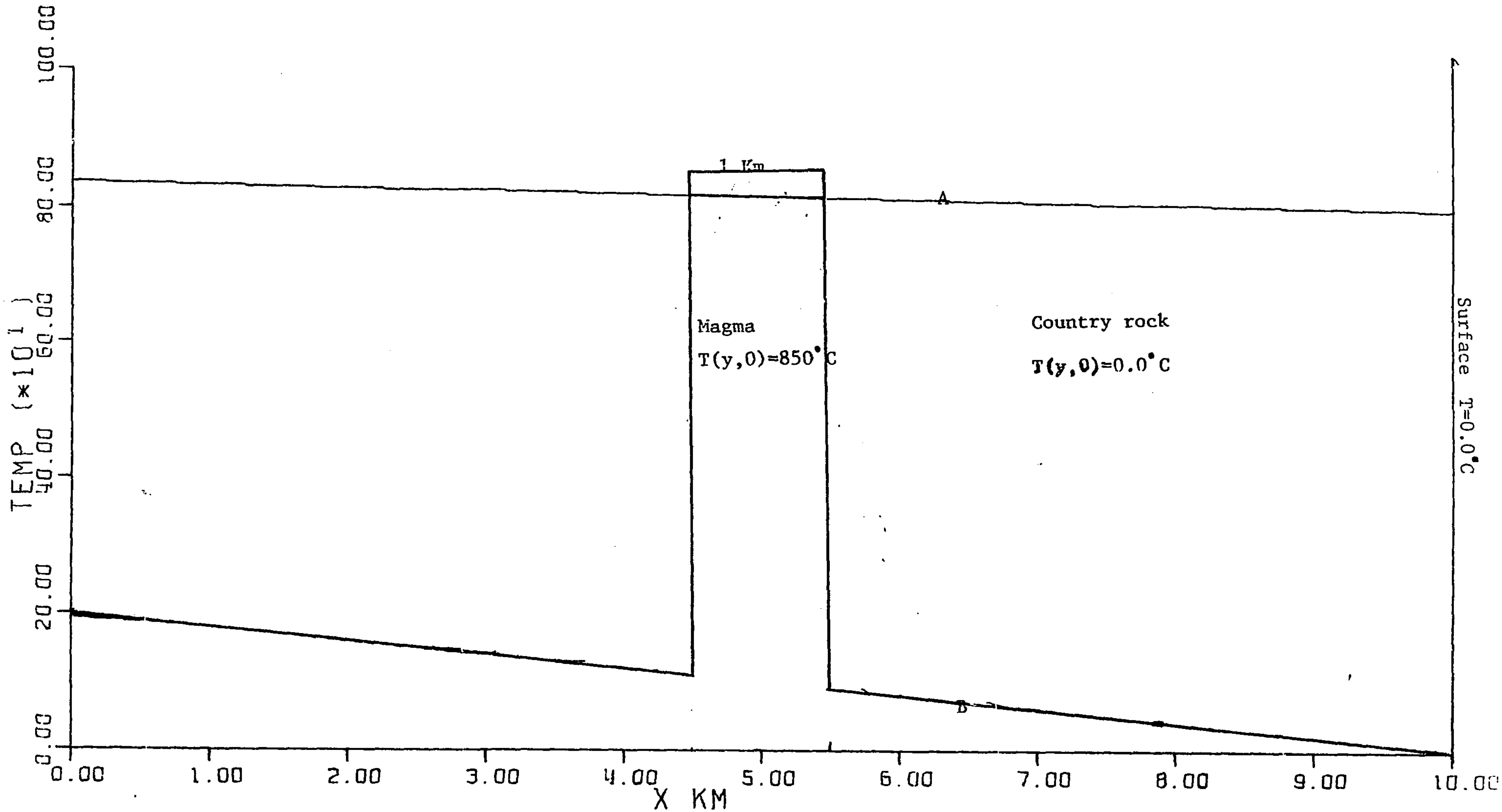

Figure 5-7. Boundary and initial condition of the magma intruded into the country rock which has been subjected to the geothermal gradient (A; slope of the melting temperature, B; slope of the geothermal gradient).

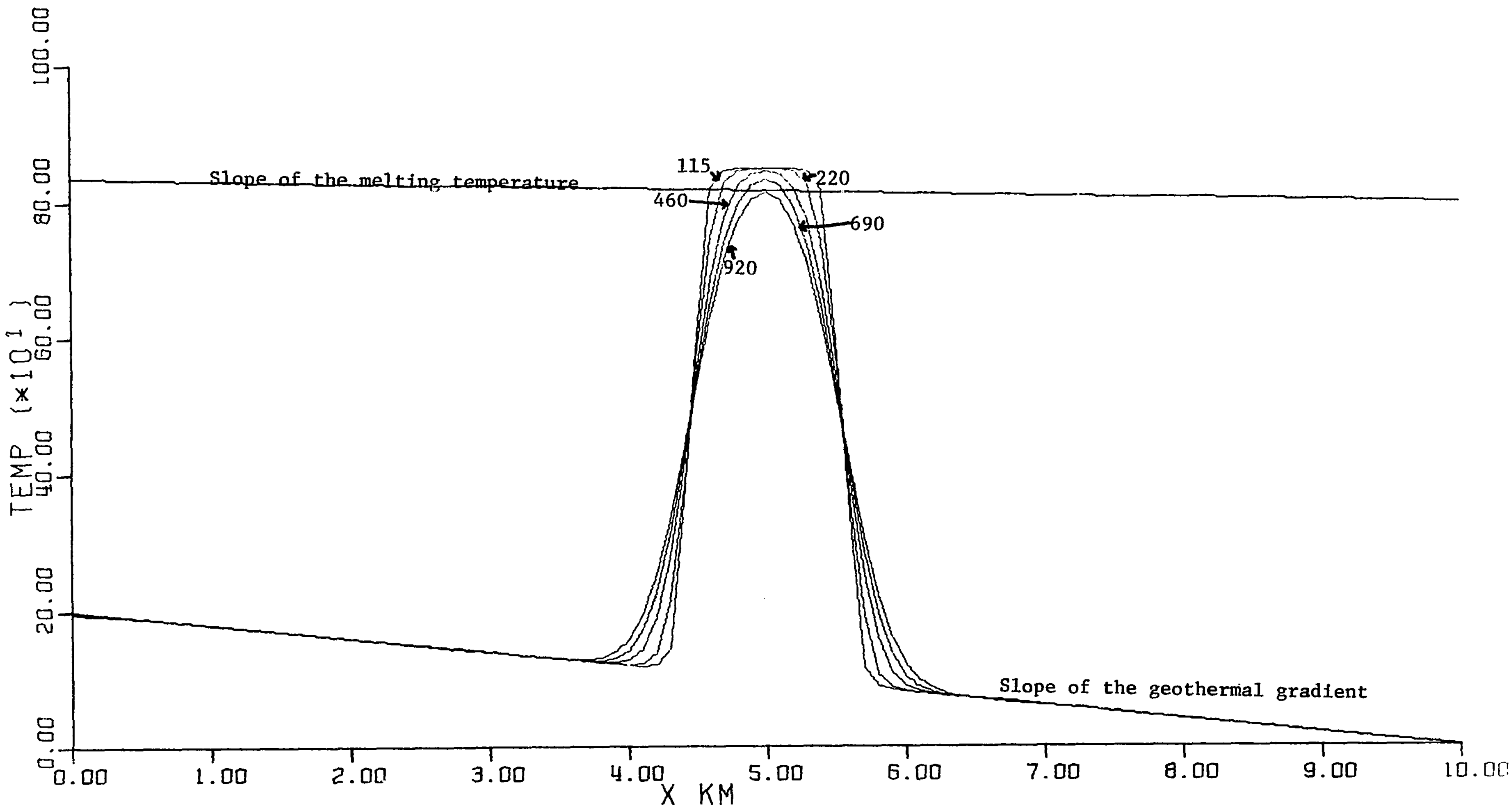

Figure 5-8. Temperature distribution changing with time for the conduction model. (Unit: years)

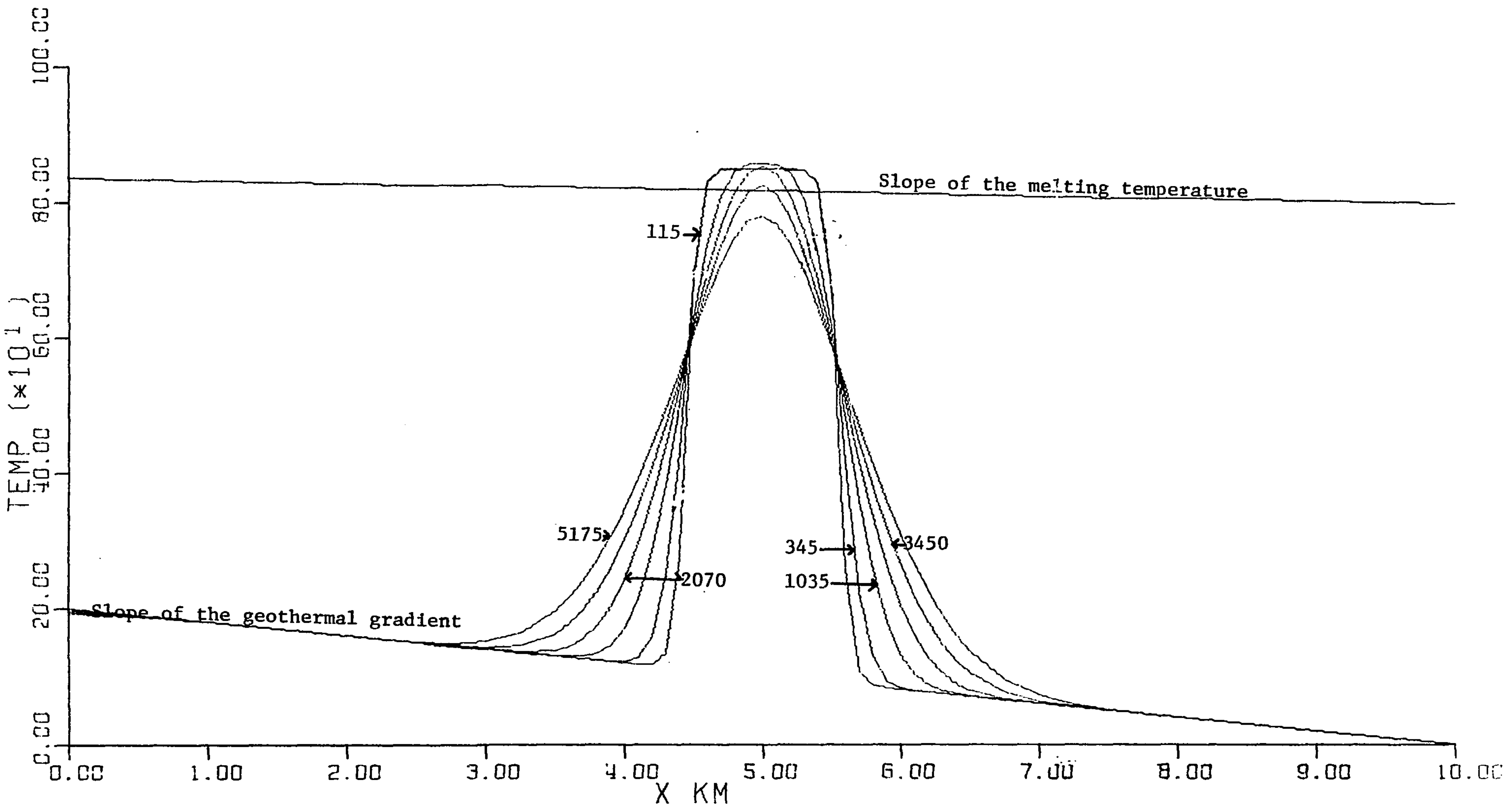

Figure 5-9. Temperature distribution changing with time for the conductive moving boundary model. Note that the effect of latent heat gives longer solidification time of the magma. (Unit:years)

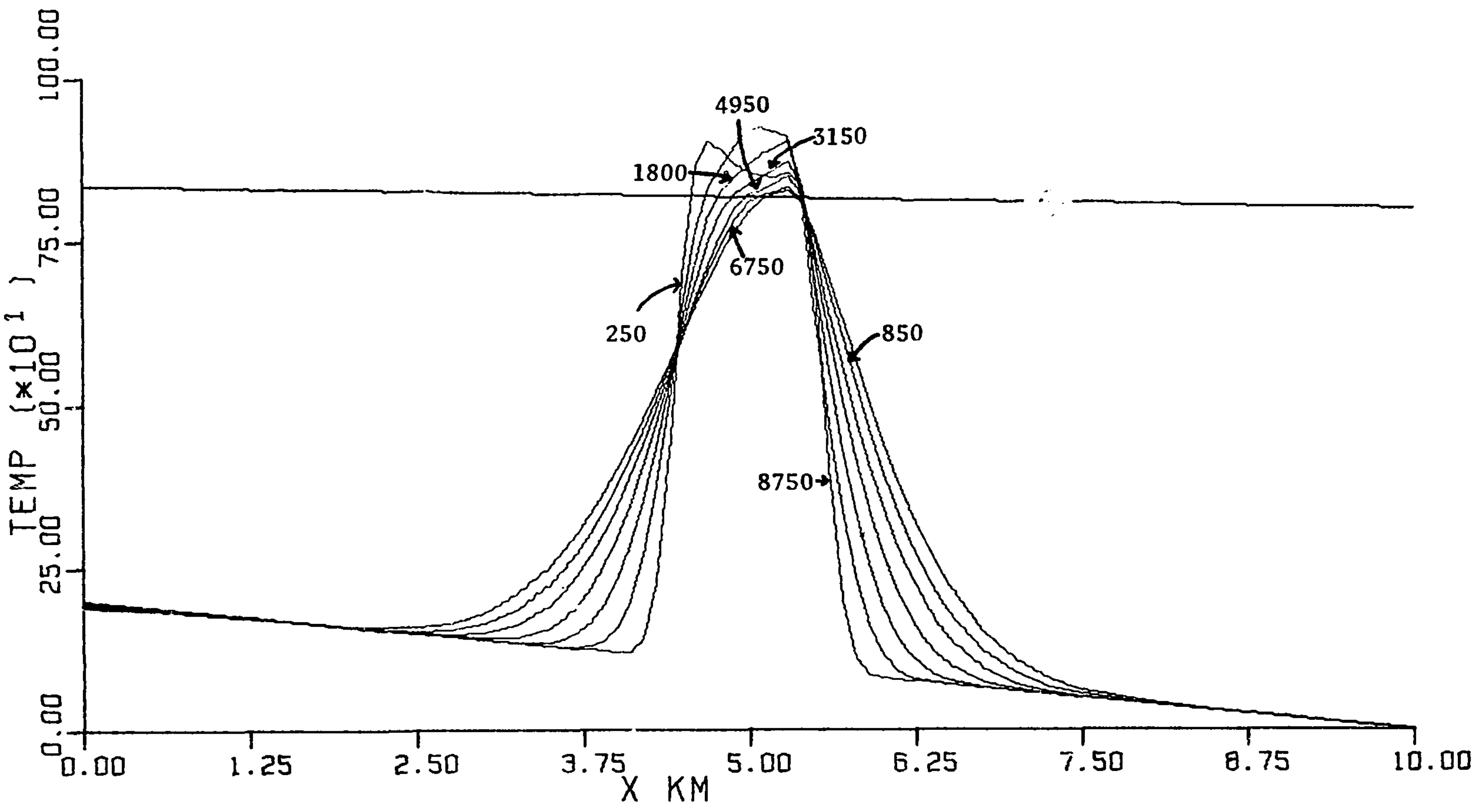

Figure 5-10. The mode of solidification of the magma. It is interesting to note the temperature gradient in the right side of the temperature distribution to be more steep than the left one. (Unit;years)

CHAPTER VI

CONCLUSION AND RECOMMENDATION FOR FUTURE RESEARCH

Problems of the heat and mass transfer in geothermal reservoirs have been extensively treated in the literature of finite element analysis. The problems under investigation in this study are unsteady free convection within a magma body and the two phase Stefan problem associated with the moving boundary. In this geological problem which requires larger computer storage created by the fine mesh discretization to provide increased resolution near an interesting small area of the huge domain, a consideration to reduce the number of unknown variables is necessary. The penalty method of finite element analysis has been employed to solve the time dependent viscous thermal flow (unsteady free convection). The purpose of this study was to investigate the effect of convection on the temperature and streamline distribution within a geothermal reservoir (magma chamber). The one dimensional, two phase Stefan problems, which have dependent melting temperature on depth, have been solved by finite element method. This method has used the Duvaut's transformation to resolve the discontinuity of the temperature gradient on the solid-liquid interface which is a principal difficulty of numerical approaches to Stefan problems. This model has been employed to investigate the effect of the latent heat of fusion on the solidification of the magma. The unsteady two dimensional conduction model developed in this study shows that

(1) Galerkin scheme, one of the θ family of approximation for a time stepping procedure of the time dependent model, gives a convergent and smooth time approximation of temperature over Crank-Nicolson's even at the point where temperature changes rapidly.

From the penalty finite element analysis of unsteady free convection

(2) The penalty parameter $\varepsilon=10^{15}$ showed to be desirable for this problem where the temperature is a more dependent variable than pressure and Prantdl number has a large value.

(3) The convection is generated by a change of density due to the difference in the temperature between hot magma and cold country rock.

(4) Below the critical Rayleigh number for the onset of convection (about 1500), the temperature distribution is simply governed by conduction with no movement of flow. Above that value, the larger the value, the more vigorous the convection of the fluid.

(5) Turbulent flow seems to be prevented because of large viscosity even if the modified Rayleigh number of this model exceeds the critical value for the onset of turbulent flow defined by Lipps (1971).

(6) The rate of heat diffusion into the country rock by convection exceeds the value of conduction for the stock-like bodies of magma more than 30 m. in diameter before the convection motion dies out.

(7) Hot magma tends to rise near the center, and cold magma tends to fall along the boundary of country rock by thin thermal

boundary layers emerged on the interface between the magma and the country rock.

(8) As the speed of convective currents increase, a secondary cell with anticlockwise circulation occurs in the upper central region of the magma.

(9) After 10.2 years the convection motion reaches a steady state.

(10) The convection in the magma body gives larger temperature gradients at the upper portion of magma than at lower portions indicating a possibility of upward migration of the magma.

From the conductive moving boundary model

(11) The numerical results from the model developed herein agree with the analytical solutions by Jaeger (1961) of the magma.

(12) The effect of latent heat of fusion gives longer solidification time of the magma.

From the convective moving boundary model

(13) A freezing front proceeds from the bottom to the top by transferring heat at the bottom upward suggesting the possibility of inhibiting the freezing of the top of magma body until all of the magma is solidified completely.

(14) The convection gives steeper temperature gradients in the upper portion of the magma than those in the lower.

(15) The effects of convection and latent heat of fusion would play an important role on the mode of solidification of the magma.

Finally, as a result of this study the following future research is recommended;

(1) To investigate the two dimensional analysis of upward magma migration, the general formulation is recommended by introducing moving boundary conditions into the unsteady free convection model.

(2) The penalty finite element formulation developed herein can be applied to the problems of flow in porous media.

APPENDIX I

DERIVATION OF THE GOVERNING EQUATION

1. Energy Equation

The relation between heat flux Q and temperature T is defined by the Fourier law

$$Q = -K \frac{\partial T}{\partial \tilde{x}}$$

where $\tilde{x}$ is a vector coordinate.

The general 3-D differential equation of heat conduction is derived as follows. Let;

E_I = net rate of heat entering by conduction into given element

E_{II} = rate of energy generated in element

E_{III} = rate of increase of internal energy of element

E_I can be expressed in mathematical form

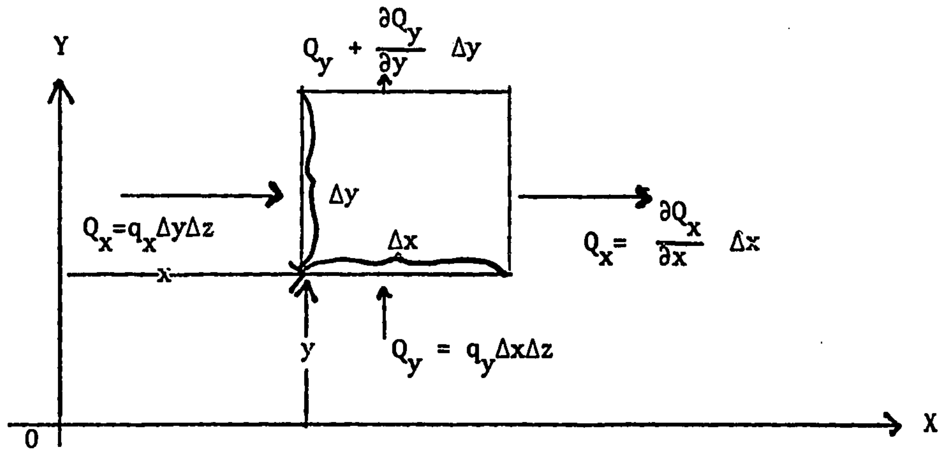

Figure I-1 Symbols for the Derivation of the Heat-Conduction Equation

The rate of heat flow Q_x in the x direction is given by:

$$Q_x = q_x \cdot \Delta y \cdot \Delta z \qquad \text{at } x$$

$$Q_{x+\Delta x} = Q_x + \frac{\partial Q_x}{\partial x} \Delta x \qquad \text{at } x+\Delta x$$

The net rate of heat flow in x direction is

$$Q_x - Q_{x+\Delta x} = -\frac{\partial q_x}{\partial x} \Delta x \cdot \Delta y \cdot \Delta z$$

Similarly, the net rate of heat flow in y, z directions are

$$-\frac{\partial q_y}{\partial y} \Delta x \Delta y \Delta z$$

$$-\frac{\partial q_z}{\partial z} \Delta x \Delta y \Delta z$$

Thus $E_I = (-\frac{\partial q_x}{\partial x} + \frac{\partial q_y}{\partial y} + \frac{\partial q_z}{\partial z}) \Delta x \cdot \Delta y .. \Delta z$

E_{II} = rate of energy generation = $F(x,y,z,t).\Delta x \cdot \Delta y \cdot \Delta z$ where G is a generating heat per unit time, per unit volume.

E_{III} = rate of energy storage in the element = $\rho \cdot C \cdot \frac{\partial T}{\partial t} \Delta x \cdot \Delta y \cdot \Delta z$ where ρ is density, C is specific heat.

Thus from the point of view of energy balance, we obtain $E_I + E_{II} = E_{III}$.

$$-\left(\frac{\partial q_x}{\partial x} + \frac{\partial q_y}{\partial y} + \frac{\partial q_z}{\partial z} \right) + G = \rho \cdot C \cdot \frac{DT}{Dt}$$

Therefore, using the Fourier law,

$$-K \cdot \nabla^2 T + G = \rho \cdot C \cdot \frac{DT}{Dt}$$

2. Continuity Equation

The continuity equation is the equation for the conservation of mass. If the continuity equation is explained in words, the sum of the net rate of mass flow entering element in the x direction and the net rate of mass flow entering the element in the y direction equals zero.

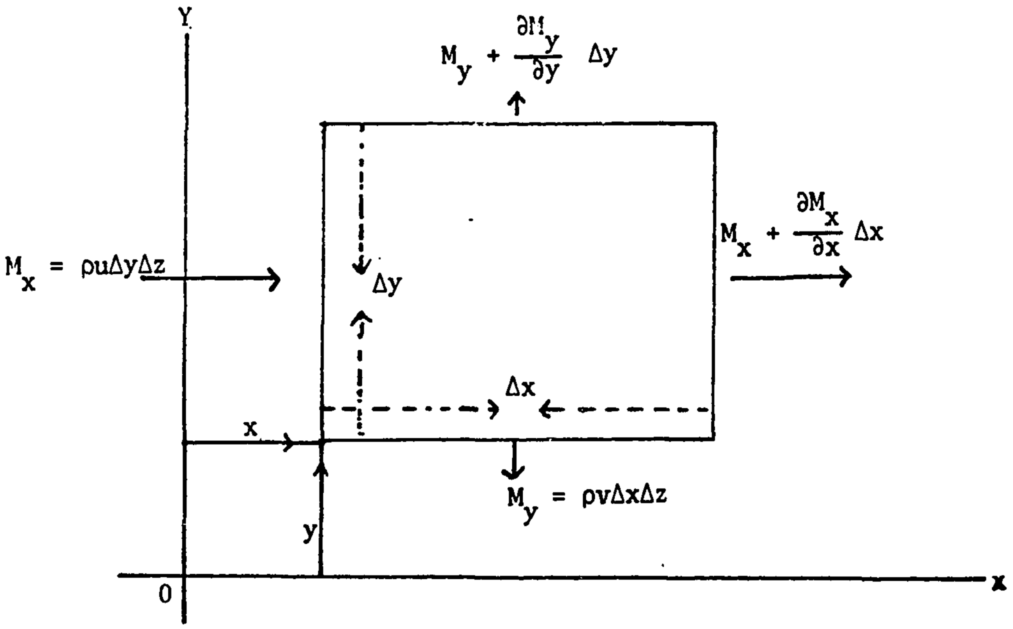

Figure I-2 Symbols for the Derivation of the Continuity Equation

The mass flow entering the element in the x direction, F_x may be expressed as

$$F_x = M_x - M_{x+\Delta x}$$

where $M_x = \rho \cdot U \cdot \Delta y \cdot \Delta z$, V is the velocity in x direction and

$$M_{x+\Delta x} = M_x + \frac{\partial M_x}{\partial x} \cdot \Delta x \quad .$$

Thus, $F_x = -\frac{\partial M_x}{\partial x} \Delta x = -\frac{\partial (\rho V)}{\partial x} \Delta x \cdot \Delta y \cdot \Delta z$

Similarly, the mass flow entering the element in the y direction, F_y, may be expressed as

$$F_y = \frac{\partial (\rho V)}{\partial y} \Delta x \cdot \Delta y \cdot \Delta z$$

Requiring that the sum of the mass flows by zero gives

$$F_x + F_y = 0$$

or $$\frac{\partial (\rho U)}{\partial x} + \frac{\partial (\rho V)}{\partial y} = 0$$

3. The Momentum Equations

The momentum equations, or the Navier-Stokes equations, are derived from Newton's second law.

$$F = M \cdot a$$

where F: the external forces

M: mass

a: acceleration

The external forces in a flow field consist of the body force and the surface force. In this appendix the time dependent two dimensional momentum equations are derived as follows:

$$M = \rho \cdot \Delta x \cdot \Delta y \cdot \Delta z$$

The body forces are given as:

$$F_x \cdot \Delta x \cdot \Delta y \cdot \Delta z \quad \text{in x direction}$$

$$F_y \cdot \Delta x \cdot \Delta y \cdot \Delta z \quad \text{in y direction,}$$

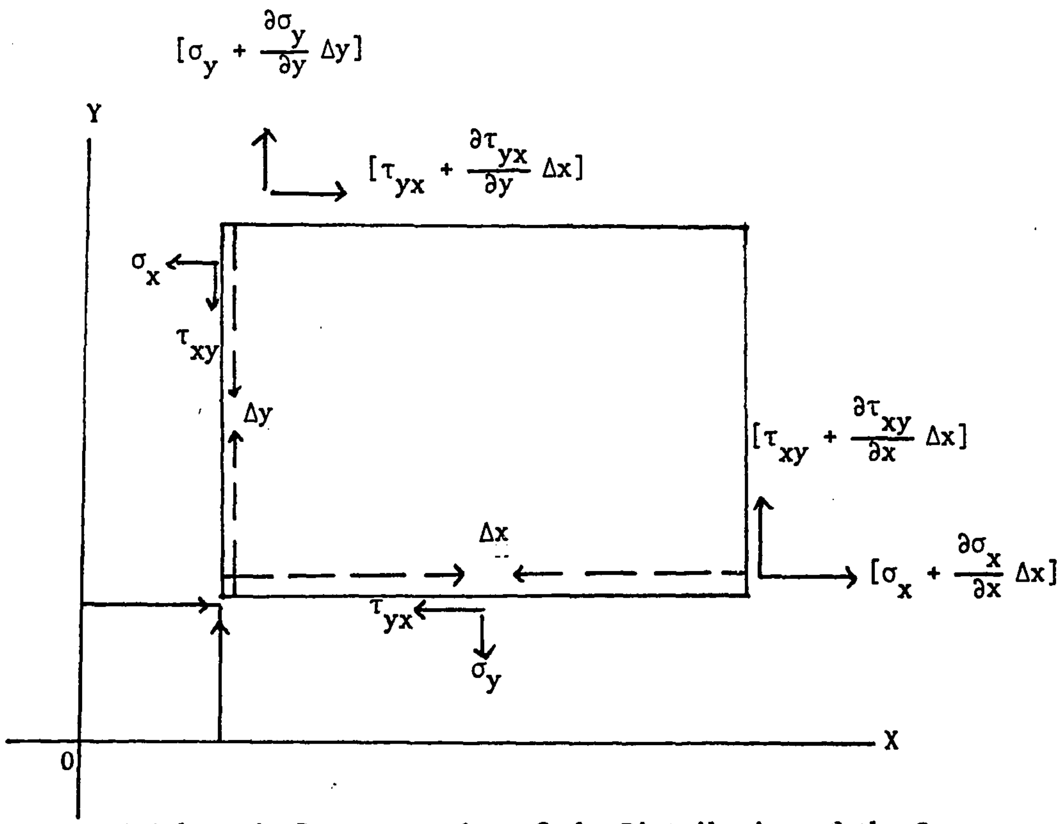

Figure I-3 A Schematic Representation of the Distribution of the Stresses for the Derivation of the Momentum Equations

The surface forces have two components depending on the acting direction; normal stress, shear stress.

The surface forces are;

σ_x, τ_{yx} at x in x direction

$\sigma_x + \frac{\partial \sigma_x}{\partial x}, \quad \tau_{yx} + \frac{\partial \tau_{yx}}{\partial x}$ at x + Δx in x direction

Thus, net surface forces in x direction is given:

$$\left(\frac{\partial \sigma_x}{\partial x} + \frac{\partial \tau_{yx}}{\partial y}\right)\Delta x \,.\, \Delta y \,.\, \Delta z$$

It is necessary to note that the first subscript indicates the axis to which the surface is perpendicular and the second subscript indicates the direction of the shear stress. Similarly net surface forces in y direction are given:

$$\left(\frac{\partial \sigma_y}{\partial y} + \frac{\partial \tau_{xy}}{\partial x}\right)\Delta x \,.\, \Delta y \,.\, \Delta z$$

The next step in the development is to introduce the relationship between the stresses and the velocity components

$$\sigma_{ij} = \rho\delta_{ij} + 2\mu e_{ij}$$

for the Newtonian flow.

where $e_{ij} = \frac{1}{2} (\frac{\partial V_i}{\partial x_j} + \frac{\partial V_j}{\partial x_i})$, $\delta_{ij} = 0$ for $i \neq j$ $\delta_{ij} = 1$ for $i=j$.

Therefore

$$\sigma_{xx} = -\rho + 2\mu \frac{\partial u}{\partial x}$$

$$\sigma_{yy} = -\rho + 2\mu \frac{\partial v}{\partial y}$$

$$\tau_{yx} = \tau_{xy} = \mu \left(\frac{\partial u}{\partial y} + \frac{\partial v}{\partial x}\right)$$

We can rewrite net surface forces in y directions

$$\left[- \frac{\partial P}{\partial y} + 2\mu \frac{\partial^2 v}{\partial y^2} + \mu \frac{\partial}{\partial x} \left(\frac{\partial u}{\partial y} + \frac{\partial v}{\partial x}\right)\right] \Delta x \cdot \Delta y \cdot \Delta z$$

Thus the momentum equation is given in y direction

$$\rho \frac{Dv}{Dt} = F_y - \frac{\partial P}{\partial y} + 2\mu \frac{\partial^2 v}{\partial y^2} + \mu \frac{\partial}{\partial x} \left(\frac{\partial u}{\partial y} + \frac{\partial v}{\partial x}\right)$$

In the free convection where the density changes due to temperature variation, the effect of density variation should be considered.

$$\rho = \rho_o + \Delta\rho$$

where ρ_o is a reference density, $\Delta\rho$ density variation. If we express the gravitational acceleration by a potential

$$\overline{g} = - \nabla\Phi \quad \text{where } \overline{g} = -gy, \text{ y is taken upward}$$

Also, the relationship between $\Delta\rho$ and T under Boussinesq approximation can be expressed as follows;

$$\Delta\rho = -\beta \cdot \rho_o \cdot \Delta T$$

where β is the coefficient of expansion of the fluid. Thus, body force is introduced to allow for the effect of gravity.

Using the above three quations, we obtain;

$$\begin{aligned} F_y &= \rho\overline{g} \\ &= (\rho_o + \Delta\rho)\overline{g} \\ &= -(\rho_o + \Delta\rho)\nabla\Phi \\ &= -\nabla(\rho_o\Phi) - \rho_o \cdot \beta \cdot \Delta T \cdot \overline{g} \end{aligned}$$

Then, if we included $\Delta\rho_o\Phi$ into the pressure term,

$$P' = P + \rho_o\Phi$$

The momentum equation is given under the Boussinesq assumption

$$\rho_o \frac{Dv}{Dt} = -\frac{\partial p'}{\partial y} + \mu\frac{\partial^2 V}{\partial y^2} - \rho_o\overline{g} \cdot \beta \cdot \Delta T$$

The pressure change is negligible if the pressure does not impose explicitly in the boundary conditions (Tritton, 1977).

Thus, we can rewrite the momentum equation in y direction as follows:

$$\frac{DV}{Dt} = \frac{1}{\rho_o} \nabla \frac{\partial p}{\partial y} + \nu \frac{\partial v^2}{\partial y^2} - \overline{g} \cdot \beta \cdot \Delta T$$

APPENDIX II

NUMERICAL INTEGRATION

The finite element method usually introduces Gaussian Quadrature, one type of numerical integration, to describe curved boundaries more accurately. In the penalty method the numerical integration is necessary to obtain the reduced integration. The transformation from the Cartesian coordinates (x,y) to the curvilinear coordinates (ξ,η) is needed to evaluate the coefficient matrix over the complicated domain.

If the unknown variable T and the shape of the elements x and y are approximated by the interpolation functions expressed in terms of the curvilinear coordinates (ξ,η), we have

$$T = T_i N_i(\xi,\eta) \tag{1}$$

$$X = X_i N_i(\xi,\eta), \qquad Y = Y_i N_i(\xi,\eta) \tag{2}$$

where N_i denotes the interpolation function corresponding to node i. Furthermore, the interpolation function $N_i(\xi,\eta)$ can be described in terms of the Cartesian components (x,y) using the chain rule of differentiation.

$$\begin{vmatrix} N_\xi \\ N_\eta \end{vmatrix} = \begin{vmatrix} X_\xi & Y_\xi \\ X_\eta & Y_\eta \end{vmatrix} \cdot \begin{vmatrix} N_x \\ N_y \end{vmatrix} \tag{3}$$

$$\begin{vmatrix} N_x \\ N_y \end{vmatrix} = [J]^{-1} \begin{vmatrix} N_\xi \\ N_\eta \end{vmatrix} \tag{4}$$

where J is Jacobian matrix;

$$\begin{vmatrix} X_\xi & Y_\xi \\ X_\eta & Y_\eta \end{vmatrix} \tag{5}$$

Substituting equations 2 into eq[illegible] [illegible]ompute the Jacobian matrix

$|J| = |X$ [illegible]

Therefore

$K_{ij} = \int N_{i,x}$ [illegible]

$$= \sum_i \sum_j G(\tau i, \tau j \text{[illegible]} \tag{7}$$

where τi, τj are Gaussian points

ωi, ωj are Gaussian weight factors.

$$\begin{vmatrix} N_x \\ N_y \end{vmatrix} = [J]^{-1} \begin{vmatrix} N_\xi \\ N_\eta \end{vmatrix} \tag{4}$$

where J is Jacobian matrix;

$$\begin{vmatrix} X_\xi & Y_\xi \\ X_\eta & Y_\eta \end{vmatrix} \tag{5}$$

Substituting equations 2 into equation 5, we can compute the Jacobian matrix

$$|J| = \begin{vmatrix} X_\xi & Y_\xi \\ X_\eta & Y_\eta \end{vmatrix} = \begin{vmatrix} \Sigma X_i N_{i,\xi} & \Sigma Y_i N_{i,\xi} \\ \Sigma X_i N_{i,\eta} & \Sigma Y_i N_{i,\eta} \end{vmatrix}$$

$$= \begin{vmatrix} X_1 & Y_1 \\ X_2 & Y_2 \\ \cdot & \cdot \\ X_n & Y_n \end{vmatrix} \cdot \begin{vmatrix} N_{1,\xi} \cdots N_{n,\xi} \\ N_{1,\xi} \cdots N_{n,\eta} \end{vmatrix}$$

Therefore

$$K_{ij} = \int N_{i,x} N_{j,x} \, dxdy = \int_{-1}^{1} \int_{-1}^{1} N_{i,\xi} N_{j,\eta} \det[J] \, d\xi d\eta$$

$$= \sum_i \sum_j G(\tau i, \tau j) \omega_i \omega_j \tag{7}$$

where τi, τj are Gaussian points

ωi, ωj are Gaussian weight factors.

APPENDIX III

A COMPARISON OF FINITE DIFFERENCE METHOD AND FINITE ELEMENT METHOD FOR UNSTEADY FORCED CONVECTION MODEL

In this appendix the validity of the finite element model is checked by comparing the finite difference solutions* for unsteady forced convection with finite element results.

In forced convection where mass transfer of fluid takes place as a result of an externally applied force, the velocity is unaffected by the temperature field.

The problem under consideration is illustrated in Figure III-1. Initially, the walls are fixed and the dimensionless temperature is zero at all points. For time greater than zero the top wall assures a temperature of 1.0 and moves in a positive x direction with a velocity of 1.0. The physical parameters used for the present model such as density, viscosity, gravitational acceleration, and thermal diffusivity take the value of a unit.

The domain of the present problem is discretized using a 10 * 10 regular sized mech of quadrilateral elements to match the discretization employed by the finite difference model.

---

*The finite difference solutions is obtained from personal communication with Ahern on May, 1981.

The numerical results of the finite difference model and the finite element model is after the dimensionless time 0.15 & 0.25 are illustrated in Table III-1, III-2. In addition, the temperature and stream line distribution, which were obtained from both models after the dimensionless time 0.25, are plotted in Figure III-2, Figure III-3, Figure III-4, Figure III-5, by using the SYSMAP plotting procedure for visual comparison. The comparison shows that the results from both models agree.

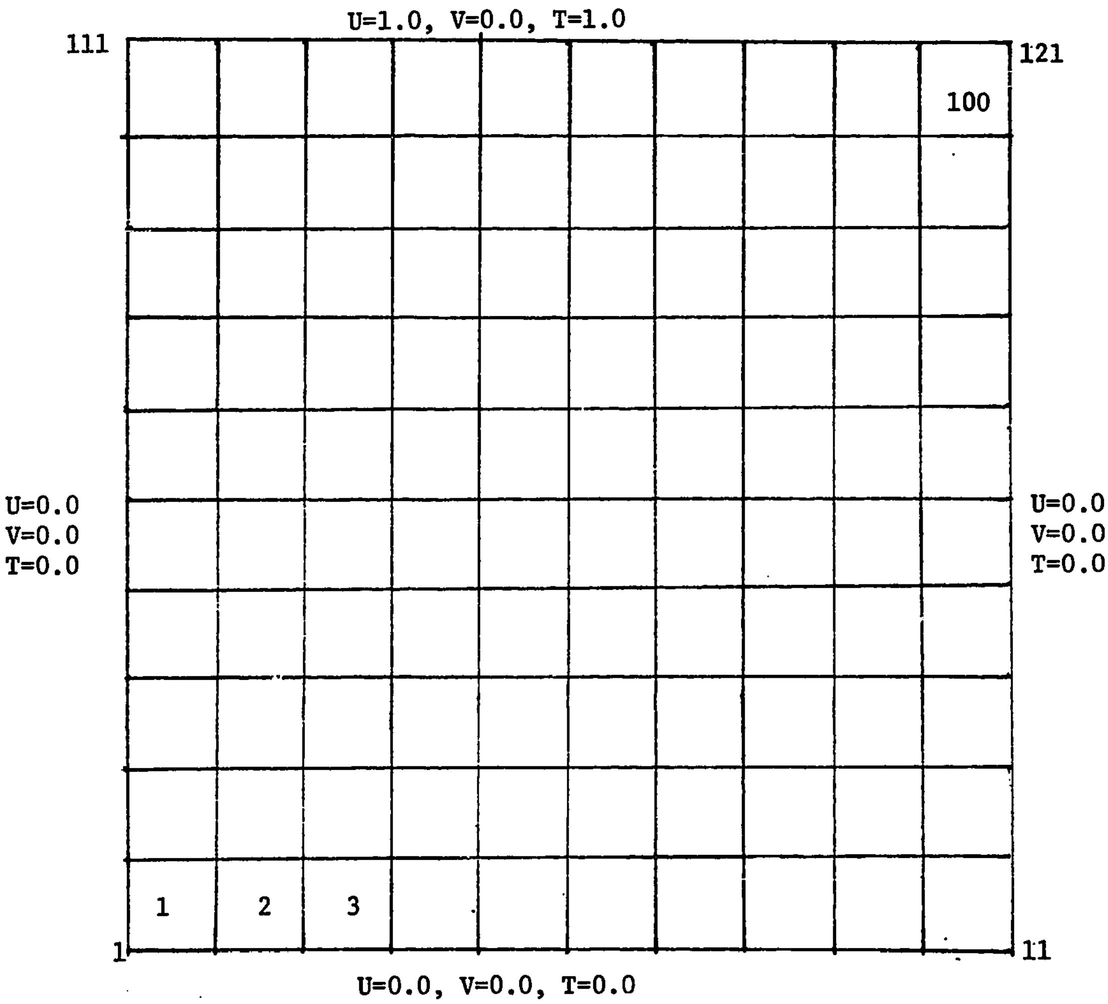

Figure III-1. Boundary and intial condtion, and mesh distribution of the forced convection model. (Element and node numbering from left to right, from down to up.)

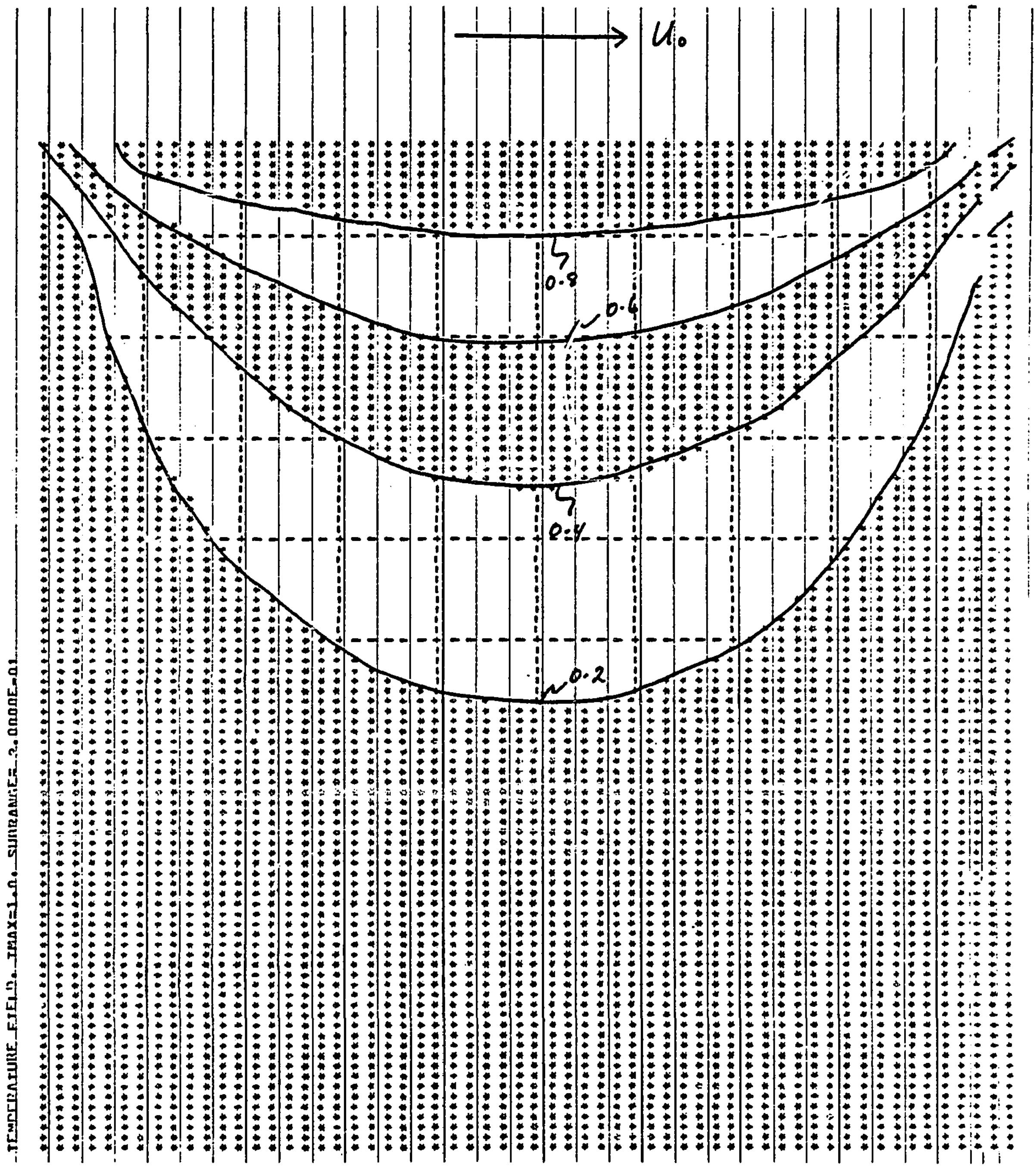

Figure III-2. Temperature distribution for finite difference model after dimensionless time 0.25.

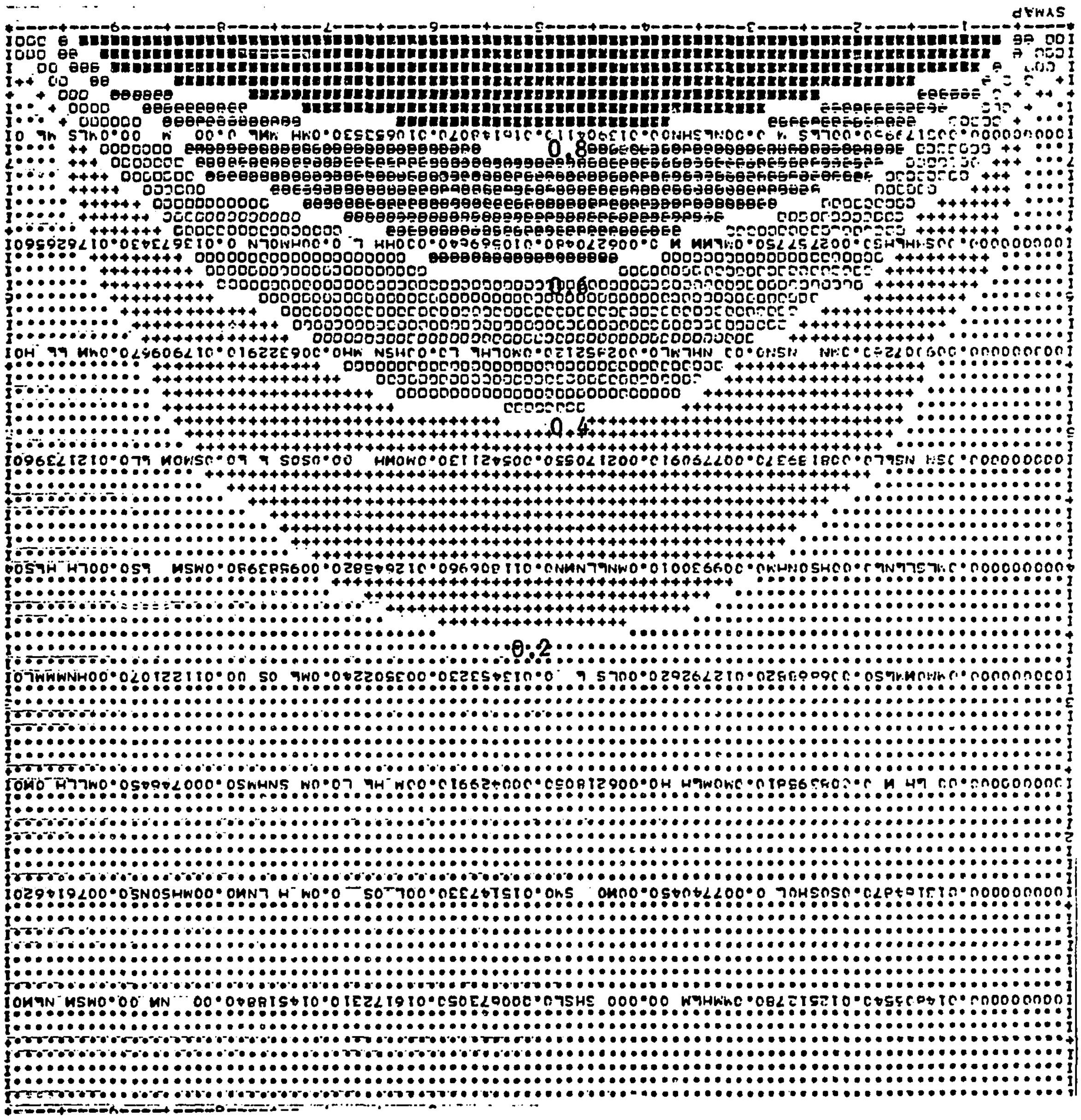

Figure III-3. Temperature distribution for finite element model after dimensionless time 0.25.

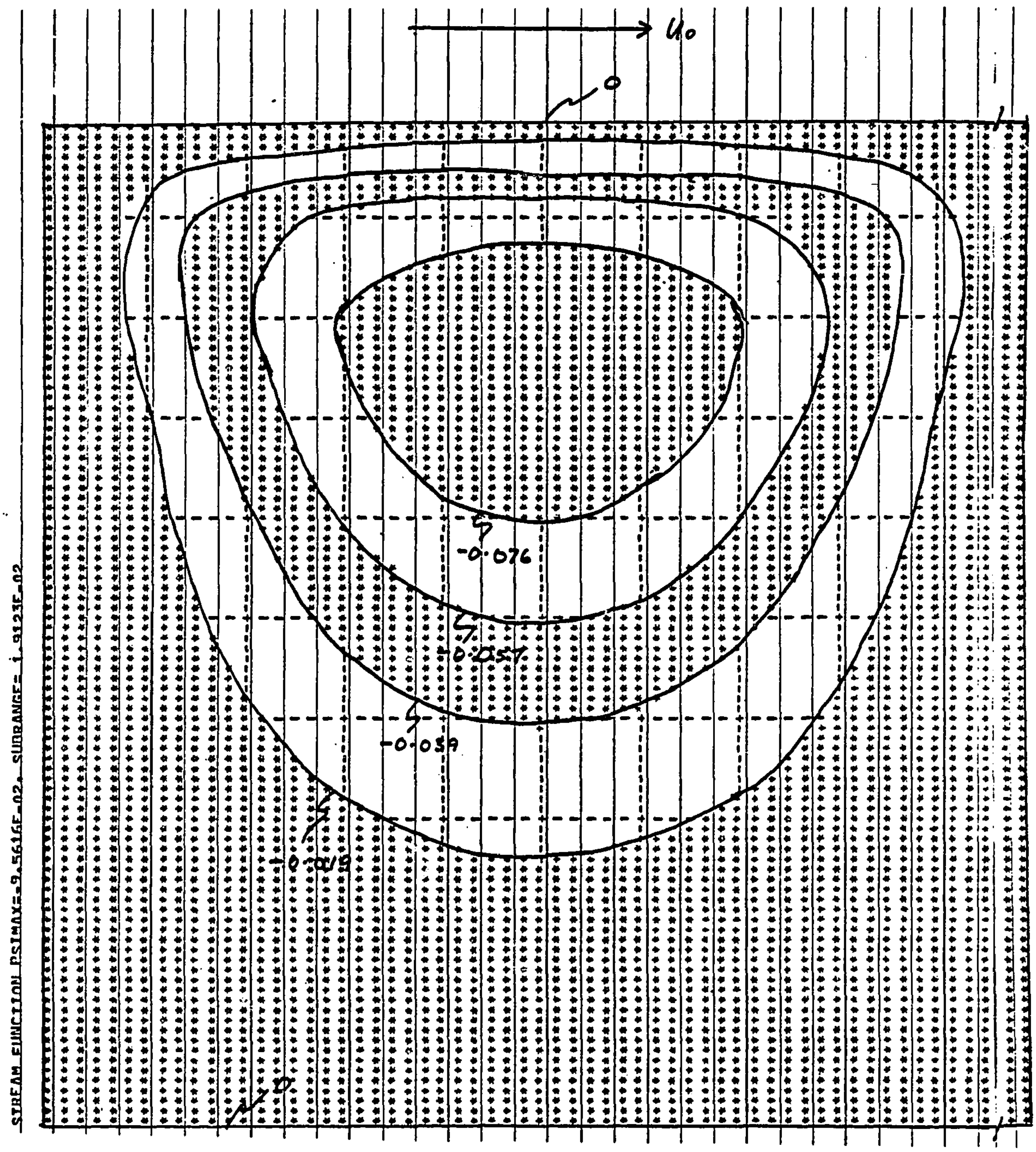

Figure III-4. Streamlines for finite difference model after dimensionless time 0.25.

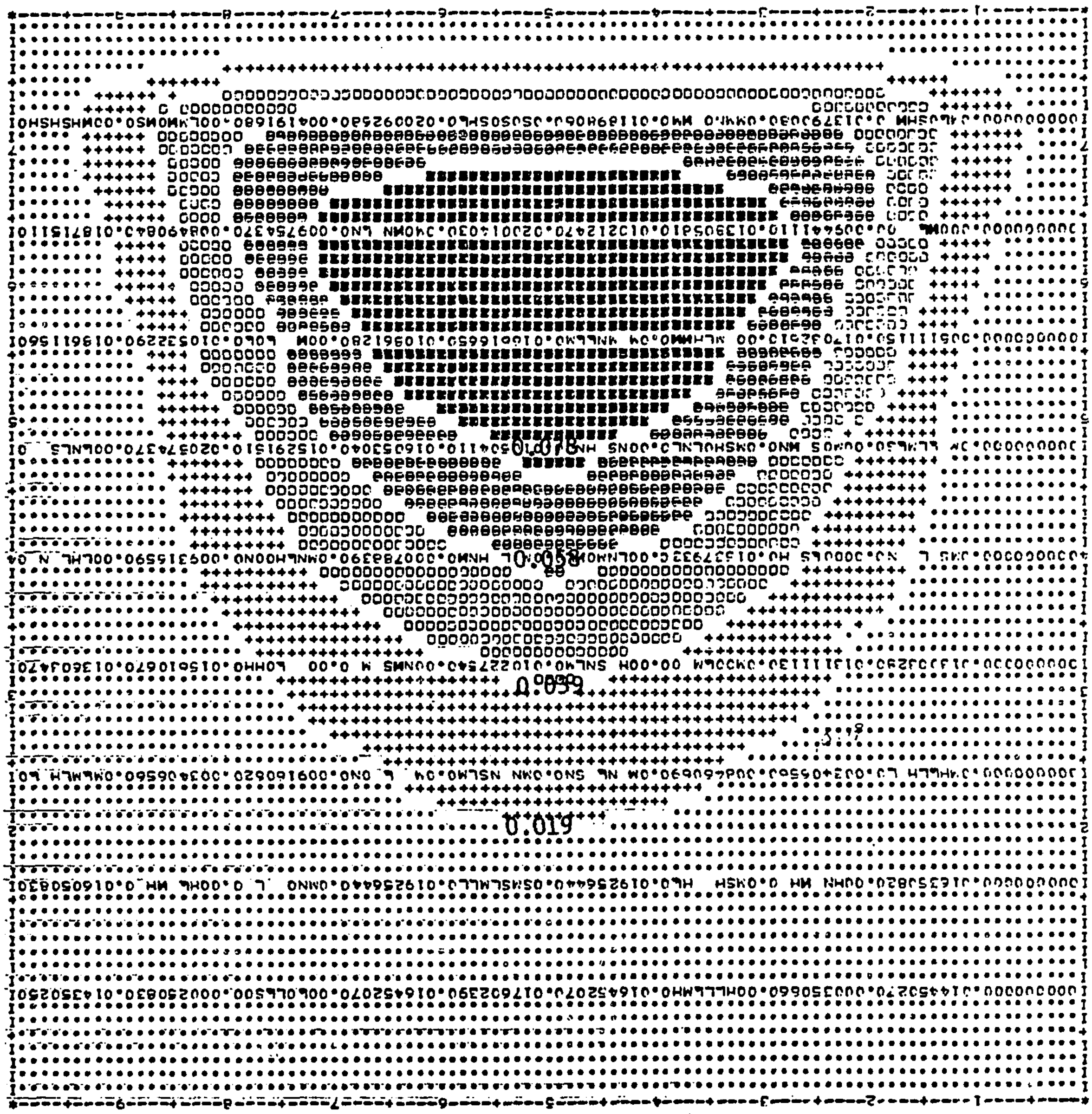

Figure III-5. Streamlines for finite element model after dimensionless time 0.25.

Table III-1. Numerical results after dimensionless time 0.15 and 0.25 for finite difference model. (Numbering from left to right, from up to down).

TIME = 0.150

TEMPERATURE (+Y DOWNWARD)

0.000	0.000	0.000	0.000	0.000	0.000	0.000	0.000	0.000	0.000	0.000
0.000	0.009	0.017	0.024	0.028	0.029	0.028	0.024	0.017	0.009	0.000
0.000	0.020	0.037	0.051	0.060	0.063	0.060	0.051	0.037	0.020	0.000
0.000	0.033	0.063	0.085	0.099	0.104	0.099	0.085	0.063	0.033	0.000
0.000	0.051	0.096	0.130	0.151	0.158	0.151	0.130	0.096	0.051	0.000
0.000	0.077	0.143	0.191	0.221	0.230	0.221	0.191	0.143	0.077	0.000
0.000	0.115	0.209	0.275	0.313	0.326	0.313	0.275	0.209	0.115	0.000
0.000	0.174	0.305	0.389	0.435	0.450	0.435	0.389	0.305	0.174	0.000
0.000	0.277	0.449	0.544	0.591	0.606	0.591	0.544	0.449	0.277	0.000
0.000	0.487	0.671	0.749	0.783	0.793	0.783	0.749	0.671	0.487	0.000
0.500	1.000	1.000	1.000	1.000	1.000	1.000	1.000	1.000	1.000	0.500

STREAM FUNCTION (+Y DOWNWARD)

0.000	0.000	0.000	0.000	0.000	0.000	0.000	0.000	0.000	0.000	0.000
0.000	-0.000	-0.001	-0.002	-0.003	-0.003	-0.003	-0.002	-0.001	-0.000	0.000
0.000	-0.001	-0.004	-0.008	-0.011	-0.012	-0.011	-0.008	-0.004	-0.001	0.000
0.000	-0.003	-0.009	-0.017	-0.022	-0.024	-0.022	-0.017	-0.009	-0.003	0.000
0.000	-0.005	-0.017	-0.028	-0.037	-0.040	-0.037	-0.028	-0.017	-0.005	0.000
0.000	-0.009	-0.026	-0.043	-0.055	-0.059	-0.055	-0.043	-0.026	-0.009	0.000
0.000	-0.013	-0.037	-0.059	-0.073	-0.078	-0.073	-0.059	-0.037	-0.013	0.000
0.000	-0.019	-0.048	-0.073	-0.088	-0.094	-0.088	-0.073	-0.048	-0.019	0.000
0.000	-0.026	-0.056	-0.079	-0.092	-0.096	-0.092	-0.079	-0.056	-0.026	0.000
0.000	-0.028	-0.050	-0.062	-0.068	-0.070	-0.068	-0.062	-0.050	-0.028	0.000
0.000	0.000	0.000	0.000	0.000	0.000	0.000	0.000	0.000	0.000	0.000

TIME = 0.250

TEMPERATURE (+Y DOWNWARD)

0.000	0.000	0.000	0.000	0.000	0.000	.000	0.000	0.000	0.000	0.000
0.000	0.011	0.021	0.028	0.033	0.035	.033	0.028	0.021	0.011	0.000
0.000	0.023	0.043	0.059	0.069	0.073	.069	0.059	0.043	0.023	0.000
0.000	0.037	0.071	0.096	0.112	0.118	112	0.096	0.071	0.037	0.000
0.000	0.056	0.106	0.143	0.167	0.174	.167	0.143	0.106	0.056	0.000
0.000	0.082	0.153	0.205	0.237	0.247	.237	0.205	0.153	0.082	0.000
0.000	0.120	0.218	0.288	0.329	0.342	.329	0.288	0.218	0.120	0.000
0.000	0.178	0.313	0.400	0.448	0.463	.448	0.400	0.313	0.178	0.000
0.000	0.280	0.455	0.552	0.601	0.616	.601	0.552	0.455	0.280	0.000
0.000	0.489	0.674	0.754	0.788	0.798	.788	0.754	0.674	0.489	0.000
0.500	1.000	1.000	1.000	1.000	1.000	.000	1.000	1.000	1.000	0.500

STREAM FUNCTION (+Y DOWNWARD)

0.000	0.000	0.000	0.000	0.000	0.000	.000	0.000	0.000	0.000	0.000
0.000	-0.000	-0.001	-0.002	-0.003	-0.003	- .003	-0.002	-0.001	-0.000	0.000
0.000	-0.001	-0.004	-0.008	-0.011	-0.012	- .011	-0.008	-0.004	-0.001	0.000
0.000	-0.003	-0.009	-0.017	-0.022	-0.024	- .022	-0.017	-0.009	-0.003	0.000
0.000	-0.005	-0.017	-0.028	-0.037	-0.040	- .037	-0.028	-0.017	-0.005	0.000
0.000	-0.009	-0.026	-0.043	-0.055	-0.059	- .055	-0.043	-0.026	-0.009	0.000
0.000	-0.013	-0.037	-0.059	-0.073	-0.078	- .073	-0.059	-0.037	-0.013	0.000
0.000	-0.019	-0.048	-0.073	-0.088	-0.094	- .088	-0.073	-0.048	-0.019	0.000
0.000	-0.026	-0.056	-0.079	-0.092	-0.096	- .092	-0.079	-0.056	-0.026	0.000
0.000	-0.028	-0.050	-0.062	-0.068	-0.070	- .068	-0.062	-0.050	-0.029	0.000
0.000	0.000	0.000	0.000	0.000	0.000	.000	0.000	0.000	0.000	0.000

Table III-2. Numerical results after dimensionless time 0.25 and 0.15 for finite element model.

* RESULT AT IT= 30 CT= 0.15,000D+00

I	T	STR
1	0.0	0.0
2	0.0	0.0
3	0.0	0.0
4	0.0	0.0
5	0.0	0.0
6	0.0	0.0
7	0.0	0.0
8	0.0	0.0
9	0.0	0.0
10	0.0	0.0
11	0.0	0.0
12	0.0	0.0
13	0.8753935D-02	0.5735981D-03
14	0.1664727D-01	0.1291720D-02
15	0.2292303D-01	0.2496113D-02
16	0.2698726D-01	0.3169118D-02
17	0.2845522D-01	0.3610207D-02
18	0.2716774D-01	0.3168653D-02
19	0.2321066D-01	0.2494362D-02
20	0.1693072D-01	0.1290075D-02
21	0.8924515D-02	0.5725121D-03
22	0.0	0.0
23	0.0	0.0
24	0.1878617D-01	0.1450899D-02
25	0.3570991D-01	0.4648541D-02
26	0.4913836D-01	0.8027702D-02
27	0.5783270D-01	0.1092351D-01
28	0.6098685D-01	0.1180548D-01
29	0.5826528D-01	0.1092307D-01
30	0.4983001D-01	0.8025027D-02
31	0.3638299D-01	0.4643313D-02
32	0.1919534D-01	0.1448571D-02
33	0.0	0.0
34	0.0	0.0
35	0.3151533D-01	0.3255197D-02
36	0.5981608D-01	0.9478589D-02
37	0.8219754D-01	0.1682621D-01
38	0.9664800D-01	0.2216755D-01
39	0.1019289D+00	0.2433297D-01
40	0.9749758D-01	0.2217581D-01
41	0.8354406D-01	0.1683259D-01
42	0.6113376D-01	0.9477904D-02
43	0.3229785D-01	0.3252519D-02
44	0.0	0.0
45	0.0	0.0
46	0.4866592D-01	0.5282417D-02
47	0.9214204D-01	0.1644502D-01
48	0.1262079D+00	0.2823371D-01
49	0.1480706D+00	0.3727530D-01
50	0.1561057D+00	0.4045647D-01
51	0.1495979D+00	0.3731305D-01
52	0.1286496D+00	0.2827992D-01
53	0.9450544D-01	0.1646993D-01
54	0.5009282D-01	0.5287987D-02
55	0.0	0.0
56	0.0	0.0
57	0.7273130D-01	0.8462695D-02
58	0.1369007D+00	0.2490214D-01
59	0.1863160D+00	0.4266005D-01
60	0.2174816D+00	0.5529344D-01

61	0.2289576D+00	0.5994898D-01
62	0.2200538D+00	0.5539446D-01
63	0.1904321D+00	0.4279689D-01
64	0.1409561D+00	0.2499686D-01
65	0.7512156D-01	0.8490225D-02
66	0.0	0.0
67	0.0	0.0
68	0.1077206D+00	0.1186508D-01
69	0.2006108D+00	0.3563113D-01
70	0.2693511D+00	0.5870156D-01
71	0.3111268D+00	0.7468274D-01
72	0.3262982D+00	0.8040268D-01
73	0.3150568D+00	0.7487569D-01
74	0.2738231D+00	0.5898186D-01
75	0.2070673D+00	0.3584762D-01
76	0.1116716D+00	0.1194002D-01
77	0.0	0.0
78	0.0	0.0
79	0.1620464D+00	0.1722939D-01
80	0.2946308D+00	0.4698088D-01
81	0.3850578D+00	0.7424186D-01
82	0.4354924D+00	0.9088979D-01
83	0.4531872D+00	0.9593008D-01
84	0.4407297D+00	0.9114931D-01
85	0.3940757D+00	0.7465849D-01
86	0.3042786D+00	0.4734529D-01
87	0.1679989D+00	0.1736452D-01
88	0.0	0.0
89	0.0	0.0
90	0.2563862D+00	0.2232590D-01
91	0.4432092D+00	0.5850314D-01
92	0.5454083D+00	0.8216714D-01
93	0.5948448D+00	0.9329669D-01
94	0.6116008D+00	0.9768838D-01
95	0.6004847D+00	0.9351676D-01
96	0.5556240D+00	0.8255626D-01
97	0.4555958D+00	0.5892361D-01
98	0.2653400D+00	0.2251998D-01
99	0.0	0.0
100	0.0	0.0
101	0.4814228D+00	0.3289035D-01
102	0.6828211D+00	0.5640147D-01
103	0.7550665D+00	0.6388058D-01
104	0.7870946D+00	0.6926618D-01
105	0.7976002D+00	0.6980399D-01
106	0.7909785D+00	0.6934817D-01
107	0.7627563D+00	0.6403543D-01
108	0.6932916D+00	0.5660132D-01
109	0.4928643D+00	0.3300371D-01
110	0.0	0.0
111	0.5000000D+00	0.0
112	0.1000000D+01	0.0
113	0.1000000D+01	0.0
114	0.1000000D+01	0.0
115	0.1000000D+01	0.0
116	0.1000000D+01	0.0
117	0.1000000D+01	0.0
118	0.1000000D+01	0.0
119	0.1000000D+01	0.0
120	0.1000000D+01	0.0
121	0.5000000D+00	0.0

* RESULT AT IT= 50 CT= 0.25000D+00

I	T	STR
1	0.0	0.0
2	0.0	0.0
3	0.0	0.0
4	0.0	0.0
5	0.0	0.0
6	0.0	0.0
7	0.0	0.0
8	0.0	0.0
9	0.0	0.0
10	0.0	0.0
11	0.0	0.0
12	0.0	0.0
13	0.1045574D-01	0.5737634D-03
14	0.1988175D-01	0.1292391D-02
15	0.2737032D-01	0.2497475D-02
16	0.3220845D-01	0.3171044D-02
17	0.3393717D-01	0.3612347D-02
18	0.3237386D-01	0.3170573D-02
19	0.2763341D-01	0.2495714D-02
20	0.2014075D-01	0.1290739D-02
21	0.1061081D-01	0.5726747D-03
22	0.0	0.0
23	0.0	0.0
24	0.2203642D-01	0.1451572D-02
25	0.4188770D-01	0.4651059D-02
26	0.5763031D-01	0.8032571D-02
27	0.6779959D-01	0.1093028D-01
28	0.7144754D-01	0.1181296D-01
29	0.6819586D-01	0.1092982D-01
30	0.5826397D-01	0.8029866D-02
31	0.4250270D-01	0.4645805D-02
32	0.2241032D-01	0.1449234D-02
33	0.0	0.0
34	0.0	0.0
35	0.3601939D-01	0.3256564D-02
36	0.6837408D-01	0.9483468D-02
37	0.9395821D-01	0.1683534D-01
38	0.1104434D+00	0.2218004D-01
39	0.1163984D+00	0.2434673D-01
40	0.1112251D+00	0.2218827D-01
41	0.9519595D-01	0.1684166D-01
42	0.6958618D-01	0.9482740D-02
43	0.3673679D-01	0.3253869D-02
44	0.0	0.0
45	0.0	0.0
46	0.5400589D-01	0.5284353D-02
47	0.1022891D+00	0.1645181D-01
48	0.1401437D+00	0.2824623D-01
49	0.1644051D+00	0.3729231D-01
50	0.1732220D+00	0.4047516D-01
51	0.1658207D+00	0.3733003D-01
52	0.1424092D+00	0.2829238D-01
53	0.1044805D+00	0.1647668D-01
54	0.5533181D-01	0.5289905D-02
55	0.0	0.0
56	0.0	0.0
57	0.7840490D-01	0.8464846D-02
58	0.1476746D+00	0.2490965D-01
59	0.2011039D+00	0.4267384D-01
60	0.2347958D+00	0.5531216D-01
61	0.2470793D+00	0.5996955D-01

62	0.2372092D+00	0.5541317D-01
63	0.2049663D+00	0.4281066D-01
64	0.1514863D+00	0.2500436D-01
65	0.8064839D-01	0.8492367D-02
66	0.0	0.0
67	0.0	0.0
68	0.1131728D+00	0.1186700D-01
69	0.2109647D+00	0.3563790D-01
70	0.2835457D+00	0.5871406D-01
71	0.3277276D+00	0.7469976D-01
72	0.3436521D+00	0.8042141D-01
73	0.3314652D+00	0.7489273D-01
74	0.2897082D+00	0.5899439D-01
75	0.2171151D+00	0.3585442D-01
76	0.1169453D+00	0.1194196D-01
77	0.0	0.0
78	0.0	0.0
79	0.1667346D+00	0.1723074D-01
80	0.3035202D+00	0.4698572D-01
81	0.3972310D+00	0.7425095D-01
82	0.4497120D+00	0.9090229D-01
83	0.4680418D+00	0.9594389D-01
84	0.4547654D+00	0.9116186D-01
85	0.4059383D+00	0.7466766D-01
86	0.3128526D+00	0.4735021D-01
87	0.1724920D+00	0.1736590D-01
88	0.0	0.0
89	0.0	0.0
90	0.2598182D+00	0.2232656D-01
91	0.4497109D+00	0.5850562D-01
92	0.5542945D+00	0.8217199D-01
93	0.6052244D+00	0.9330347D-01
94	0.6224474D+00	0.9769590D-01
95	0.6107367D+00	0.9352358D-01
96	0.5642884D+00	0.8256117D-01
97	0.4618457D+00	0.5892617D-01
98	0.2686120D+00	0.2252067D-01
99	0.0	0.0
100	0.0	0.0
101	0.4832356D+00	0.3289051D-01
102	0.6862383D+00	0.5640213D-01
103	0.7597422D+00	0.6388194D-01
104	0.7925606D+00	0.6926811D-01
105	0.8033210D+00	0.6980614D-01
106	0.7963942D+00	0.6935011D-01
107	0.7673372D+00	0.6403681D-01
108	0.6966000D+00	0.5660201D-01
109	0.4945376D+00	0.3300388D-01
110	0.0	0.0
111	0.5000000D+00	0.0
112	0.1000000D+01	0.0
113	0.1000000D+01	0.0
114	0.1000000D+01	0.0
115	0.1000000D+01	0.0
116	0.1000000D+01	0.0
117	0.1000000D+01	0.0
118	0.1000000D+01	0.0
119	0.1000000D+01	0.0
120	0.1000000D+01	0.0
121	0.5000000D+00	0.0

BIBLIOGRAPHY

1. Ahern, J. L., 1979, Magma Migration, Ph.D. Dissertation unpublished, Cornel University, Ithaca, NY.

2. Ahern, J. L. and Turcotte, D. L., and Oxburgh, E. R., 1979, On the Upward Migration of Batholith during Solidification EOS - Trans. Am. Geophys. Urion, Abstr., 60, pp. 411.

3. Ahern, J. L. and Turcotte, D. L., 1979, Magma Migration Beneath an Ocean Ridge, Earth Plan. Sci. Letters, Vol. 45, pp. 115-122.

4. Ahern, J. L., Turcotte, D. L., and Oxburgh, E. R., 1981, On the Upward Migration of an Intrusion, Journal of Geology, Vol. 89, p. 421-432.

5. Atthey , D. R., 1974, A Finite Difference Scheme for Melting Problems, J. Insti. Matha. Applics., 13, pp. 353-366.

6. Bear, J., 1972, Dynamics of Fluids in Porous Media, Elsevier, New York, NY, 1972, pp. 641-662.

7. Carnahan, B. et al, 1969, Applied Numerical Methods, John Wiley & Sons.

8. Carslaw, H. S. and Jaeger, J. C., 1959, Conduction of Heat in Solids, 2nd Edition, Oxford Press, London.

9. Chung, T. J., 1978, Finite Element Analysis in Fluid Dynamics, McGraw-Hill, New York.

10. Clark, S. P., 1966, Handbook of Physical Constants (Geological Society of America, New York, NY, 1966) p. 459-482.

11. Courant, R., Variational Methods for the Solution of Problem of Equilibrium and Vibrations, Bulletin the American Mathematical Society, Vol. 49, pp. 1-23.

12. Crowley, A. B., 1977, Numerical Solution of Stefan Problems, J. Heat and Mass Transfer, Vol. 21, pp. 215-219.

13. Duvaut, G. and Lions, J. L., 1976, Inequalities in Mechanics and Physics, Spring - Verlag, Berlin.

14. Gartling, D. K., 1977, Convective Heat Transfer Analysis by the Finite Element Method, Computer Meth. Appl. Mec. Eng., Vol. 12, pp. 365-382.

15. Hargraves, R. B., 1980, Physics of Magmatic Processes, Princeton University Press.

16. Hulbert, M. K., 1937, Theory of Scale Models as Applied to Study of Geological Structures, Bulletin Geol. Soc. Amer., Vol. 48, pp. 1459-1520.

17. Ichikawa, Y. et al, 1979, A One-Phase Multi-Dimensional Stefan Problem by the Method of Variational Inequalities, International Journal for Numerical Methods in Engineering, Vol. 14, pp. 1197-1220.

18. Jaeger, J. C., 1961, Cooling and Solidification of Igneous Rocks, Basalts, Vol. 2, pp. 503-536.

19. Jaeger, J. C., 1964, Thermal Effects of Intrusions, Rev. Geophysics 2, pp. 443-466.

20. Kang, J. M., 1979, Salt Dome Utilization in Gulf Coast, (unpublished)

21. Kikuchi, N. et al, 1979, Numerical Method for a Two-Phase Stefan Problem by Variational Inequalities, International Journal for Numerical Methods in Engineering, Vol. 14, pp. 1221-1239.

22. Kono, Y. et al, 1979, Simulation of the Time Dependent Thermal Convection Within the Earth's Mantle, J. Phys. Earth, Vol. 27, pp. 315-336.

23. Lipps, F. B., 1971, Two-Dimensional Numerical Experiments in Thermal Convection with Vertical Shear, Jour. Atmos. Sci. 28, No. 1, pp. 3-19.

24. Lovering, T. S., 1955, Temperature In and Near Intrusions, Econ. Geology, Vol. 51, pp. 249-281.

25. McKenzie, D. P., 1968, The Influence of the Boundary Conditions and Rotation on Convection in the Earth's Mantle, Geophys. J. R. Astron. Soc., Vol. 15, pp. 457-500.

26. Oxburgh, E. K., 1980, Heat Flow and Magma Genesis, Princeton University Press, pp. 161-199.

27. Ozisik, M. N., 1977, Basic Heat Transfer, McGraw-Hill, New York.

28. Reddy, J. N. and Patil, K. H., 1977, Alternate Finite Element Formulations of Incompressible Fluid Flow with Applications, Computer Methods in Engineering, University of Southern California, LA.

29. Reddy, J. N., 1979-a, Penalty Finite Elements: Theory and Application, Research Report No OU-AME-79-6, University of Oklahoma.

30. Reddy, J. N., 1979-b, On the Finite Element Method with Penalty for Incompressible Fluid Flow Problems, The Mathematics of Finite Elements and Applications II, Academic Press, pp. 227-235.

31. Richter, F. M., 1973, Dynamical Models for Sea Floor Spreading, Rev. Geophy. Spacephys., Vol. II, pp. 223-287.

32. Roberts, G. O., 1977, Fast Viscous Convection, Geophys, Astrophys, Fluid Dynamics, Vol. 8, pp. 199-233.

33. Satake, A. and Reddy, J. N., 1980, A Comparison of a Penalty Finite Element Model with the Stream Function - Vorticity Model of Natural Convection in Enclosures, J. Heat Transfer, Vol. 102, pp. 659-666.

34. Shaw, H. R., 1965, Comments on Viscosity, Crystal Settling and Convection in Granite Magmas, American Journal of Science, Vol. 263, February, pp. 120-152.

35. Shimazu, Y., 1961, A Physical Theory of Generation, Upward Transfer, Differentiation, Solidification and Explosion of Magmas: Nagoya University, Jour. Earth Sci., Vol. 9, pp. 185-223.

36. Spera, F. J., 1980, Aspects of Magina Transport, Princeton University Press, pp. 265-323.

37. Stern, J., and Shankland, T. J., 1981. Radiative Thermal Conductivity in Obsidian and Estimates of Heat Transfer in Magma Bodies, Journal of Geophysical Research, Vol. 86, No. B5, pp. 3685-3688.

38. Taylor, C. and Hood, P., 1974, Convective Flow Under Thermal Gradients, Internal Report C.R. 105, University of Swansea, England.

39. Taylor, C. and Ijam, A., 1975, Coupled Convective/Conductive Heat Transfer Including Velocity Field Evaluation, Proceeding of the Brunel University of Conference of Institute of Mathematics and Its Applications, pp. 333-347.

40. Taylor, C. and Ijam, B., 1979, A Finite Element Numerical Solution of Natural Convection in Enclosed Cavities, Computer Methods in Applied Mechanics and Engineering, Vol. 7, pp. 429-466.

41. Tikhonov, A. N., 1963, Equations of Mathematical Physics, Pergamon Press, Oxford, pp. 283-288.

42. Turcotte, D. L. and Oxburgh, E. R., 1967, Finite Amplitude Convective Cells and Continental Drift, J. Fluid Mech., Vol. 28, Part 1, pp. 29-42.

43. Tritton, D. J., 1977, Physical Fluid Dynamics, Van Nostrand Reinhold.

44. Wilson, D. G. et al, 1978, Moving Boundary Problems, Academic Press.

45. Yoder, H. S., 1976, Generation of Basaltic Magma, National Academy of Science, Washington, D.C.

46. Zienkiewicz, O. C. and Gallagher, R. H. and Hood, P., 1975, Newtonian and Nonnewtonian Viscous Incompressible Flow, Temperature Induced Flows, Finite Element Solution, 2nd Conference Mathematics of Finite Element and Applications, Brunel University, pp. 235-267.

47. Zienkiewicz, O. C. and Heinrich, J. C., 1978, Penalty Function Solution of Coupled Convective and Conductive Heat Transfer, Int. Conf. Numr. Mech., in Laminar and Turbulent Flow, University of Swansea, England.

48. Zienkiewicz, O. C., 1979, The Finite Element Method, 3rd Edition, McGraw-Hill, New York.